The Pennsylvania State University

The Graduate School

IDENTIFYING NOVEL MECHANISMS OF SENSITIVITY AND RESISTANCE TO POLY-ADP-RIBOSE POLYMERASE (PARP) INHIBITORS THROUGH GENOME-WIDE CRISPR KNOCKOUT AND ACTIVATION SCREENS

A Dissertation in

Biomedical Sciences

by

Kristen E. Clements

Submitted in Partial Fulfillment
of the Requirements
for the Degree of

Doctor of Philosophy

May 2020

The dissertation of Kristen E. Clements was reviewed and approved* by the following:

George-Lucian Moldovan
Dissertation Adviser
Chair of Committee
Associate Professor, Department of Biochemistry and Molecular Biology

James R. Broach
Professor and Chair, Department of Biochemistry and Molecular Biology

Kristin A. Eckert
Professor, Department of Pathology

Raymond Hohl
Director, Penn State Hershey Cancer Institute

Zhonghua Gao
Assistant Professor, Department of Biochemistry and Molecular Biology

Ralph L. Keil
Associate Professor, Department of Biochemistry and Molecular Biology
Chair, Biomedical Sciences Graduate Program

ABSTRACT

Inhibitors of poly-ADP-ribose polymerase 1 (PARPi) are highly effective in killing cells deficient in the homologous recombination (HR) DNA repair pathway, such as those lacking BRCA1 or BRCA2. In light of this, PARPi have been utilized in recent years to treat BRCA2-mutant tumors, with many patients deriving impressive clinical benefit. However, positive response to PARPi is not universal, even among patients with HR-deficient tumors. In this dissertation, I present the results of three genome-wide CRISPR knockout and activation screens which provide an unbiased look at genetic determinants of PARPi response in wildtype or BRCA2-knockout cells. Additionally, I reveal the novel mechanisms through which depletion of two hits from the screens—E2F7 and TIP60—lead to resistance to PARPi in BRCA2-deficient cells.

Strikingly, I reveal that depletion of the transcription factor E2F7, a top hit from the screens, robustly reverses the PARPi sensitivity caused by BRCA2 deficiency. Moreover, I show that the mechanism underlying this activity involves increased expression of RAD51, a target for E2F7-mediated transcriptional repression, which enhances both HR DNA repair and replication fork stability in BRCA2-deficient cells. Notably, restoration of homologous recombination independent of a reversion mutation has not previously been associated with PARPi resistance in BRCA2-deficient cells.

In addition, I demonstrate that loss of the histone acetyltransferase TIP60, a second hit from the screen, also abolishes the sensitivity of BRCA2-deficient cells to PARPi. Mechanistically, I reveal that TIP60 depletion rewires double strand break repair in BRCA2-deficient cells by promoting 53BP1 binding to double strand breaks to suppress end resection. My work provides a comprehensive set of putative biomarkers that serve to better understand and predict PARPi response, and identifies novel pathways of PARPi resistance in BRCA2-deficient cells.

TABLE OF CONTENTS

LIST OF FIGURES

LIST OF TABLES

ACKNOWLEDGEMENTS

I would like to thank Drs. James Broach, Jeremy Stark, Roger Greenberg, Robert Brosh, Mariano Russo, and Jacob Hornick for materials and advice; and the following Penn State College of Medicine core facilities: Flow Cytometry, Genomic Analyses, and Imaging. Thank you, also, to my Thesis Committee members, for their support and advice.

I am eternally grateful to my mentor, Dr. Lucian Moldovan, for providing me with the guidance and encouragement necessary not only to complete this work, but to mature as a scientist. I also owe a huge debt of gratitude to Dr. Claudia Nicolae, who is truly the heart and soul of the lab. I would like to thank her and the rest of my lab family—Michael O'Connor, Tanay Thakar, and Emily Schleicher—for many productive scientific discussions and unproductive coffee breaks.

Thank you to my friends near and far, especially my MD/PhD cohort, for making the highs of this long journey sweeter and the lows bearable. To Yun, Colin, and Alfred, thank you for always being there for me when I need it the most.

Finally, I want to thank my amazing family, especially my mother, father and sister, for sharing more love and support than I could have ever imagined; without you, this work would not have been possible.

Experimental design schemes and summary models were created with Biorender.com. This work was supported by: NIH R01ES026184 and the St. Baldrick's Foundation (to George Lucian Moldovan). The findings and conclusions within this dissertation do not necessarily reflect the views of the funding agencies.

Chapter 1: Introduction

1.1 Precision Medicine

Cancer precision medicine seeks to characterize both the tumor and the patient themselves by examining areas such as genetics, epigenetics, transcriptomics, and lifestyle factors, in order to predict, as best as possible, which treatment will be most effective for that tumor, in that patient (1). Synthetic lethality is an important concept in precision medicine, and describes the phenomenon in which interference with the functions of two proteins at the same time results in cell death, even though depletion of either protein alone does not affect viability (2). This ideally allows for maximum tumor killing efficacy, with lesser side effects than non-targeted chemotherapy. The first, and one of the most successful, clinically-approved applications of synthetic lethality is the use of inhibitors of poly-ADP-ribose polymerase to treat cancers deficient in the proteins BRCA1 or BRCA2 (3). Although tremendous progress has been made in the 15 years since the discovery of this synthetically lethal interaction, researchers are still trying to better identify specifically which patients will benefit from this treatment.

1.2 BRCA1 and BRCA2: Molecular Functions and Implications for Cancer

The gene BRCA1 (Breast Cancer Type 1) was first cloned in 1994, shortly after being linked to chromosome 17 based on analysis of families afflicted with early-onset breast cancer (4). Soon after, the gene associated with Breast Cancer Type 2 (BRCA2) was cloned from chromosome 13 (4). Now, these two proteins are well-known for their connection to cancer susceptibility as well as their well-studied roles in homologous recombination DNA repair (HR). Despite similarities in name, these two proteins have very distinct features and functions, even within the shared process of homologous recombination (Figure 1.1).

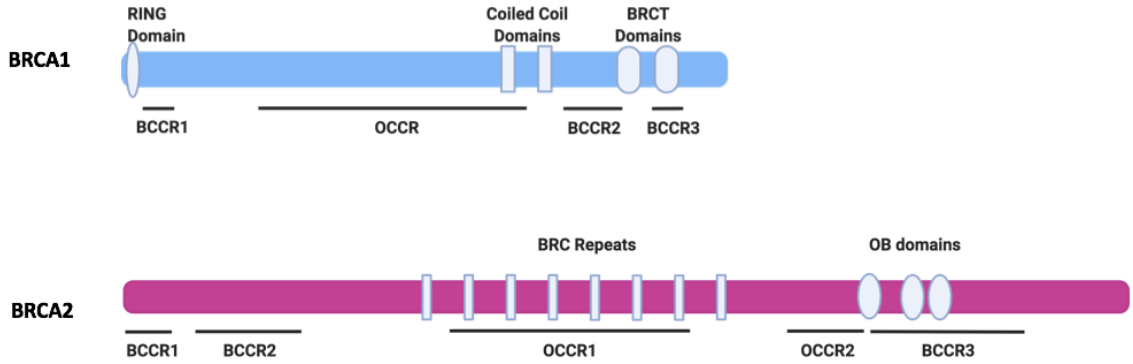

Figure 1.1. Structure of BRCA1 and BRCA2. Relevant domains referenced within the text are labelled above the structure. Below the structure, breast cancer cluster regions (BCCR) and ovarian cancer cluster regions (OCCR) are labelled. These are regions that are frequent sites of pathogenic missense mutations associated with the disease indicated. Image made with Biorender.com.

BRCA1 is a 1863 amino acid protein containing multiple domains, including a RING domain which confers its activity as an E3 ubiquitin ligase; it exists as a heterodimer with BRCA1-associated RING domain protein (BARD1) to exert its function as an E3 (5). Other structural components include tandem BRCT domains through which it interacts with many other proteins, including abraxas, CtIP, and BACH1 (5). BRCA1 is recruited to double-strand breaks (DSBs) early in the HR process through its interaction with abraxas and RAP80 (abraxas receptor-associated protein-80) (6). Through its interaction with CtIP and the MRN (MRE11-RAD50-NBS1) complex, BRCA1 antagonizes 53BP1 activity by displacing it from the DSB site and subsequently promoting end resection and subsequent repair through HR (7). During homologous recombination, BRCA1 and BRCA2 interact, in a complex bridged by the protein PALB2 at the RAD51-recruitment step (5). Overall, BRCA1 acts early in the DSB repair process by directing the choice of repair pathway towards HR via end resection, in a competing role with 53BP1 (Figure 1.2). BRCA1 has been implicated in several additional

processes other that HR. In complex with BACH1 (FANCJ), BRCA1 is recruited to replication forks upon replication stress (8, 9). BRCA1 is also responsible for activating signaling of the G2/M and replication (S-phase) checkpoints, and is implicated in such diverse processes as chromatin remodeling, transcriptional regulation, apoptosis, mitophagy, and centrosome regulation (5).

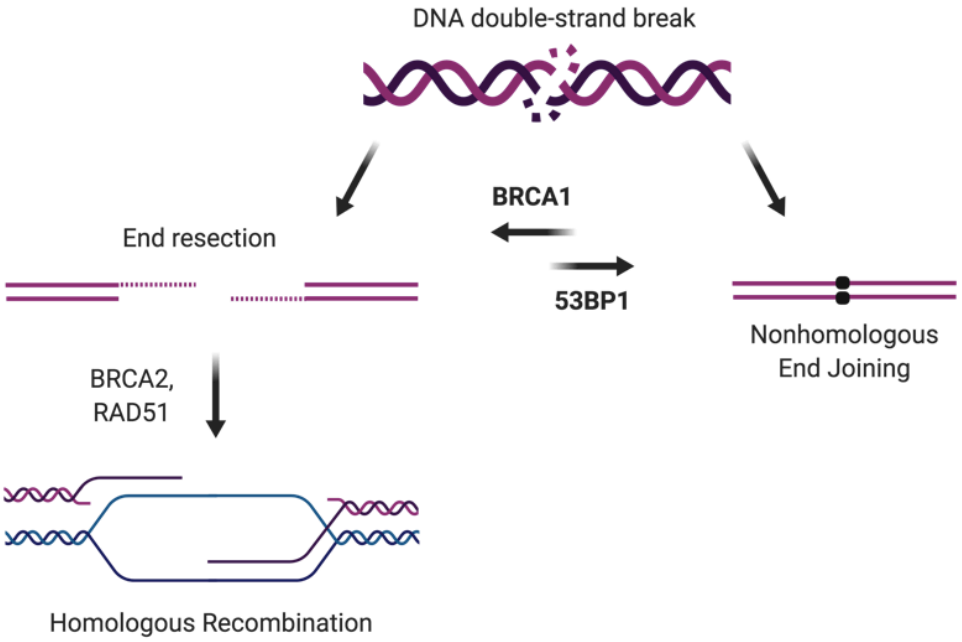

Figure 1.2. General scheme of the roles of BRCA1, 53BP1, BRCA2, and RAD51 in homologous recombination. Briefly, BRCA1 acts early in the double-strand break repair process to promote end resection, a key step for homologous recombination. 53BP1 exerts the opposite effect, suppressing end resection to promote Nonhomologous end joining. After the end resection step, BRCA2 functions to load RAD51 onto the single-stranded DNA, promoting strand invasion, D-loop formation, and ultimately error-free repair.

In contrast, BRCA2 is a protein of 3418 amino acids with no known enzymatic activity (10). It possesses three OB (oligonucleotide binding) domains, which allow it to bind both double-stranded DNA and single-stranded DNA with high affinity (11). Furthermore, the center of BRCA2 consists of eight BRC repeats, which confer the RAD51-binding function necessary to complete its essential role in HR (10). BRCA2

functions downstream of BRCA1 in homologous recombination, meditating the formation of RAD51 nucleofilaments on single-stranded DNA (ssDNA) produced by resection of the DSB end (11). Subsequently, the C-terminus of BRCA2 promotes nucleofilament extension and strand invasion to form the D-loop with the sister chromatid (12). Thus, BRCA2 is essential for HR and acts in steps distinct from BRCA1, in particular for RAD51 loading. More recently, BRCA2 has also been connected to other cellular functions, including cytokinesis, centrosome duplication, limiting R-loops, and protecting telomeres as well as stalled replication forks (see Section 1.5.5) (10, 11).

BRCA1 and BRCA2 are tumor suppressor proteins, meaning that their cellular function works to prevent carcinogenesis. Typically, patients with germline BRCA1/2 mutations are carriers, having inherited one mutant allele from one parent. However, through chromosomal instability and mutagenesis during the process of carcinogenesis, tumor cells lose the other wild type allele; thus, tumor cells have lost heterozygosity and are deficient in BRCA1/2 function, while the rest of the patient's cells remain heterozygous (13–15). While there are thousands of reported BRCA1 and 2 variants, only a small fraction of these are confirmed to be pathogenic; most are "Variants of Unknown Significance" (VUS) (16). The majority of pathogenic mutations are nonsense mutations and are distributed throughout the genes; however, pathogenic mutations that are missense tend to cluster in hotspots, which interestingly differ by cancer type (Figure 1.1) (16, 17).

BRCA1/2 mutations are responsible for 25% of hereditary breast cancer, and roughly 10% of total breast cancer cases (18). One systematic review of the international prevalence of germline deleterious BRCA mutations in sporadic breast cancer found wide variations, from 1.8% of patients in a study in Spain, to 36.9% of patients in a U.S. study (19). BRCA1 and BRCA2 are considered highly penetrant with regards to the development of breast cancer, as the risk for mutation carriers is 10- 20 times higher

than the risk for those without mutations (20). A recent prospective study evaluated the risk of developing breast and ovarian cancer in more than 6000 carriers of pathogenic mutations in BRCA1 and nearly 4000 carriers of pathogenic mutations in BRCA2 (21). This study revealed that the risk of developing breast cancer by age 80 was 72% for patients with BRCA1 mutations and 69% for BRCA2 carriers. For ovarian cancer, the risk was 44% for BRCA1 mutation carriers and 17% for BRCA2 mutation carriers (21). Mutations in these proteins increase the risk for other cancer types as well, including pancreatic and prostate cancer (16). Thus, there is a great need for effective therapies to target BRCA1 and BRCA2-mutant tumors.

1.3 PARP inhibitor treatment is synthetically lethal with BRCA1/2 deficiency

In 2005, two groups hypothesized that increasing the cellular requirement for homologous recombination repair could lead to specific killing of cells deficient in this DNA repair pathway, such as those deficient in BRCA1 or BRCA2. In particular, these groups focused their studies on poly-ADP-ribose polymerase (PARP1), a protein important for single strand break repair; previous work had indicated that depletion of PARP1 led to an increase in lesions repaired by homologous recombination, as indicated by an increase in RAD51 foci (22). To test this hypothesis, these groups employed both PARP1 knockdown as well as PARP1 inhibition using small molecule inhibitors of the enzyme. These PARP inhibitors (PARPi), which block the NAD+ binding pocket of the enzyme, had been previously investigated as possible means to improve DNA damage-based chemotherapy; however, these researchers were interested in testing PARPi as a single agent against HR-deficient cells (23, 24).

Excitingly, these studies revealed that cells deficient in BRCA1, BRCA2, or other homologous recombination proteins were exceedingly sensitive to PARP1 knockdown or inhibition, whereas wildtype controls were not (23, 24). In fact, these cells were even

more sensitive to PARPi than to cisplatin, the mainstay of treatment for many tumors with such DNA repair defects. For example, BRCA2-mutant embryonic stem cells were 3-fold more sensitive to cisplatin than wildtype controls, however these cells were 133-fold more sensitive to PARPi (24). Importantly, PARP1 was equally inhibited in BRCA1/2 mutant and wildtype control cells, indicating that the differences in cytotoxicity were due to differences in downstream response to PARP inhibition rather than differential efficacy of the inhibitor (23).

As described in the previous section (I.2), patients who inherit defects in BRCA proteins are heterozygous for the mutation in most cells, but tumors lose heterozygosity. Therefore, in order to be a viable clinical treatment for these patients, PARPi would need to demonstrate efficacy against homozygous mutant tumor cells, but not heterozygous mutant cells, to prevent side effects. Indeed, experiments revealed that even though cells homozygous for BRCA1/2 mutations were increasingly sensitive to PARPi treatment, cells heterozygous for mutations in these proteins were not (24). Furthermore, as BRCA mutation carriers frequently develop breast cancer, PARPi were tested in BRCA1 or BRCA2- depleted breast cancer cell lines. In both cell culture experiments as well as mouse xenografts, PARPi efficiently killed BRCA1 or 2 -deficient breast cancer cells (23, 24). Together, these experiments suggested that this novel synthetically lethal interaction between PARP1 inhibition and BRCA1/2 deficiency may be clinically actionable.

1.4 Clinical Trials Summary

Although PARPi had been pursued as a potential therapeutic for many years, the discovery that BRCA1 and BRCA2 deficient cells were sensitive to these agents as a single agent provided increased incentive for development, and within only a few years an orally bioavailable PARPi was developed and under evaluation in the clinic (25).

Currently, over 100 phase I and more than 100 phase II clinical trials are registered with ClinicalTrials.gov. Furthermore, six different PARPi are being evaluated for safety and efficacy in a variety of clinical contexts through phase III trials (Table 1.1).

Table 1.1. PARP inhibitors under investigation in Phase III clinical trials

Generic Name	Brand Name	FDA-approved indications?
Niraparib	Zejula (Tesaro/GlaxoSmithKline)	Yes
Olaparib	Lynparza (AstraZeneca/Merck)	Yes
Pamiparib	N/A (BeiGene)	No
Rucaparib	Rubraca (Clovis Oncology)	Yes
Talazoparib	Talzenna (Pfizer)	Yes
Veliparib	N/A (AbbVie)	No

1.4.1 Use of PARPi in the treatment of ovarian cancer

Due largely to the connections between BRCA1/2 deficiency, ovarian cancer, and the predicted susceptibility to PARPi treatment, ovarian cancer has remained a major focus of PARPi-based clinical trials, with half of all registered phase III trials enrolling specifically ovarian cancer patients (Table 1.2). Several of these trials have tested the use of PARPi as maintenance therapy for platinum-sensitive and/or BRCA1/2-mutant recurrent disease (7 trials). As HR-deficient cells are often sensitive to platinum therapy, which is often used in the first-line setting, platinum sensitivity is used in many trials as a surrogate biomarker for patients who may respond to PARPi (26). Although many of these trials are still currently active, several have reached primary endpoints and produced survival analyses.

Table 1.2. Phase III clinical trials evaluating PARPi in ovarian cancer patients

PARPi	Application tested	Clinical Trial #	Study Start
Niraparib	Maintenance for platinum-sensitive recurrent disease	NCT01847274	2013
	Maintenance after front-line platinum-based chemotherapy in patients with newly diagnosed Stage III/IV (advanced) disease	NCT02655016	2016
	Maintenance treatment in patients with platinum-sensitive relapsed disease	NCT03705156	2017
	Anti-PD-1 therapy and maintenance Niraparib added to standard chemotherapy in newly diagnosed advanced disease	NCT03602859	2018
	Addition of Anti-PD-L1 therapy to platinum-based chemotherapy and maintenance Niraparib in recurrent disease	NCT03598270	2018
	Maintenance after front-line platinum-based chemotherapy in patients with newly diagnosed Stage III/IV (advanced) disease	NCT03709316	2018
	Chemotherapy-free treatment of recurrent disease using the combination of Niraparib and anti-VEGF therapy, with or without anti-PD-1	NCT03806049	2019
	Niraparib with or without anti-PD-1 therapy, vs chemotherapy for the treatment of metastatic or recurrent Carcinosarcoma	NCT03651206	2020
Olaparib	Maintenance after front-line platinum-based chemotherapy in patients with newly diagnosed Stage III/IV (advanced) disease with BRCA1/2 mutations ("SOLO1")	NCT01844986	2013
	Maintenance for BRCA1/2 mutant, platinum-sensitive recurrent disease ("SOLO2")	NCT01874353	2013
	Olaparib monotherapy vs. standard chemotherapy for relapsed, previously platinum-sensitive, BRCA1/2-mutant disease	NCT02282020	2015
	Maintenance added to anti-VEGF therapy after front-line platinum and anti-VEGF-based chemotherapy in patients with newly diagnosed Stage III/IV (advanced) disease	NCT02477644	2015
	Olaparib monotherapy, or olaparib with anti-VEGF therapy, vs. standard chemotherapy for relapsed, previously platinum-sensitive disease	NCT02446600	2016
	Olaparib and anti-VEGF therapy, alone or in combination, vs. standard chemotherapy for relapsed, platinum-resistant disease	NCT02502266	2016
	Maintenance re-treatment in patients with platinum- sensitive disease recurrence after maintenance therapy with PARPi	NCT03106987	2017
	Maintenance for BRCA1/2 wildtype, platinum-sensitive recurrent disease	NCT03402841	2018
	Maintenance for platinum-sensitive recurrent disease	NCT03534453	2018
	Maintenance with or without anti-VEGF therapy for platinum-sensitive recurrent disease	NCT03278717	2018
	Maintenance with anti-PD-1 therapy after front-line platinum-based chemotherapy with anti-PD-1 therapy in patients with newly diagnosed, Stage III/IV (advanced), BRCA1/2- wildtype disease	NCT03740165	2018
	In newly-diagnosed, advanced disease, platinum-based and anti-VEGF therapy followed by maintenance anti-VEGF therapy as monotherapy, in combination with anti-PD-L1 therapy, or in combination with anti-PD-L1 therapy and olaparib	NCT03737643	2019
Pamiparib	Maintenance for platinum-sensitive recurrent disease	NCT03519230	2018
Rucaparib	Maintenance for platinum-sensitive recurrent disease	NCT01968213	2014
	Rucaparib monotherapy vs. standard chemotherapy as treatment for relapsed, BRCA1/2 mutant disease	NCT02855944	2016
	Rucaparib with Nivolumab (anti-PD-1) as maintenance after front-line platinum-based chemotherapy in patients with newly diagnosed Stage III/IV (advanced) disease	NCT03522246	2018
Veliparib	Veliparib concurrent with front-line platinum-based chemotherapy and as maintenance in patients with newly diagnosed Stage III/IV (advanced) disease	NCT02470585	2015

In the ENGOT-OV16/NOVA trial (NCT01847274), niraparib maintenance treatment significantly improved progression-free survival (PFS) in ovarian cancer patients with platinum-sensitive, recurrent disease, regardless of status as a “complete” or “partial” responder to previous platinum therapy (27). Furthermore, this trial stratified patients based on germline BRCA1/2 mutation (“gBRCA”) status, and found that both gBRCA and non-gBRCA patients benefited from niraparib treatment (28). Strikingly, median PFS improved from 5.5 months to 21.0 months upon niraparib treatment in the cohort with BRCA1/2 mutations, and from 3.9 months to 9.3 months in the non-gBRCA group (28). Olaparib treatment was tested under similar conditions in the SOLO2/ENGOT-Ov21 trial (NCT01874353), which focused specifically on patients with platinum-sensitive recurrent disease and a predicted deleterious mutation in BRCA1/2 (29). PARPi maintenance treatment produced a remarkable improvement in PFS in these patients, with a median PFS of 19.1 months in the group receiving olaparib as compared to 5.5 months in the placebo group (29). A third PARPi, rucaparib, was also investigated as maintenance treatment for recurrent, platinum-sensitive ovarian cancer. Overall, rucaparib treatment doubled median PFS in this study (named “ARIEL3,” NCT01968213), from 5.4 months in the placebo group to 10.8 months in the rucaparib group (30). Investigators also analyzed subgroups of the study population, finding that the therapeutic benefit was even more robust in the cohort of patients with BRCA1/2-mutant carcinoma: median PFS in this cohort was 16.6 months—up from 5.4 months in the BRCA1/2-mutant cohort receiving placebo (30). Altogether, these trials demonstrate that PARPi maintenance treatment in women with relapsed, platinum-sensitive ovarian cancer improved PFS while not affecting (or in some respects improving) quality of life (31, 32). Indeed, the United States Food and Drug Administration (FDA) has approved these agents (niraparib, rucaparib, and olaparib) for use in patients with recurrent

platinum-sensitive ovarian cancer or recurrent BRCA1/2-mutated ovarian cancer (33–35).

In light of these outstanding results, other trials have investigated PARPi treatment earlier on in the patient's treatment regimen: as maintenance therapy after first-line chemotherapy in newly diagnosed disease. The SOLO1 trial (NCT01844986) evaluated olaparib maintenance therapy in patients with platinum-sensitive, BRCA1/2-mutated, newly diagnosed advanced ovarian cancer (36). This study estimated that the addition of olaparib maintenance treatment led to a remarkable increase in median PFS of approximately 3 years compared to the placebo group (36). In 2018, the FDA approved olaparib for use in this context (35). The efficacy of niraparib treatment was similarly tested in women with newly-diagnosed, platinum-sensitive advanced ovarian cancer (the PRIMA/ENGOT-OV26/GOG-3012 trial, NCT 02655016) (37). In the overall study population, the niraparib-treated group demonstrated a significant improvement in PFS, with a median of 13.8 months (compared to 8.2 months in the placebo group). Similar to studies done in the recurrent setting as described above, investigators also analyzed the effects of niraparib treatment in a subgroup of the patients, who had tumors with homologous recombination deficiency (HRD); once again, this cohort experienced an even more substantial benefit from niraparib treatment, with median PFS increasing from 10.4 months in the placebo group to 21.9 months in the niraparib-treated group (37). A third PARPi, veliparib, was also investigated in this setting. The VELIA/GOG-3005 trial (NCT02470585) tested the addition of veliparib both to first-line induction chemotherapy (carboplatin and paclitaxel) and continued as maintenance therapy in newly-diagnosed advanced ovarian cancer (38). In the overall study population, patients receiving the veliparib-containing regimen demonstrated a significantly improved median PFS of 23.5 months, up from 17.3 months for those receiving the induction chemotherapy alone (38). Once again, patient cohorts with BRCA1/2 mutations (median

PFS of 34.7 months vs. 22 months in the control group) or HRD (31.9 months compared to 20.5 months for the control group) showed the greatest increase in PFS upon the addition of PARPi (38). Taken together, these clinical trials support the use of PARPi—namely olaparib, niraparib, and veliparib—as maintenance treatment in newly-diagnosed advanced ovarian cancer, regardless of BRCA1/2 mutation or HRD status.

In addition to use as a monotherapy in the maintenance setting, PARPi are being investigated in combination with other non-chemotherapeutic agents. Recently, results were published from the PAOLA-1 trial (NCT02477644), which combined olaparib with bevacizumab, an agent which targets vascular endothelial growth factor (VEGF) to interfere with tumor vascularization (39). Patients with newly diagnosed, advanced ovarian cancer who responded to first-line chemotherapy plus bevacizumab were placed on bevacizumab maintenance therapy with or without maintenance olaparib. Treatment with olaparib yielded a median PFS of 22.1 months, a significant improvement over the placebo group for which median PFS was 16.6 months (39). Strikingly, patients with tumors demonstrating HRD (which included BRCA1/2-mutant tumors) showed even greater gains in PFS, with median PFS increasing from 17.7 months with placebo to 37.2 months upon the addition of olaparib. BRCA1/2 mutations were not the only drivers of this effect, as patients with HRD-positive tumors that did not have mutations in BRCA1 or 2 also benefitted from olaparib treatment, with median PFS of 28.1 months in the olaparib group compared to 16.6 months in the placebo group (39). PARPi are also being tested in combination with modulators of the immune response to tumors, including anti-PD-1 and anti-PD-L1 monoclonal antibodies, however the data are not yet mature (Table 1.2). Furthermore, clinical trials are underway to test the use of PARPi, both as a single agent as well as in combination with anti-VEGF or anti-PD-1 therapy, as a chemotherapy-free approach to treat recurrent disease rather than as a maintenance drug (Table 1.2).

1.4.2 Use of PARPi in the treatment of non-ovarian cancer

There are many Phase III clinical trials evaluating the efficacy of PARPi against tumor types other than ovarian cancers; one major area of research is breast cancer, once again owing to the relationship between BRCA1/2 deficiency, breast cancer, and PARPi sensitivity (Table 1.3). The OlympiAD trial (NCT02000622) enrolled patients with human epidermal growth factor receptor type 2 (HER2)-negative metastatic breast cancer and germline mutations in BRCA1 or 2, and evaluated the efficacy of olaparib monotherapy versus standard chemotherapy. Investigators found that in this population of patients, olaparib treatment significantly improved median PFS, from 4.2 months for those receiving standard chemotherapy, to 7.0 months for those receiving olaparib monotherapy (40). Despite this promising increase in PFS, there was not a significant difference in overall survival (OS) between the two groups (41). However, patient surveys indicated that the cohort receiving olaparib treatment experienced a consistent improvement in health-related quality of life (42). Talazoparib was also evaluated in a similar context in the EMBRACA trial (NCT01945775). In this study, talazoparib treatment provided a significant improvement in median PFS (8.6 months vs 5.6 months in group receiving standard chemotherapy) in patients with advanced breast cancer and germline mutations in BRCA1/2 (43). Furthermore, analysis of patient-reported outcomes revealed that whereas quality of life scores for patients in the standard chemotherapy cohort showed a significant decline over the treatment period, these scores showed a significant improvement over time in the group receiving talazoparib (44). Ultimately, the FDA approved olaparib and talazoparib for the treatment of advanced or metastatic HER2-negative breast cancer in patients with a deleterious germline BRCA1/2 mutation (35, 45). However, results of trials investigating PARPi in breast cancer treatment were not universally positive. The BrighTNess trial (NCT02032277), which tested the addition of veliparib to treatment with carboplatin and

paclitaxel in patients with triple negative breast cancer, found no difference in the proportion of patients achieving a pathological complete response between the veliparib-containing regimen and controls (46).

Table 1.3. Phase III clinical trials evaluating PARPi in non-ovarian cancers

Cancer site	Other inclusion criteria	PARPi	Clinical Trial #	Study Start
Brain	Glioblastoma multiforme, newly diagnosed, tumor MGMT promoter hypermethylation	Veliparib	NCT02152982	2014
Breast	Germline BRCA1/2 mutated	Niraparib	NCT01905592	2013
	Germline BRCA1/2 mutated	Olaparib	NCT02032823	2014
	Germline BRCA1/2 mutated, metastatic	Olaparib	NCT02000622	2014
	HR-deficient, newly diagnosed Stage III	Olaparib	NCT02810743	2017
	BRCA1/2 mutated, metastatic	Olaparib	NCT03286842	2018
	Triple-negative and/or germline BRCA1/2-mutated	Olaparib	NCT03150576	2019
	Triple-negative, newly diagnosed, inoperable	Olaparib	NCT04191135	2020
	Advanced/metastatic, germline BRCA1/2-mutant	Talazoparib	NCT01945775	2013
	Advanced/metastatic, BRCA1/2-mutant, HER2-neg	Veliparib	NCT02163694	2014
	Triple-negative, newly diagnosed	Veliparib	NCT02032277	2014
Gastric	Advanced Stage	Olaparib	NCT01924533	2013
	Platinum-sensitive, advanced/metastatic	Pamiparib	NCT03427814	2018
Lung	Small cell, Extensive stage	Niraparib	NCT03516084	2018
	Newly diagnosed, metastatic, squamous non-small cell	Olaparib	NCT03976362	2019
	Newly diagnosed, metastatic, nonsquamous non-small cell	Olaparib	NCT03976323	2019
	Recurrent, Stage IV, Squamous cell, HR-deficient	Talazoparib	NCT02154490	2014
	Newly diagnosed, advanced/metastatic, squamous non-small cell	Veliparib	NCT02106546	2014
	Advanced/metastatic, nonsquamous non-small cell, history of smoking	Veliparib	NCT02264990	2014
Not specified	Advanced malignancy, enrolled in BeiGene parent study	Pamiparib	NCT04164199	2019
Pancreas	Germline BRCA1/2 mutated, metastatic	Olaparib	NCT02184195	2014
Prostate	Metastatic	Niraparib	NCT03748641	2019
	Metastatic, castration-resistant, HR-mutant	Olaparib	NCT02987543	2017
	Newly diagnosed, metastatic, castration-resistant	Olaparib	NCT03732820	2018
	Metastatic, castration-resistant	Olaparib	NCT03834519	2019
	Metastatic, castration-resistant, BRCA1/2 or ATM mutant	Rucaparib	NCT02975934	2017
	Metastatic, castration-resistant	Talazoparib	NCT03395197	2017
Sarcoma	Soft-tissue; advanced or metastatic	Olaparib	NCT03784014	2019

Phase III clinical trials were also initiated to investigate the effect of PARPi in many other types of cancer. Results were underwhelming from a clinical trial investigating the addition of olaparib to paclitaxel as second-line therapy in Asian adults with advanced gastric cancer (NCT01924533), which showed no difference in overall

survival upon olaparib treatment (47). However, results were much more positive from the POLO trial (NCT02184195), which evaluated olaparib maintenance treatment in patients with newly-diagnosed, platinum-sensitive metastatic pancreatic cancer and a germline mutation in BRCA1/2. In this study, olaparib treatment significantly improved PFS from 3.8 months in the placebo group to 7.4 months, while preserving quality of life (48, 49). Just this week (December 27, 2019), the FDA approved olaparib for use in these patients (35). Trials are also underway in patients with lung and prostate cancers, as well as in those with rare tumor types such as glioblastoma multiforme and soft-tissue sarcoma (Table 1.3).

Given the impressive success of PARPi in many of these populations of patients, there is great interest in identifying cohorts of BRCA1/2-proficient patients who may be able to benefit from this therapy, as well (50). However, even though a large number of patients experience great clinical benefit from PARPi treatment, a significant subpopulation either do not respond or quickly develop resistance to PARPi, despite being predicted to be sensitive based on their BRCA1/2 status (29, 51). In light of this, efforts have been made to better understand the mechanisms underlying the efficacy of PARPi, as well as to characterize the roles of individual proteins in mediating resistance to PARPi in the background of BRCA1/2 deficiency.

1.5 Proposed Mechanisms of Action of PARPi, and corresponding reported mechanisms of PARPi resistance

As described in previous sections, inhibition of PARP1 has proven to be synthetically lethal with proteins causing homologous recombination deficiency, including BRCA1 and BRCA2 (52, 53). However, the specific details underlying this synthetic lethality have remained elusive. In fact, both arms of this interaction have been controversial: 1) Which effects of PARP inhibition make these agents effective against

BRCA2 deficient cells? and 2) Which functional defects caused by depletion of HR proteins sensitizes cells to PARP inhibition? Here, I discuss mechanisms which have been proposed to contribute to the synthetic lethality observed between HR deficiency and PARPi (Table 1.4). Notably, these mechanisms are not in all cases mutually exclusive and it is likely that multiple mechanisms are responsible for this phenomenon. Furthermore, for each mechanism of cytotoxicity, I review mechanisms through which BRCA1/2-deficient cells may demonstrate resistance to PARPi.

Table 1.4. Major mechanisms of PARPi cytotoxicity & resistance

Proposed Mechanism of Cytotoxicity	Related Resistance Mechanisms*

Accumulation of double-strand breaks	• Reversion mutations in BRCA1/2
	• Restoration of HR via E2F7 depletion (Chapter 3)
	• Modulation of end resection/pathway choice
	  ○ 53BP1 loss in BRCA1-deficient cells
	  ○ Shieldin loss in BRCA1-deficient cells
	  ○ Loss of CST complex in BRCA1-deficient cells
	  ○ DYNLL1/ASCIZ loss in BRCA1-deficient cells
	  ○ TIP60 loss in BRCA2-deficient cells (Chapter 4)

Trapping of PARP1	• Mutations in PARP1 • Loss of PARG in BRCA2-deficient cells
Replication fork degradation	• Depletion of PTIP • Loss of EZH2 • Depletion of RADX • Loss of ZRANB3/HLTF/SMARCAL1

*See text in Section 1.5 for descriptions of mechanisms and citations.

1.5.1 Proposed model: PARP1 inhibition causes persistence of single-strand breaks, which are converted to double-strand breaks that are unable to be repaired in HR-deficient cells.

PARP1 is critical for efficient repair of single-strand DNA breaks (54–56). Accordingly, the rationale behind initially testing PARPi in BRCA1/2-deficient cells was based on the hypothesis that PARP1 inhibition would prevent the repair of single-strand breaks (SSBs), which would persist and be converted during replication to one-ended double-strand breaks (DSBs) toxic to HR-deficient cells (23, 24). Results from these

initial studies were consistent with this hypothesis. They found that PARPi treatment induced formation of gamma-H2AX foci in both wildtype and BRCA1/2 mutant cells, and from this suggest that DSBs are similarly formed regardless of BRCA status (23, 24). Furthermore, RAD51 foci were formed in BRCA1/2-wildtype cells upon PARPi treatment, suggesting the formation of lesions typically repaired by HR (23, 24). PARPi treatment led to an increase in chromatid breaks and radial chromosomes in BRCA1/2-mutant, but not -wildtype, cells, suggesting more error-prone repair in BRCA1/2-mutant cells (24). Collectively, these findings support the proposed model in which PARPi treatment leads to the production of DSBs which would be repaired through HR. However, although classically considered to be a marker of DSBs, gamma-H2AX foci may be induced by other types of damage, such as single-strand breaks or replication stress (57, 58). Thus, although formation of DSBs may explain these findings, alternative pathways may cause similar results. Furthermore, the above experiments do not address the cause of the proposed DSBs. To address this, the authors hypothesized that if defects in SSB repair were the cause of the DSBs and ultimately of cytotoxicity, depletion of other critical SSB repair proteins would cause similar results; indeed, XRCC1-deficient cells also showed increased gamma-H2AX and RAD51 foci in BRCA-wildtype cells, supporting the concept that SSB repair defects could result in lesions that are normally repaired by HR (23). However, the authors did not present results addressing if XRCC1 depletion is also synthetically lethal with BRCA1/2 deficiency, which is crucial to support the claim that this is the mechanism of cytotoxicity. Interestingly, this question was later addressed in a separate study, which found that in fact, depletion of XRCC1 did not reduce viability of BRCA2-deficient cells (54, 59). Additionally, others have unexpectedly reported that PARP1 knockdown or inhibition is not associated with any detectable increase in SSBs, despite a critical role for the protein in SSB repair (54, 60, 61). Overall, this model is only partially supported by the literature: while these findings are consistent with the induction

of DSB formation by PARPi treatment, DSB-independent roles of BRCA1/2, RAD51, and gamma-H2AX may also be consistent with these results. Furthermore, if DSB formation ultimately does contribute, it seems unlikely that SSB repair defects caused by loss of PARP1 catalytic activity contribute to the cytotoxicity caused by PARPi treatment in BRCA-deficient cells.

1.5.2 Restoration of DSB repair as a mechanism of PARPi resistance in BRCA1/2-deficient cells

Defects in DSB repair as a mechanism underlying the synthetic lethality observed between BRCA1/2-deficient cells and PARPi is further supported by many studies connecting restoration of DSB repair with PARPi resistance. In fact, reversion mutations restoring the function of mutant BRCA1 or BRCA2 and subsequently correcting the HR defects are frequently identified as underlying mechanisms of PARPi resistance in patients (50, 62). Independent of reversion mutations, restoration of HR through modulation of end resection at the DSB is an extensively studied mechanism of resistance to PARPi, specifically in BRCA1-deficient cells (63). This has been observed specifically in BRCA1, but not BRCA2, deficient cells, due to the distinct roles for each protein in HR—BRCA1 functions early on, promoting the end resection step—therefore BRCA1 deficiency can be corrected for by reducing anti-resection factors (64). In particular, loss of 53BP1 in BRCA1-deficient cells was shown to restore the defects in HR and rescue sensitivity to PARPi (Figure 1.2) (65, 66). Subsequently, factors upstream or downstream of 53BP1 were found to have similar effects. In particular, the shieldin complex, composed of SHLD1 (also known as C20orf196 or RINN3), SHLD2 (FAM35A or RINN2), SHLD3 (CTC-534A2.2 or RINN1) and REV7, was recently identified as a downstream effector complex of 53BP1, and depletion of Shieldin components resulted in PARPi resistance in BRCA1-deficient cells (67–71). Additionally,

another potential effector complex downstream of 53BP1, the CTC1-STN1-TEN1 (CST) complex, was recently identified, and depletion of these proteins restored end resection and rescued PARPi sensitivity in BRCA1-deficient cells (72). Finally, loss of DYNLL1 or its transcriptional regulator ASCIZ increased end resection and HR and also caused PARPi resistance in BRCA1-deficient cells (73–76), although whether this axis acts as a regulator (73) or effector (74) of 53BP1 remains controversial. Altogether, modulation of end resection to restore HR in BRCA1-deficient cells is a well-established mechanism of PARPi resistance.

1.5.3 Proposed model: "Trapping" of PARP1 on DNA, rather than loss of PARP1 catalytic activity, is the main consequence of PARP inhibition responsible for cytotoxicity.

PARP1 is activated by binding to sites of SSBs and DSBs, where it functions to modify target proteins with poly-ADP-ribose (PAR) chains to orchestrate the repair response (77). Importantly, PARP1 itself is a substrate of its own enzymatic activity, and ultimately the negative charge accumulated due to extending PAR chains on PARP1 leads to repulsive forces with DNA and release of the enzyme from the break site (77). Thus, it was hypothesized that PARP inhibitors would not only prevent the catalytic activity of PARP1, but also result in the formation of PARP1-DNA complexes owing to the binding, but not release, of PARP1 on damaged DNA—termed "PARP trapping" (54, 78). Although this phenomenon had been previously proposed, Murai *et al*. first detected increased PARP1 present on chromatin after PARPi treatment using chromatin fractionation assays, and further suggested that PARP1 is trapped not only due to catalytic inhibition, but also due to the inhibitors allosterically promoting stabilization of PARP1 on the DNA (78). This model is supported by later publications demonstrating that the cytotoxicity of various PARPi may correlate more with the PARP-trapping ability

of the inhibitor rather than the efficacy of catalytic inhibition (79, 80). Subsequent studies visualized PARP trapping using microscopy-based single-cell analyses, and supported the contribution of PARP trapping to cytotoxicity (81, 82). Additionally, PARP trapping could explain the observations that PARP1 is required for the cytotoxicity of PARP inhibitors (79, 83, 84), and that PARP inhibition is more cytotoxic than depletion of PARP1 protein (23, 24). Still, the fact that depletion of PARP1 protein does yield synthetic lethality in BRCA-mutant cells demonstrates that loss of PARP1 function also contributes to cytotoxicity, and PARP trapping is not the exclusive mechanism. Importantly, exactly how trapped PARP1 contributes to cytotoxicity is not known, although it is hypothesized to be associated with replication (54, 81). Altogether, this evidence supports PARP1 trapping as an important mechanism of the cytotoxicity of PARPi, together with loss of PARP1 catalytic activity; however, additional research is needed in order to determine the processes connecting trapping to cell death.

1.5.4 Modulation of PARP1 activity and trapping as a mechanism of PARPi resistance

Consistent with PARP trapping as an important mechanism of cytotoxicity, perturbations that reduce trapped PARP1 have been connected to PARPi resistance (85). For example, in one recent study, the investigators performed a CRISPR/Cas9 mutagenesis screen to identify mediators of PARPi resistance; of 24 resistant clones identified, 9 clones contained guide RNAs targeting PARP1 (86). Eight of these nine clones demonstrated loss of the PARP1 protein, consistent with other reports that depletion of PARP1 causes PARPi resistance (79, 83, 84). Further analysis of the ninth clone revealed two in-frame mutations in PARP1, which abolished binding of PARP1 to chromatin, thus alleviating PARP trapping (86). In light of these findings, the investigators performed a focused CRISPR mutagenesis screen, designed to produce

in-frame mutations in PARP1. Analysis of PARP1 mutations conferring resistance identified PARP1 residues essential for PARPi sensitivity. Interestingly, they found that many PARP1 mutations that caused PARPi resistance altered PARP1 trapping, but not catalytic activity (86). Additionally, a mutant form of PARP1, which demonstrated reduced PARP trapping ability, was isolated from cells derived from an ovarian cancer patient showing clinical resistance to PARPi treatment (86). Poly-ADP-ribose glycohydrolase (PARG) degrades PAR chains, therefore counteracting PARP1 activity (85). Recently, one study showed that loss of PARG in BRCA2-deficient cells led to PARPi resistance, restored catalytic activity of PARP1 and reduced the accumulation of PARP1-DNA complexes (87). Thus, these studies indicate that the amelioration of PARP trapping is a mechanism of resistance to PARPi.

1.5.5 Proposed model: Degradation of nascent DNA at stalled replication forks in BRCA1/2- deficient cells contributes to the cytotoxicity of PARPi.

As mentioned in Section 1.2, BRCA1 and BRCA2 have several other functions apart from their classical roles in homologous recombination. Schlacher et *al*. sought to investigate the role of BRCA2 at replication forks stalled by treatment with hydroxyurea (HU) (88). Surprisingly, they found that BRCA2 acts to protect newly replicated DNA at stalled replication forks, rather than to repair damage after fork collapse. This was based on the observation nascent DNA tracts were degraded after HU treatment in BRCA2-deficient hamster cells, or in cells containing BRCA2 mutated at the RAD51 binding site within the BRCA2 C-terminal region (Figure 1.3) (88). Importantly, mutations in this domain compromise the stability of stalled replication forks, but not the role of BRCA2 in HR, suggesting that these functions are distinct. Furthermore, the data show that the nuclease MRE11 is responsible for this degradation of nascent DNA at stalled forks in

BRCA2-deficient cells (88). Further studies confirmed this fork degradation phenotype, and showed that another nuclease, MUS81, contributes to degradation.(89–91)

Interestingly, fork degradation was not originally proposed as a mechanism of PARPi cytotoxicity. In fact, in the original study by Schlacher et *al.*, the authors tested whether this fork degradation phenotype affected cellular survival by treating cells with BRCA2-deficiency, or cells expressing BRCA2 with a mutation in the domain responsible for fork protection, with HU. They found that HU treatment did not cause any significant impact on survival, despite an observed increase in fork degradation and chromosomal aberrations (88). Importantly, Schlacher et al. also tested the sensitivity of BRCA2-deficient cells, which are defective in both HR and fork protection, as well as cells expressing the mutant BRCA2 which results in defective fork protection but preserved HR, to PARPi treatment. While the BRCA2-deficient cells were profoundly sensitive to olaparib treatment (less than 5% of cells surviving at a dose of 1.5 μM), cells corrected with wildtype BRCA2 or mutant BRCA2 (which caused fork degradation but preserved HR) were resistant to olaparib, with more than 80% of cells surviving at 1.5 μM olaparib (88). Furthermore, while BRCA2-deficient cells demonstrate fork protection defects upon HU-induced replication fork stalling, the validity of fork degradation as a mechanism of cytotoxicity of PARPi would depend on PARPi similarly causing stalled replication forks. However, in a recent study, PARPi treatment in BRCA1-deficient cells did not lead to an increase in replication fork stalling (92). Still, despite this evidence, replication fork degradation as a mechanism explaining the cytotoxicity of PARPi in BRCA-deficient cells has remained widely regarded in the field for years, propelled by the well-established observation that protein perturbations which cause replication fork protection are often associated with resistance to PARPi as described in the next section.

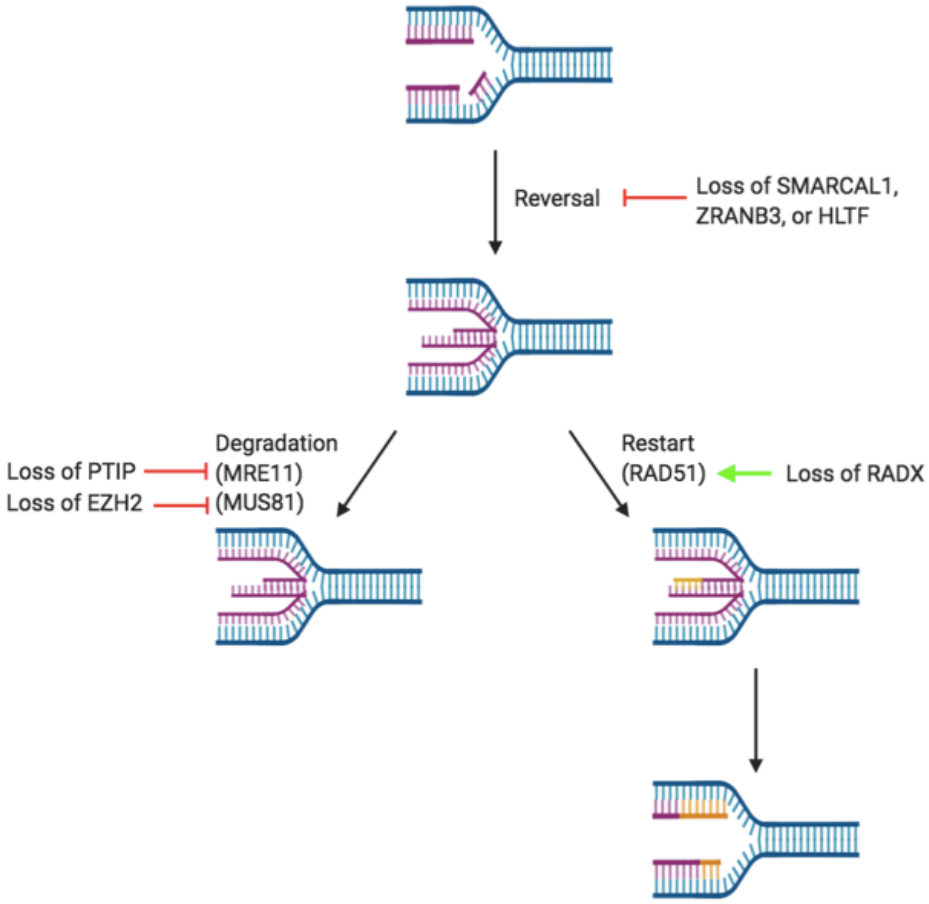

Figure 1.3. Schematic representation of replication fork degradation in PARPi sensitivity. As described in the text, stalled replication forks are susceptible to degradation in BRCA2-deficient cells. Replication fork protection and restart are associated with PARPi resistance. Proteins whose loss is implicated in conferring PARPi resistance through these mechanisms are indicated (described in detail in Section 1.5.6).

1.5.6 Fork protection as a mechanism of PARPi resistance

Several different proteins have been shown to rescue both fork degradation upon HU treatment as well as PARPi sensitivity in BRCA1/2- deficient cells (Figure 1.3). The first group to establish this relationship demonstrated that depletion of PTIP reduces recruitment of MRE11 to stalled replication forks, thus preventing degradation (93). Additionally, PTIP depletion reduced PARPi-induced chromosomal aberrations in BRCA2-deficient cells (93). Similarly, EZH2 depletion led to stabilization of stalled

replication forks, but not HR, by reducing recruitment of MUS81, and also rescued the cytotoxicity caused by PARP inhibition in BRCA2- deficient cells (91, 94). Dungrawala et *al*. characterize a novel protein, RADX, which binds to single-strand DNA at stalled replication forks, thereby antagonizing RAD51 and regulating fork processing (95). Depletion of RADX in BRCA2-deficient cells rescued fork protection, but not HR, and was associated with PARPi resistance (95). Finally, loss of SNF2 family fork remodelers including ZRANB3, HLTF, and SMARCAL1 in BRCA1/2-deficient cells restores fork protection as well as improves replication stress-induced DNA damage and chromosomal instability (96). Thus, the association between response to HU-induced replication fork stalling and PARPi response is well- established, and fork protection remains an extremely valuable predictor/ potential biomarker for PARPi response, although fork protection as a true **cause** of PARPi resistance remains to be definitively shown.

1.5.7 Proposed model: PARPi-induced increase in replication fork speed contributes to PARPi cytotoxicity

Recently, a new potential mechanism of cytotoxicity was proposed for PARPi: that PARPi treatment leads to an aberrant increase in replication fork speed (92). Specifically, the Maya-Mendoza et *al.* show that treatment with PARPi for 24 hours led to a 60% increase in replication fork speed as measured using the DNA fiber combing assay, as well as an accumulation of cells in mid-to-late S or G2 phases (92). They also report that PARPi treatment caused replication stress and the activation of the DNA damage response as evidenced by gamma-H2AX, RAD51, RPA, and 53BP1 foci and phosphorylated RPA and CHK1. Further experiments led to the conclusion that the threshold of the increase in replication fork speed required for DDR induction was a 40% increase from baseline (92, 97). The authors propose that these phenotypes are

governed by a “fork speed regulatory network” in which PARylation by PARP1 acts as a sensor of replication stress at ongoing forks, keeping speed in check; speed is also restrained by p21, which is transcriptionally downregulated by PARP1 (Figure 1.4) (92, 97). In their model, PARPi leaves replication fork speed unchecked, as PARylation is inhibited, but the transcriptional repression of p21 via PARP1 is still intact; PARP1 knockdown prevented the increase in fork speed and DDR caused by PARPi by increasing p21 levels. Supporting a role for the PARP1-p21 axis proposed, PARP1 knockdown in HeLa cells, which have low p21 expression, did not produce an increase in p21 or prevent PARPi-induced increase in fork speed (92). However, the relationship between these phenotypes and cytotoxicity is not clear, as experiments involving cellular viability or death in this study were extremely limited. In fact, according to the proposed model, if an aberrant increase in replication fork speed underlies PARPi cytotoxicity, one would expect that depletion of PARP1 in HeLa cells would not rescue PARPi sensitivity, as it did not affect replication fork speed in this cellular background. However, our lab and others have shown that mutations or depletion of PARP1 in HeLa cells does, in fact, rescue PARPi sensitivity, challenging the extent to which this proposed mechanism contributes to cytotoxicity (86, 98). Finally, this study does not provide a clear explanation regarding why BRCA-deficient cells are more sensitive to PARPi than BRCA-wildtype cells; while the reported phenotypes were also observed in BRCA1-depleted U2OS and MDA-MB-436 (breast cancer) cells, the PARPi-induced increase in fork speed (above the 40% threshold) is seen in both BRCA-deficient and –wildtype cells (92). Overall, while this study provides an interesting and well-supported perspective on the effects of PARP inhibition on replication forks, the contribution of this mechanism to the cytotoxicity of PARPi is not clear.

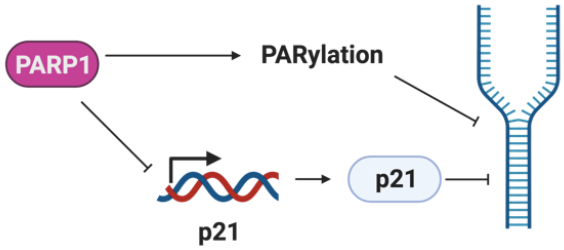

Figure 1.4. Overview of model proposed by Maya-Mendoza et al. Please see the text for details but briefly, the PARylation activity of PARP1 is important for replication fork slowing after replication stress. PARP1 also inhibits the expression of p21, a protein which also acts to appropriately restrain fork speed.

1.5.8 General mechanisms of PARPi resistance, not attributed to a particular model of cytotoxicity

Finally, mechanisms of PARPi resistance have been described which do not fall into any of the above described categories, as they do not relate to a specific proposed mechanism of cytotoxicity. One such resistance mechanism is disruption of the amount of PARPi available within the cell through upregulation of drug efflux pumps within the ABC transporter family (85). Overexpression of ABC transporters has been reported as a mechanism of PARPi resistance in mouse models of BRCA1-deficient or -wildtype tumors (99, 100), as well as a human ovarian cancer cell line (101) and even recently in breast and ovarian cancers from chemotherapy-treated patients (102). Another proposed mechanism of resistance is EMI1 depletion, which causes mitotic bypass (103). Schoonen et *al*. proposed that cells treated with PAPRi incur damage during DNA replication, which causes failure of DNA to properly segregate during mitosis, leading to more damage which ultimately results in lethality; thus, forced bypass of mitosis via depletion of EMI1 caused resistance to PARPi (103). Lastly, recent work has suggested

that activation of Wnt signaling and subsequent increase in activity of the transcription factor TCF (T-cell factor) contributes to PARPi resistance (104). Yamamoto et al. detected these changes in olaparib-resistant ovarian cancer lines, then confirmed that activation of Wnt signaling via overexpression of WNT3A led to PARPi resistance in a previously PARPi-sensitive ovarian cancer cell line.

1.6. Brief overview of dissertation

Overall, it is clear that despite a great deal of work and progress towards understanding the mechanisms underlying the cytotoxicity of PARPi as well as mechanisms of resistance, much remains uncertain. Additionally, despite showing great promise in clinical trials, identifying precisely which patients would benefit from PARPi therapy remains a challenge. In the following chapters, I present the results of three genome-wide CRISPR screens aimed at improving the understanding of mechanisms governing sensitivity and resistance to PARPi. Additionally, I further validate three hits from the screen—E2F7, HUWE1, and TIP60—and subsequently identify two novel mechanisms of PARPi resistance in BRCA2-deficient cells.

Chapter 2: CRISPR Knockout and Activation screens reveal mediators of PARPi resistance and sensitivity

Adapted from: Clements, K.E. et al. (2019) bioRxiv; and
Clements, K.E. et al. (2018) Nucleic Acids Res.

2.1 Rationale

Based on the laboratory and clinical data described in previous sections, it is clear that more than simply BRCA1/2 status determines the response to PARPi. A comprehensive, genome-wide characterization of potential mediators of PARPi sensitivity and resistance would both advance the fundamental understanding of the processes underlying these effects, as well as potentially promote more effective usage in the clinic. Genome-wide CRISPR (clustered regularly interspaced short palindromic repeats) screen technology has emerged as a powerful method for identifying essential genes as well as genetic determinants of drug sensitivity in human cell lines. In side-by-side comparisons, CRISPR screens have performed equally well or better than short hairpin RNA (shRNA) screen approaches (105–107). CRISPR screens have several advantages over shRNA screens, including more robust depletion of targets and reduced off-target effects, leading to more reproducible phenotypes and greater sensitivity (107–110).

Using CRISPR knockout (loss-of-function) screens, others have identified proteins which cause sensitivity to the PARPi olaparib when depleted in HR-proficient cells (82, 111). Additionally, several groups have employed CRISPR knockout screens to search for proteins which cause PARPi resistance when depleted in BRCA1-deficient cells (70, 72, 75). However, PARPi resistance in BRCA2-deficient cells has not been investigated using this technology. In order to better understand the mechanisms regulating cellular sensitivity and resistance to PARP inhibitors, we designed complementary genome-wide CRISPR screens in a pair of parental wildtype and

BRCA2-knockout (BRCA2^{KO}) HeLa cell lines. This approach allowed us to investigate which specific genetic changes lead to PARPi sensitivity in inherently resistant cells (parental) or to resistance in intrinsically sensitive cells (BRCA2^{KO}) in an otherwise isogenic background.

2.2 Results

In order to gain a broader understanding of factors governing PARPi response, I first created BRCA2-knockout HeLa cell lines using the CRISPR/Cas9 technology. BRCA2^{KO} cells lack any detectable full-length BRCA2 protein expression by western blot (Figure 2.1A) and have similar sensitivity to olaparib as parental cells treated with BRCA2-targeting siRNA (Figure 2.1B). I then used this isogenic pair of wildtype and BRCA2-knockout HeLa cell lines to perform a series of CRISPR knockout and transcriptional activation (overexpression) screens.

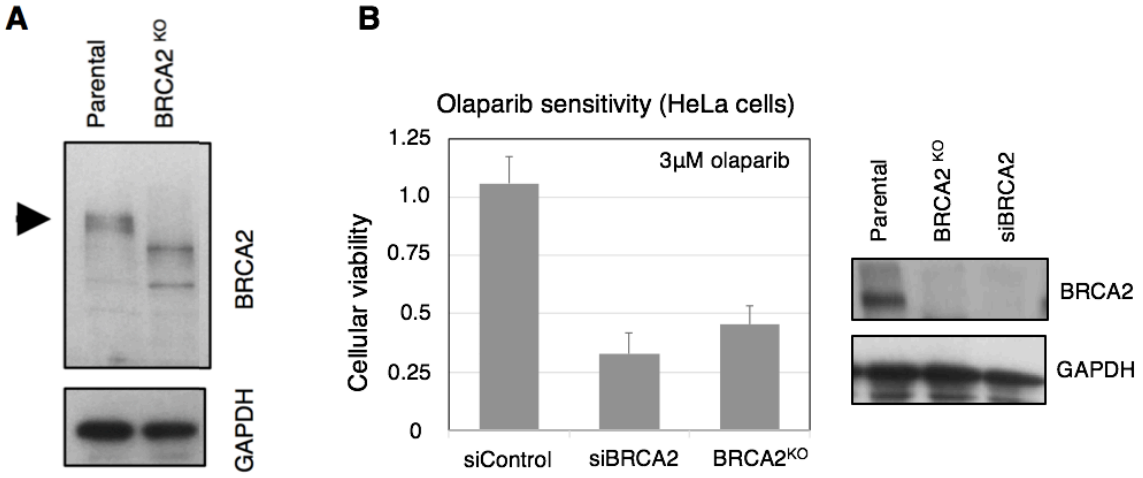

Figure 2.1. Generation and validation of a BRCA2-knockout HeLa cell line. (**A**) Western blot showing loss of full-length BRCA2 (indicated by an arrowhead) in HeLa cells with CRISPR/Cas9-mediated BRCA2 knockout. (**B**) BRCA2KO HeLa cells have similar olaparib sensitivity as HeLa cells treated with BRCA2 siRNA. Results are shown as normalized to control (no drug treatment) for each sample. The average of three biological replicates, with standard deviations as error bars, is shown.

2.2.1. CRISPR knockout screen identifies determinants of PARPi sensitivity in HeLa cells

To identify genetic changes which sensitize cells to PARPi treatment, I employed the Brunello human CRISPR knockout pooled library, which targets 19,114 genes with four single-guide RNAs (sgRNAs) per gene (112). HeLa cells infected with the Brunello library were divided into PARPi (5 μM olaparib)- or vehicle (DMSO)- treated arms, and after 4 days surviving cells were harvested for sgRNA sequencing and bioinformatic analysis (Figure 2.2A). By treating parental HeLa cells with a relatively low dose of olaparib and identifying sgRNA sequences which dropped out in the olaparib-treated arm as compared to the DMSO-treated arm, I was able to generate a list of genes which, when knocked out, sensitize wildtype cells to PARPi (Figure 2.2B). Importantly, RAD51, an essential component of the homologous recombination pathway, was one of the most significant hits from this screen. In addition, several RAD51 paralogs including RAD51B, XRCC3, and RAD51C were among the top hits; indeed, RAD51C loss via mutation or promoter hypermethylation in tumors has been connected to favorable PARPi response in patients (113). Other notable top hits include multiple RNase H2 subunits, consistent with previous findings implicating loss of RNase H2 in sensitizing HR-proficient cells to PARPi (82). Collectively, top hits were enriched for biological processes including homologous recombination, DNA replication, translational initiation, and DNA repair (Figure 2.2C).

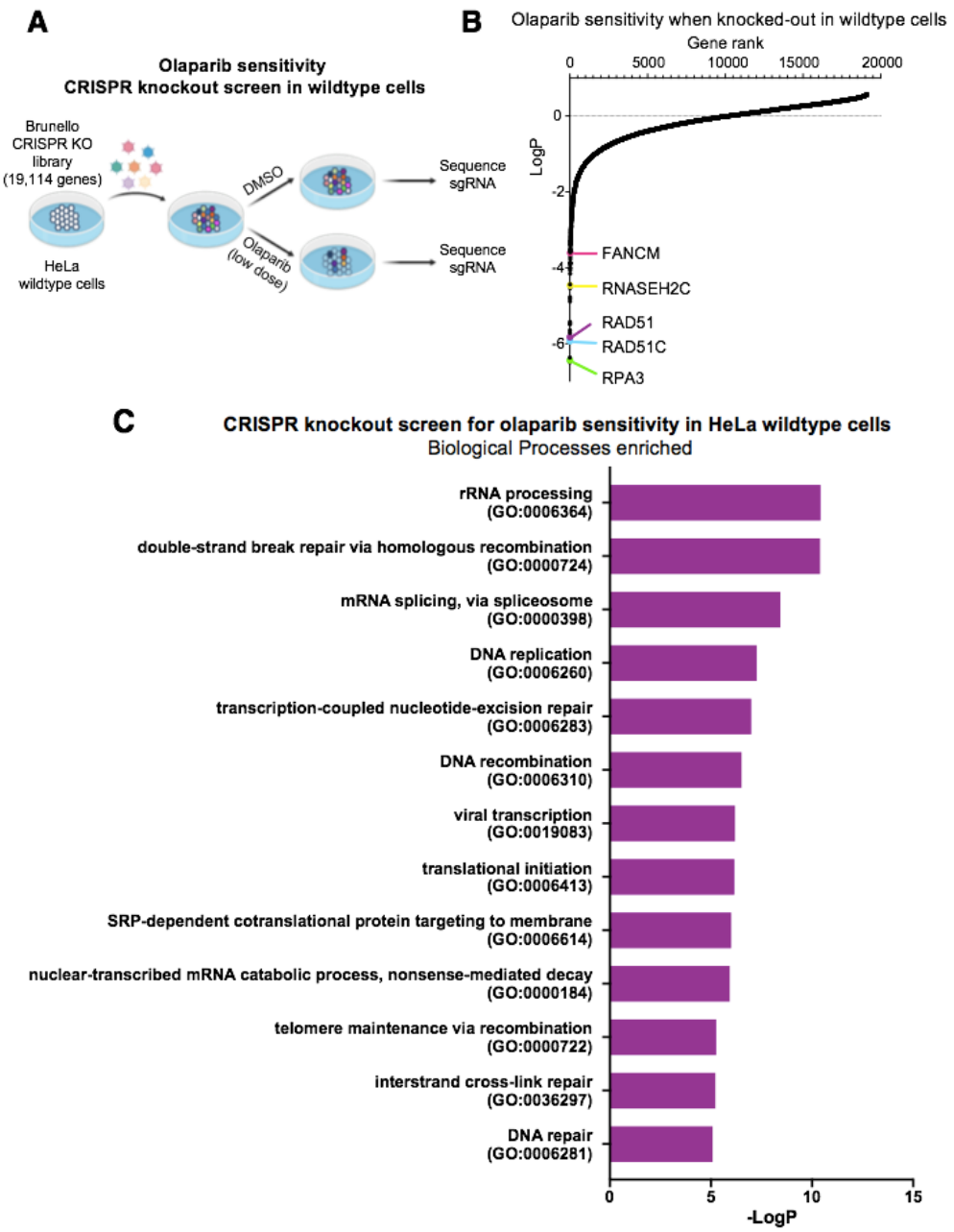

Figure 2.2. CRISPR knockout screen identifies determinants of PARPi sensitivity in HeLa cells. (A) Schematic representation of the screen. HeLa cells were infected with the Brunello CRISPR knockout library. Infected cells were divided into PARP inhibitor (olaparib) -treated or control (DMSO) arms. Genomic DNA was extracted from cells surviving the drug treatment and single-guide RNAs (sgRNAs) were identified using Illumina sequencing. **(B)** Scatterplot showing the results of this screen. Each gene targeted by the library was ranked according to P-values calculated using RSA analysis. The P-values are based on the fold change of the guides targeting each gene between the olaparib- and DMSO-treated conditions. Several biologically interesting hits are highlighted. **(C)** Gene ontology analysis of the top candidates from the CRISPR knockout screen for olaparib sensitivity in wildtype cells. Top hits with LogP less than or equal to -2 were entered into NIH DAVID and pathways were analyzed for Gene Ontology Biological Processes (GO_BP) terms. GO_BP terms with a logP of -5 or lower are shown.

2.2.2. CRISPR knockout screen identifies determinants of PARPi resistance in BRCA2-knockout HeLa cells

Next, I sought to identify genes which cause PARPi resistance when depleted in $BRCA2^{KO}$ cells. To identify resistant cells, I treated CRISPR knockout library-infected $BRCA2^{KO}$ cells with a dose olaparib (4 μM) which killed more than 90% of cells over 4 days (Figure 2.3A). Then, I searched for sgRNA sequences which were enriched in the cells surviving olaparib treatment as compared to DMSO (Figure 2.3B). It has been well-established in previous studies that PARP1 itself is required for the cytotoxicity of PARPi (78, 114, 115). In line with this, I found that PARP1 was ranked among the most significant of hits in my screen, as well (Figure 2.3B). Further investigations of novel hits from this screen, namely E2F7, TIP60, and HUWE1, are developed in the following chapters (Chapters 3 and 4). Unlike as seen in the sensitivity screen, the pathway analysis of the resistance screen implicated more unexpected pathways such as vesicle-mediated transport and tRNA processing in PARPi resistance (Figure 2.3C). While this finding could reflect a role for these pathways in PARPi resistance, an alternative explanation may be that proteins in these pathways have heretofore underappreciated roles in DNA repair.

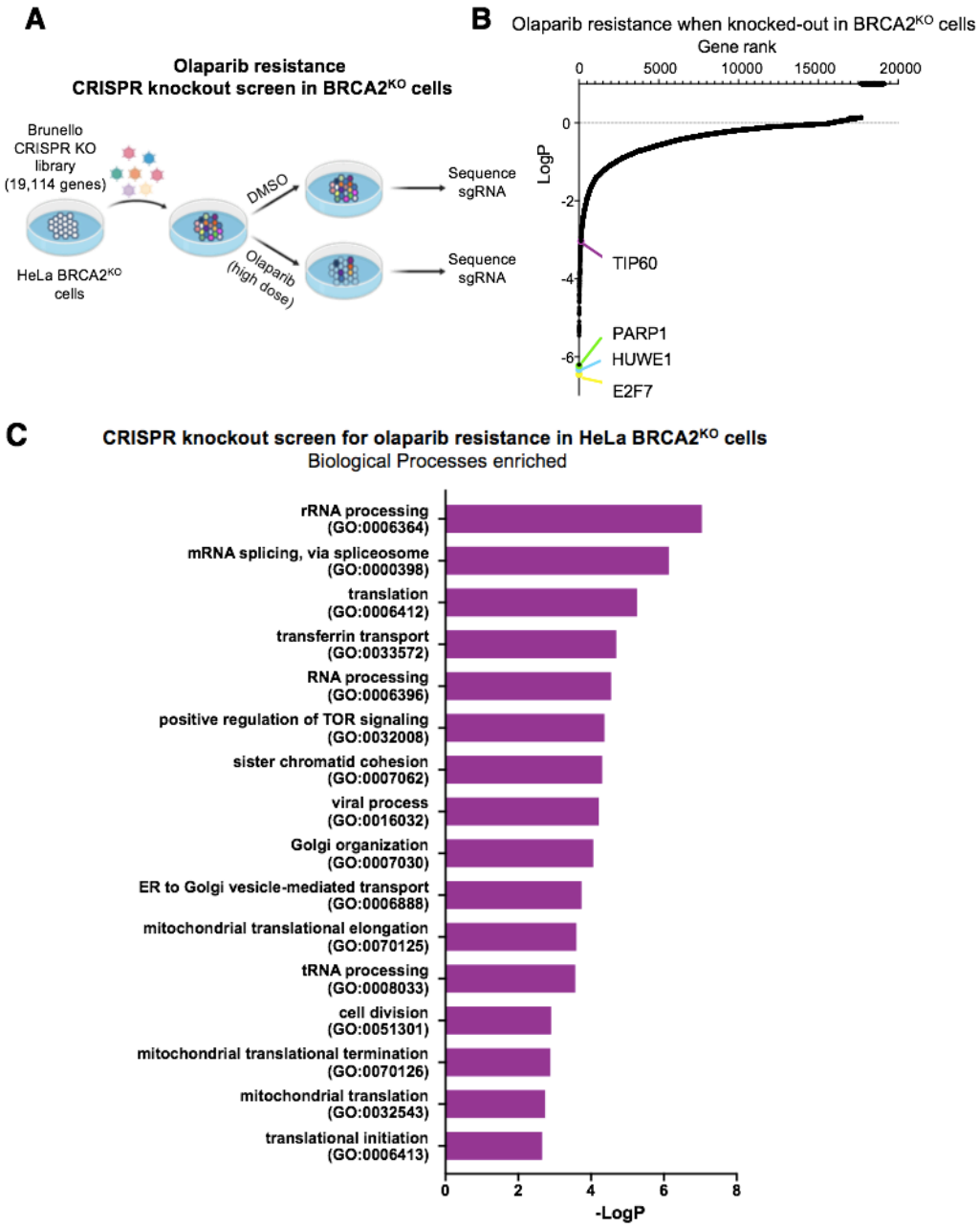

Figure 2.3. CRISPR knockout screen identifies determinants of PARPi resistance in BRCA2-knockout HeLa cells. (A) Schematic representation of the CRISPR knockout screen for olaparib resistance in BRCA2^{KO} cells. HeLa BRCA2^{KO} cells were infected with the Brunello CRISPR knockout library. Infected cells were divided into PARP inhibitor (olaparib) -treated or control (DMSO) arms. **(B)** Scatterplot showing the results of this screen, with several biologically interesting hits highlighted. **(C)** Gene ontology analysis of the top candidates from the CRISPR knockout screen for olaparib resistance in BRCA2^{KO} cells. Top hits with LogP less than or equal to -2 were entered into NIH DAVID and pathways were analyzed for GO_BP terms. GO_BP terms with a logP of -2.5 or lower are shown.

2.2.3. CRISPR activation screen identifies determinants of PARPi resistance in BRCA2-knockout HeLa cells

Finally, I performed a CRISPR activation screen to identify genes which cause PARPi resistance when overexpressed in BRCA2^{KO} cells. I utilized the Calabrese human CRISPR activation library, which transcriptionally activates 18,885 genes individually by using guide RNA sequences to recruit an enzymatically dead Cas9 (dCas9) and transcriptional activators to the region near the transcriptional start site of the gene (116). Screening conditions were maintained as performed in the resistance CRISPR knockout screen. Briefly, HeLa BRCA2^{KO} cells expressing dCas9 were infected with the activation library and divided into high dose PARPi (4 μM olaparib)- or vehicle (DMSO)-treated arms (Figure 2.4, Figure 2.5A). Roughly 90% of cells were killed after 4 days of treatment; surviving cells were harvested and analyzed to identify genes which cause resistance to PARPi when transcriptionally activated (Figures 2.5 B and C).

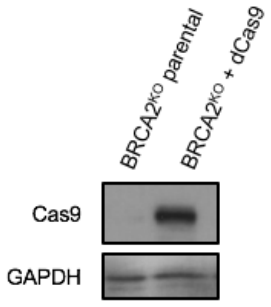

Figure 2.4. Western blot confirming expression of dCas9 in HeLa BRCA2^{KO} cells.

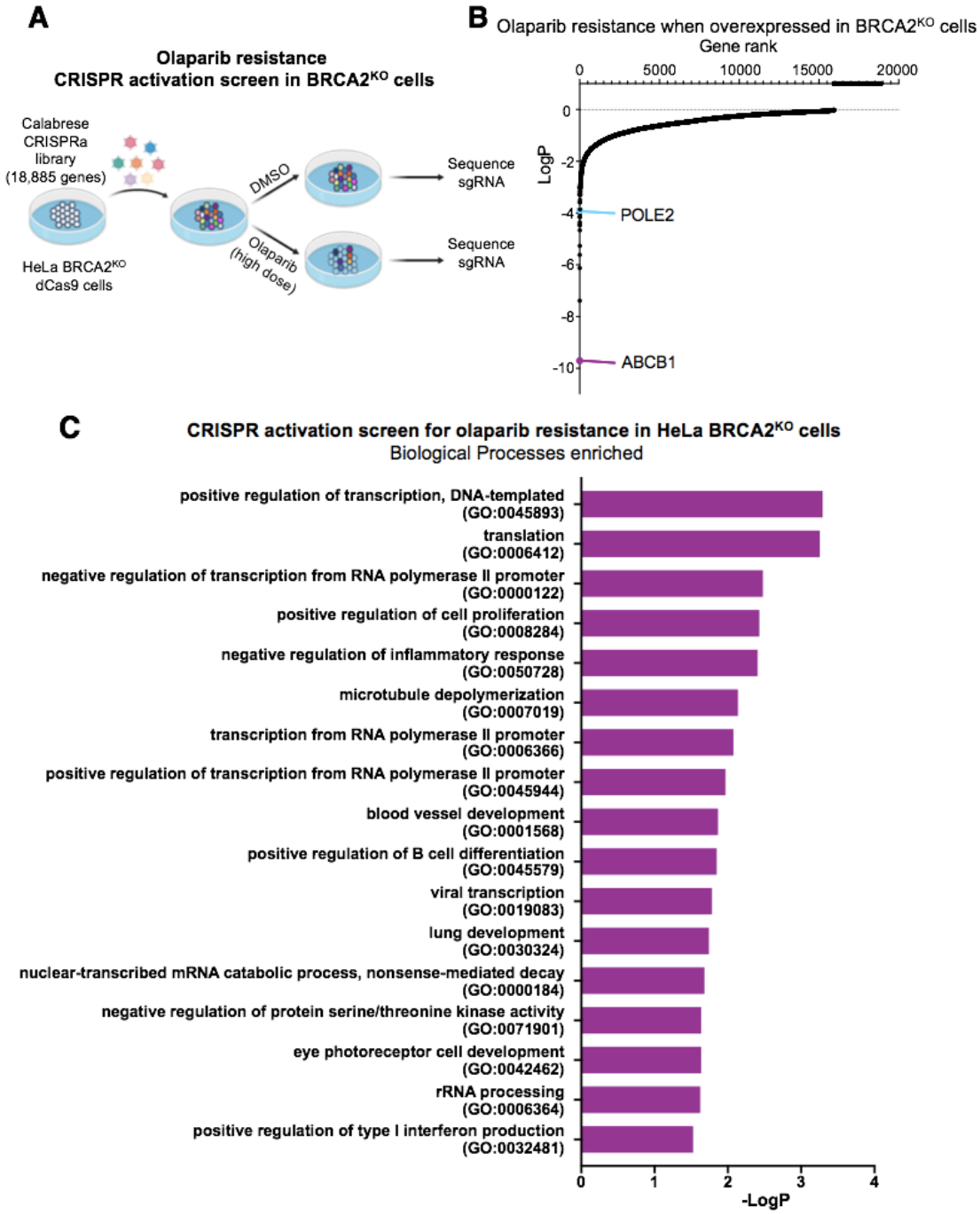

Figure 2.5. CRISPR activation screen identifies determinants of PARPi resistance in BRCA2-knockout HeLa cells. (A) Schematic representation of the CRISPR activation screen for olaparib resistance in BRCA2^{KO} cells. HeLa BRCA2^{KO} cells stably expressing the modified dCas9 enzyme were infected with the Calabrese CRISPR activation library. Infected cells were divided into PARP inhibitor (olaparib) -treated or control (DMSO) arms. **(B)** Scatterplot showing the results of this screen, with several biologically interesting hits highlighted. **(C)** Gene ontology analysis of the top candidates from the CRISPR activation screen for olaparib resistance in BRCA2^{KO} cells. Hits with LogP less than or equal to -2 were entered into NIH DAVID and pathways were analyzed for GO_BP terms. GO_BP terms with a logP of -1.5 or lower are shown.

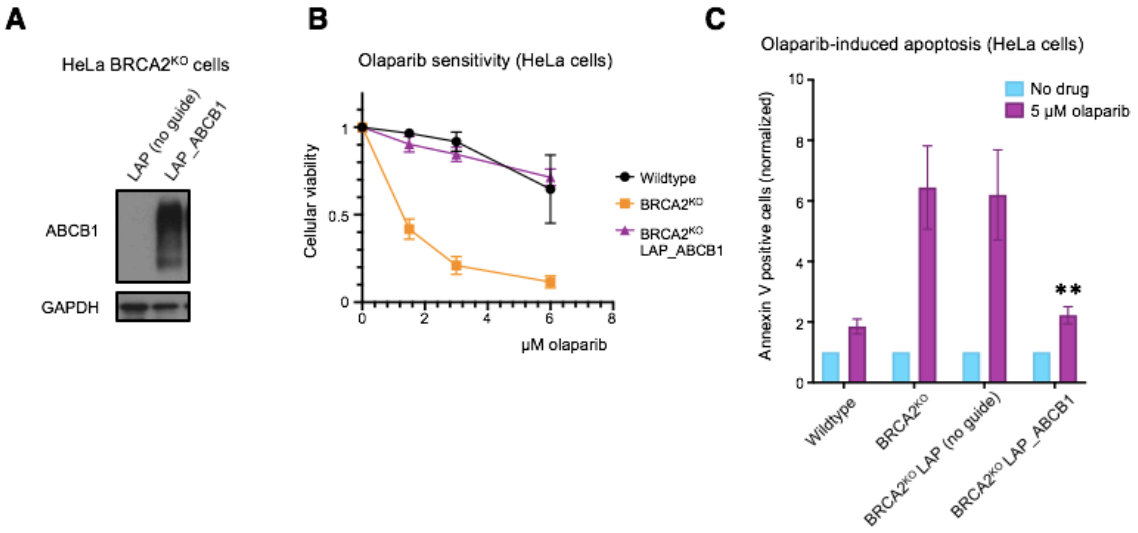

Figure 2.6. Overexpression of ABCB1, the top hit from the CRISPR activation screen, causes PARPi resistance in BRCA2-deficient cells. (A) Western blot showing overexpression of ABCB1 in the cell line containing all three components of the CRISPR lentiviral activation particle (LAP) system (dCas9, activator helper complex, and sgRNA targeting the ABCB1 gene) but not in the control cell line lacking the sgRNA. **(B)** Cellular viability assay showing that ABCB1 transcriptional activation rescues PARPi sensitivity in HeLa BRCA2-knockout cells. The averages of 4 biological replicates are shown, with standard deviations as error bars. **(C)** Olaparib-induced apoptosis in BRCA2-knockout cells is suppressed by ABCB1 overexpression. The averages of 4 biological replicates are shown, with standard deviations as error bars. Asterisks indicate statistical significance (compared to "no guide" sample).

There are few studies reporting proteins which cause PARPi resistance when overexpressed; however, interestingly, our top hit from the screen, ABCB1, has previously been identified as a mechanism of PARPi resistance (101). This gene encodes the protein MDR-1 (multidrug resistance protein 1), a drug efflux pump whose overexpression was associated with acquired resistance to olaparib in ovarian cancer cell lines (101). To validate these results in our system, I generated HeLa BRCA2^{KO} cells with transcriptional activation of the ABCB1 gene (Figure 2.6A). I found that the BRCA2-knockout, ABCB1-overexpressing cell line was as resistant to PARPi as the BRCA2-proficient parental HeLa line (Figure 2.6B). Previously, PARPi treatment has been shown to induce apoptosis in BRCA2-deficient cells (103). In line with this, I found that olaparib treatment led to a more than 6-fold increase in cells positive for annexin V, a

marker of apoptosis, in BRCA2-knockout cells; however, overexpression of ABCB1 restored olaparib-induced apoptosis to control levels (Figure 2.6C). Overall, these findings validate the results of the CRISPR activation screen.

2.3 Discussion

Identifying potential predictors of response to PARPi serves to both identify additional patients who may benefit from this therapy, and to avoid ineffective treatment for those who will not. Additionally, beyond simply predicting treatment response, achieving a better understanding of mechanisms of sensitivity and resistance to PARPi brings us closer to potential therapeutic interventions that may be able to sensitize or re-sensitize patients to treatment. Therefore, there has been great interest in investigating PARPi sensitivity and resistance through genome-wide CRISPR knockout screens in cells with various genetic backgrounds (75, 82, 117).

Here, I have completed a series of genome-wide screens based on CRISPR technology as an unbiased approach towards better understanding determinants of PARPi response. First, I present data from a CRISPR-knockout screen in wildtype HeLa cells, which identified genes which, when depleted, lead to PARPi sensitivity. Additionally, I investigated PARPi resistance in BRCA2-knockout HeLa cells by identifying genes which cause resistance when depleted (CRISPR knockout library) or overexpressed (CRISPR activation library). By utilizing two different types of libraries and otherwise isogenic cell lines differing only in BRCA2 levels, I am able to not only examine the results of each screen individually, but also to consider the results in relationship to one another. For example, loss of POLE3 or POLE4, subunits of DNA polymerase Epsilon, sensitized parental HeLa cells to PARPi treatment, while transcriptional activation of polymerase Epsilon subunit POLE2 was associated with PARPi resistance in BRCA2-knockout HeLa cells. This is especially interesting given

that depletion of polymerase Epsilon subunits was recently shown to lead to sensitivity to ATR inhibitors (118). Overall, these results identified several hits which were consistent with previous findings from other groups, as well as novel hits which have not previously been connected to PARPi response.

2.4 Materials and Methods

Cell culture. Unless otherwise indicated, cells used in this dissertation (including RPE1, HeLa, and U2OS) were obtained from ATCC. Authentication was performed regularly based on morphology and gene/protein expression (in case of genetic alterations). Human HeLa cells were grown in Dulbecco's modified Eagle's medium (DMEM), supplemented with 10% fetal bovine serum. HeLa $BRCA2^{KO}$ cells were generated in our laboratory using the commercially available BRCA2 CRISPR/Cas9 KO plasmid (Santa Cruz Biotechnology sc-400700). Transfected cells were FACS-sorted into 96-well plates using a BDFACSAria II instrument. Resulting colonies were screened by western blot.

HeLa BRCA2-knockout cells overexpressing ABCB1 via transcriptional activation were created by consecutive rounds of transduction and selection. Cells were first infected with dCas9 (Addgene, 61425-LV) and colonies were selected with blasticidin, 3 μg/ml. dCas9-expressing cells were then infected with the MS2-P65-HSF1 activator helper complex (Addgene, 61426-LVC) and treated with 0.5 mg/ml hygromycin. Finally, hygromycin-resistant cells were infected with lentivirus containing guide RNA targeting ABCB1 (Sigma Custom CRISPR in lentiviral backbone LV06), guide sequence (5'-3'): GGGAGCAGTCATCTGTGGTG. Infected cells were selected using puromycin (0.6 μg/ml).

Gene knockdown was performed using Lipofectamine RNAiMAX reagent for transfection of Stealth siRNA (Life Tech). Oligonucleotide sequence used was:

BRCA2: GAGAGGCCTGTAAAGACCTTGAATT.

Genome-wide CRISPR screens. For the CRISPR knockout screens, wildtype or BRCA2-knockout HeLa cells were transduced with the Brunello Human CRISPR knockout pooled library (Addgene, 73179) (112). To achieve a representation of 250 cells per sgRNA, 50 million cells were transduced at a low multiplicity of infection (MOI) (0.4). Selection with puromycin (0.6 μg/ml) was initiated at 48 hours post-transduction and maintained for 4-6 days. For the resistance screen in BRCA2-deficient cells, puromycin-resistant cells were divided into olaparib- or vehicle- (DMSO) treated arms at 250 fold library coverage per arm. Olaparib was used at 4μM for 4 days, and yielded 7% survival relative to the DMSO condition. After treatment, cells were pelleted and flash-frozen for DNA extraction. For the sensitivity screen in wildtype cells, puromycin-resistant cells were seeded at a representation of 150 cells per sgRNA and treated with DMSO or olaparib (5μM) for 4 days. After the 4 days of treatment, survival of the olaparib-treated population was 43% of the vehicle-treated cells; cells were pelleted and flash-frozen for DNA extraction.

For the CRISPR activation screen, HeLa BRCA2-knockout cells were infected with dCas9 (Addgene, 61425-LV) and selected with blasticidin (3 μg/ml). dCas9-expressing cells were then transduced with the Calabrese Human CRISPR Activation Pooled Library (Set A, Addgene, 92379-LV) using enough cells to obtain a library coverage of 500 cells per sgRNA at an MOI of 0.4 (116). Selection with puromycin (0.6 μg/ml) was initiated at 48 hours post-transduction and maintained for 5 days. After puromycin selection, cells were divided into olaparib- (4 μM) or vehicle- (DMSO) treated arms at 500-fold library coverage per arm. After 4 days of treatment, survival of the

olaparib-treated cells was 12% relative to the DMSO-treated condition; cells were flash-frozen as pellets for DNA extraction.

Sequencing and analysis of CRISPR screens. Genomic DNA (gDNA) was extracted per manufacturer's instructions using the DNeasy Blood & Tissue Kit (Qiagen, 69504). A maximum of 5 million cells were used per column. Isolated gDNA was quantified using Nanodrop. The genomic DNA equivalent of 125-fold library coverage (knockout screens) or 250-fold library coverage (activation screen) was used as template for PCR amplification of the sgRNA sequences. Each PCR reaction included no more than 10 μg of gDNA, in addition to the following components: 3 μl of Radiant HiFi Ultra Polymerase (Stellar Scientific, RAD-HF1100), 20 μl of 5X HiFi Ultra Reaction Buffer, 4 μl of 10 μM P5 primer, 4 μl of 10 μM uniquely-barcoded P7 primer, and water to bring the total reaction volume to 100 μl. Primers were synthesized by Eurofins Genomics using the sequences listed in the user guide provided for the CRISPR libraries. PCR cycling conditions were as follows: an initial 2 min at 98˚C; followed by 10 s at 98˚C, 15 s at 60˚C, 45 s at 72˚C, for 30 cycles; and lastly 5 min at 72˚C (119). The E.Z.N.A. Cycle Pure Kit (Omega, D6493-02) was used per manufacturer's instructions to purify PCR products. Products were then further purified and sequenced by the Penn State College of Medicine Genome Sciences Facility using the following protocol. PCR products were further purified with Agencourt AMPure XP SPRI beads according to manufacturer's instructions (Beckman Coulter, A63880). The final product was assessed for its size distribution and concentration using BioAnalyzer High Sensitivity DNA Kit (Agilent Technologies) and qPCR (Kapa Biosystems). Pooled libraries were diluted to 2 nM in EB buffer (Qiagen) and then denatured using the Illumina protocol. The denatured libraries were diluted to 10 pM by pre-chilled hybridization buffer and loaded onto a TruSeq v2 Rapid flow cell on

an Illumina HiSeq 2500 and run for 50 cycles using a single-read recipe according to the manufacturer's instructions (Illumina).

For bioinformatic analysis, de-multiplexed and adapter-trimmed sequencing reads were generated using Illumina bcl2fastq (released version 2.18.0.12) allowing no mismatches in the index read. Analysis was then performed following a previously described protocol (120). Briefly, sgRNA representation was analyzed for each condition using the provided custom python script (count_spacers.py) (step 38 (120)). The sgRNA fold change due to olaparib treatment was then determined for each cell line as follows (Step 65 (120)): A pseudocount of 1 was added to each sgRNA read count, which was then normalized by the total reads for that condition; the normalized sgRNA read counts of the olaparib-treated condition were then divided by those of the DMSO-treated condition, and the base 2 logarithm of the resulting ratios were calculated. These values were then used as inputs for analysis using the redundant siRNA activity (RSA) method (121). For the analysis, the Bonferroni correction option was used. Bounds were adjusted such that for the sensitivity screen, guides which were 2-fold less present in the olaparib treated condition were counted as guaranteed hits. For the resistance screens the default bounds were used, in which guides which were 2-fold more enriched in cells surviving olaparib treatment were counted as guaranteed hits.

Protein techniques. Total cellular protein extracts and western blots were performed as previously described (122). Antibodies used were: BRCA2 (Bethyl A303-434A), ABCB1 (Santa Cruz Biotechnology, sc-13131), Cas9 (BioLegend 844302), and GAPDH (Santa Cruz Biotechnology, sc-47724).

Drug Sensitivity Assays. Olaparib was obtained from Selleck Chemicals. To test cellular viability after olaparib treatment, cells were seeded in 96-well plates at a density

of 2000 cells per well, treated with the indicated doses of olaparib for 3 days, and assessed using CellTiter-Glo reagent (Promega, G7572) per manufacturer's instructions. For apoptosis assays, cells were treated with olaparib (5 μM) for 3 days, prepared for flow cytometry using the FITC Annexin V kit (Biolegend, 640906) and quantified using a BD FACSCanto 10 flow cytometer.

Statistical analyses. For the viability and apoptosis assays, the statistical analysis performed was the t-test (two-tailed, unequal variance unless indicated). Statistical significance is indicated for each graph (ns = not significant, for $P > 0.05$; * for $P \leq 0.05$; ** for $P \leq 0.01$; *** for $P \leq 0.001$; **** for $P \leq 0.0001$).

Chapter 3: Loss of E2F7 confers resistance to PARPi in BRCA2-deficient cells.

Adapted from: Clements, K.E. et al. (2018) Nucleic Acids Res.

3.1 Rationale

One of the top hits from the CRISPR knockout screen identifying proteins which cause PARPi resistance when depleted in BRCA2-deficient cells was E2F7, a member of the E2F transcription factor family. Together with E2F8, E2F7 is considered an atypical E2F family member, as they mediate transcription repression rather than activation (123, 124). E2F7 levels are induced by DNA damage (125). E2F7 transcriptional repression targets include replication proteins such as CDC6 and MCM2—thereby its induction by DNA damage contributes to G1/S-arrest (126, 127). However, among its targets for repression are also HR proteins, including RAD51 and BRCA1 (127). Although restoration of HR through reversion mutations in BRCA2 is a common mechanism of PARPi resistance, restoration of HR independent of reversion mutations had not been connected to PARPi resistance in BRCA2-deficient cells. In this chapter, I show that E2F7 promotes sensitivity to PARPi, and its depletion can rescue chemosensitivity of BRCA2-deficient cells by promoting both HR and fork stability. Furthermore, I report that E2F7 depletion causes these phenotypes through an increase in RAD51 mRNA and protein levels and a subsequent rescue of the defects in RAD51 chromatin loading caused by BRCA2 deficiency.

3.2 Results

3.2.1. Depletion of E2F7 reverses the PARPi sensitivity of BRCA2-deficient cells

In order to investigate the involvement of E2F7 in mediating PARPi resistance in BRCA2- deficient cells, I knocked down E2F7 in $BRCA2^{KO}$ cells and measured olaparib sensitivity. E2F7 knockdown resulted in significant rescue of olaparib sensitivity of these

cells (Figure 3.1A). In order to rule out a non-specific effect caused by the CRISPR editing, I also knocked-down E2F7 in parental HeLa cells at the same time with BRCA2 depletion. E2F7 knockdown with three different siRNA oligonucleotides rescued olaparib sensitivity of BRCA2-knockdown cells (Figure 3.1B). In contrast, E2F7 knockdown by itself (without BRCA2 co-depletion) did not show a significant effect on olaparib sensitivity (Figure 3.2A). All three siRNA oligonucleotides efficiently knocked-down E2F7 expression as shown by qPCR-based detection of E2F7 mRNA levels (Figure 3.2B). Further confirming the specificity of the phenotype, Western blot experiments showed that BRCA2 is equally depleted in cells treated with BRCA2 siRNA alone or in combination with E2F7 siRNA (Figure 3.2C). Moreover, cellular proliferation and cell-cycle distribution of BRCA2-knockdown cells were not affected by E2F7 co-depletion (Figure 3.2 D and E).

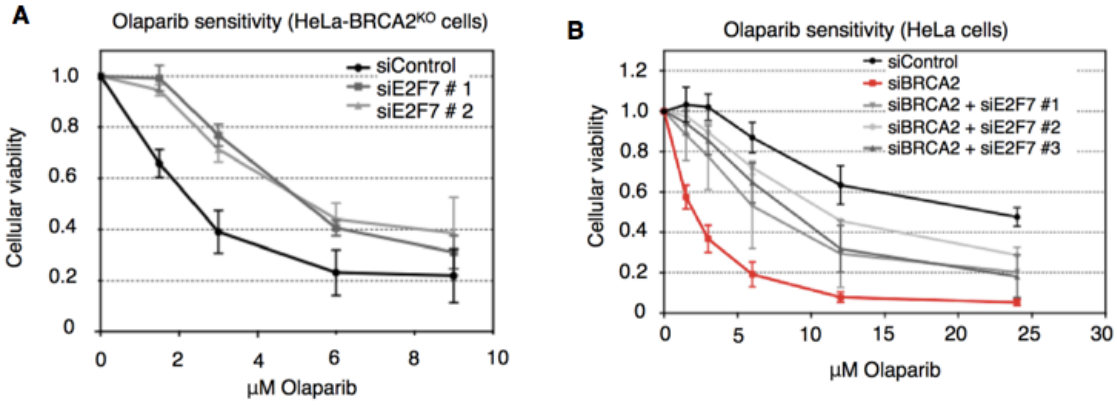

Figure 3.1. E2F7 depletion in BRCA2-deficient HeLa cells results in olaparib resistance. (**A** and **B**) E2F7 knockdown rescues the olaparib sensitivity of BRCA2-knockout **(A)** and BRCA2-knockdown **(B)** HeLa cells. The average of three biological replicates, with standard deviations as error bars, is shown. Knockdown also rescued sensitivity of a second, independently obtained BRCA2-knockout clone (data not shown).

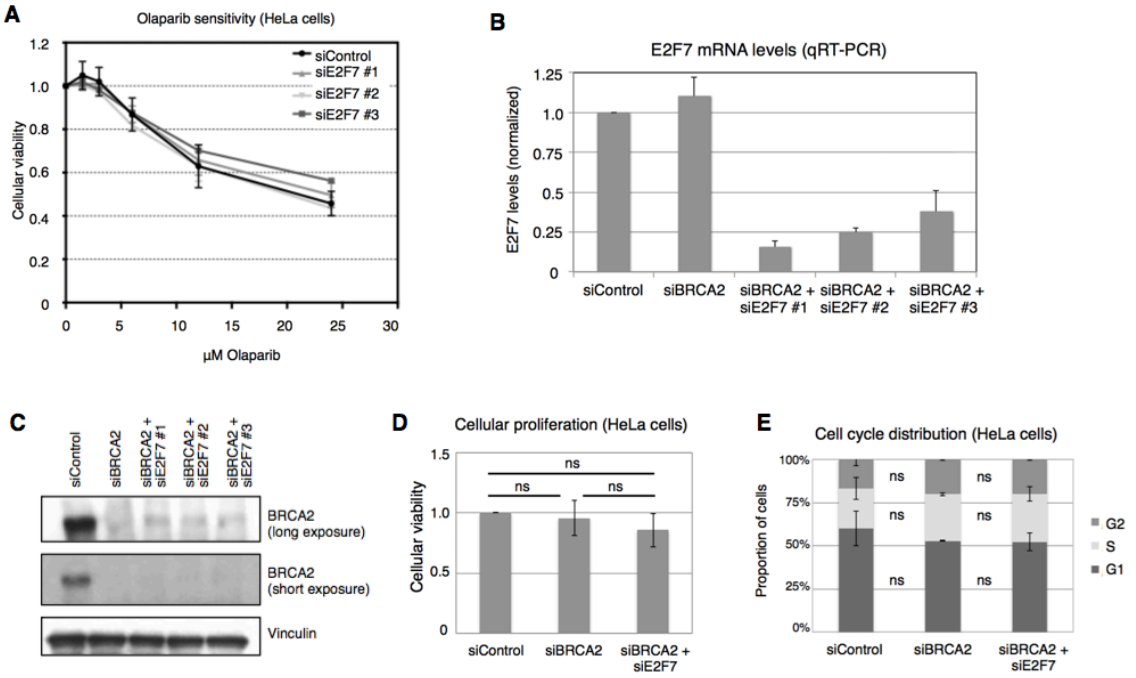

Figure 3.2. The effects of E2F7 depletion on PARPi sensitivity are specific for BRCA2-deficiency. (A) E2F7 knockdown alone does not affect olaparib sensitivity of HeLa cells. The average of three biological replicates, with standard deviations as error bars, is shown. **(B)** Quantitative RT-PCR experiment showing efficient E2F7 knockdown by the siRNA oligonucleotides employed. HeLa cells were treated with the indicated siRNA oligonucleotides then incubated with 10 μM olaparib for 24 h before harvesting. The average of three biological replicates, with standard deviations as error bars, is shown. **(C)** Western blot showing that BRCA2 is efficiently knocked down by the siRNA oligonucleotide employed singly or in combination with E2F7 siRNA oligonucleotides. HeLa cells were treated with the indicated siRNA oligonucleotides then incubated with 10 M olaparib for 24 h before harvesting. **(D)** Cellular viability assay indicating that BRCA2 or BRCA2-E2F7 co-depletion do not affect cellular proliferation rates. HeLa cells were treated with siRNA as indicated, seeded in 96-well plates, and viability was analyzed three days later using CellTiterGlo. The average of four biological replicates, with standard deviations as error bars, is shown. **(E)** Quantification of cell cycle distribution showing no impact of BRCA2 or BRCA2-E2F7 co-depletion on the cell cycle profile of HeLa cells. Cells were treated with siRNA as indicated, and cell cycle distribution was analyzed three days later by Propidium Iodide staining. The average of three experiments, with standard deviations as error bars, is shown.

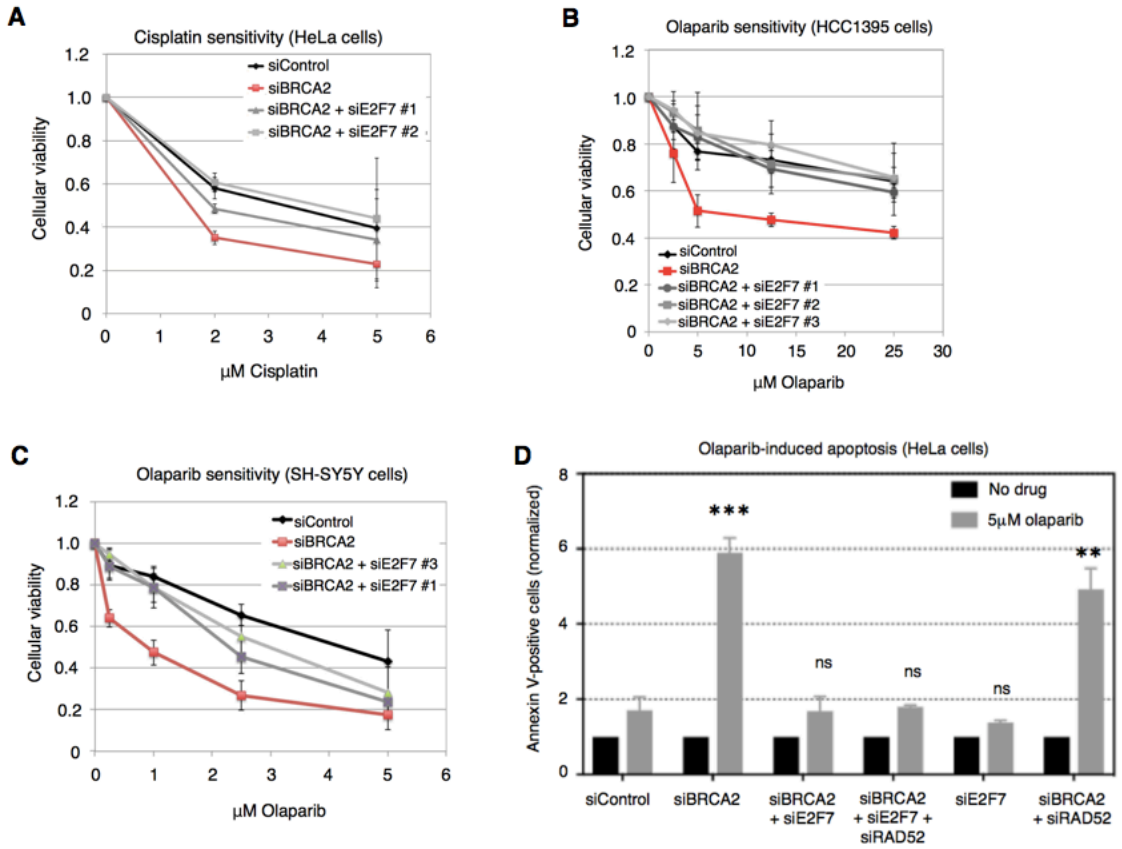

Figure 3.3. E2F7 depletion mediates cisplatin sensitivity, and PARPi sensitivity in multiple cell lines. (A) E2F7 knockdown rescues the cisplatin sensitivity of BRCA2-knockdown HeLa cells. **(B and C)** E2F7 knockdown rescues the olaparib sensitivity of BRCA2-knockdown HCC1395 breast cancer (B) and SH-SY5Y neuroblastoma (C) cells. **(D)** Quantification of AnnexinV-positive cells indicating that E2F7 knockdown suppresses olaparib-induced apoptosis of BRCA2- depleted cells. HeLa cells were treated with the indicated siRNA oligonucleotides then incubated with 5 µM olaparib for 3 days. Results are presented as normalized to control (no drug treatment condition) for each knockdown sample. Asterisks indicate statistical significance compared to siControl olaparib-treated condition. Similar results were obtained using two other siRNA oligonucleotide sequences for E2F7 (data not shown). For A-D, the average of three biological replicates, with standard deviations as error bars, is shown.

BRCA2-deficient cells are sensitive to many genotoxic agents used in cancer therapy, including cisplatin (128). Interestingly, it was recently suggested that PARPi and cisplatin have similar mechanisms of action (129). In order to test the specificity of this novel E2F7-mediated response, I treated E2F7/BRCA2-co-depleted HeLa cells with cisplatin. E2F7 knockdown was able to rescue the cisplatin sensitivity of BRCA2-depleted cells (Figure 3.3A), indicating that E2F7 has a broad impact on the

chemosensitivity of BRCA2-deficient cells. Altogether, these findings show that E2F7 is a novel regulator of DNA damage sensitivity of BRCA2-deficient cells.

I next investigated if the suppression of olaparib sensitivity by loss of E2F7 is restricted to HeLa cells, or is a general phenomenon. BRCA2 depletion in HCC1395 breast cancer cells resulted in olaparib sensitivity, which was rescued by E2F7 knockdown (Figure 3.3B). Similarly, olaparib sensitivity of BRCA2-depleted SH-SY5Y neuroblastoma cells was rescued by E2F7 depletion (Figure 3.3C). Olaparib treatment is known to induce apoptosis in BRCA2-deficient cells (103). E2F7 depletion did not only rescue cellular viability of olaparib-treated BRCA2-deficient cells, but also reduced olaparib-induced apoptosis (Figure 3.3D). Altogether, these results indicate that E2F7 is a novel factor controlling PARPi resistance in BRCA2-deficient cells.

I next investigated if E2F7 depletion suppresses olaparib-induced genomic instability in these cells. First, I employed the neutral comet assay to detect double stranded DNA breaks in BRCA2-knockout HeLa cells. I found that E2F7 depletion reduces comet tail length, indicating a suppression of DNA damage accumulation (Figure 3.4A). In line with this, immunofluorescence experiments with these cells showed a reduction in olaparib-induced formation of H2AX and 53BP1 foci, generally considered markers of double stranded breaks (Figure 3.4 B-E). These findings indicate that E2F7 depletion protects against olaparib-induced genomic instability, suggesting that E2F7 suppresses DNA repair in BRCA2-deficient cells.

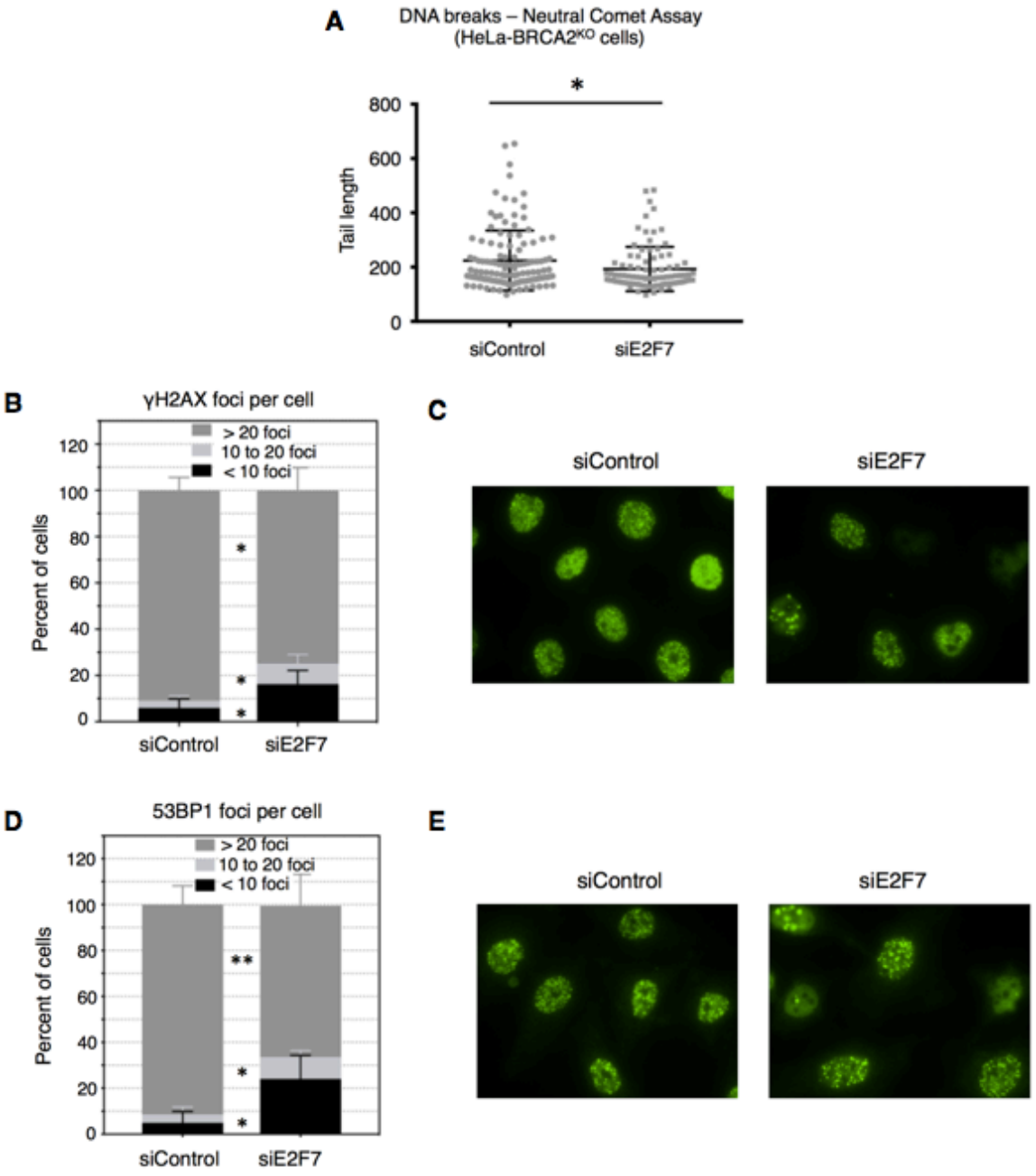

Figure 3.4. Impact of E2F7 depletion on genomic stability of BRCA2-deficient cells. **(A)** Neutral comet assay showing that E2F7 depletion reduces olaparib-induced double-strand breaks in BRCA2-knockout HeLa cells. Cells were treated with 10 μM olaparib for 24 h. At least 90 comet tails, pooled from three biological replicates, were quantified for each sample. The means with standard deviations are shown. The asterisk indicates statistical significance. **(B-E)** E2F7 depletion reduces olaparib-induced γH2AX **(A, B)** and 53BP1 **(C, D)** foci in BRCA2-knockout HeLa cells. Cells were treated with 6μM (γH2AX) or 3μM (53BP1) olaparib for 24 hours. The average of three biological replicates, with standard deviations as error bars, is shown. At least 50 cells were imaged in each experiment. The asterisks indicate statistical difference (paired t-test) between siControl and siE2F7 for each foci number category. Representative micrographs are also shown.

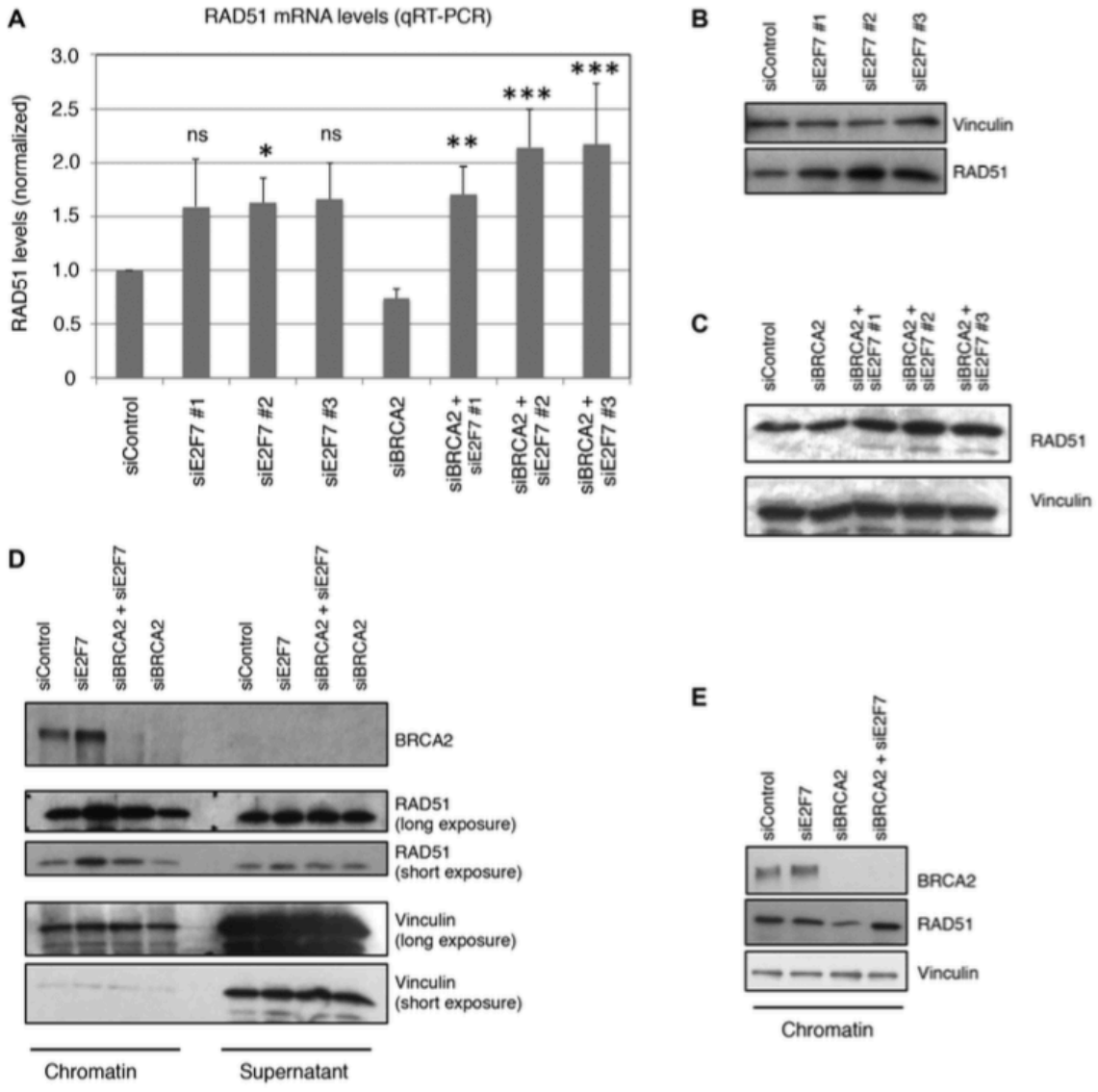

Figure 3.5. E2F7 regulates RAD51 levels to control olaparib sensitivity. (A) Quantitative RT-PCR experiment showing increased RAD51 mRNA levels upon E2F7 depletion in BRCA2-knockdown HeLa cells incubated with 10 μM olaparib for 24 h before harvesting. The average of three biological replicates, with standard deviations as error bars, is shown. Asterisks denote statistical significance compared to siControl condition (for single E2F7 depletion samples), or siBRCA2 condition (for E2F7/BRCA2 co-depletion samples). **(B and C)** Western blots showing that E2F7 knockdown results in increased RAD51 protein levels in U2OS **(B)** and HeLa **(C)** cells treated with 10 μM olaparib for 24 h. **(D and E)** Chromatin fractionation experiments showing that E2F7 depletion results in increased chromatin-bound RAD51. HeLa **(D)** or U2OS **(E)** cells, treated with 10 μM olaparib for 24 h, were used. Vinculin is used as loading control.

3.2.2. E2F7 regulates RAD51 levels to promote olaparib resistance of BRCA2-deficient cells

Previously, RAD51 was identified as a possible target for transcriptional repression by E2F7 (127). RAD51 is an essential HR factor, which is loaded by BRCA2 on resected ssDNA and catalyzes the strand invasion step in the recombination process (12). Thus, I decided to investigate the levels of RAD51 in E2F7-depleted HeLa and U2OS cells treated with olaparib. E2F7 knockdown, by itself or in combination with BRCA2 depletion, resulted in increased RAD51 expression at both the mRNA and protein levels (Figure 3.5 A–C). Moreover, E2F7 knockdown resulted in an increase in the levels of chromatin-bound RAD51 upon olaparib treatment (Figure 3.5 D and E). While RAD52 has been previously described to function as a RAD51 loader in BRCA2-deficient cells, its downregulation did not affect the E2F7 depletion-mediated rescue of olaparib sensitivity in BRCA2-knockout cells (Figures 3.3D and 3.6 A), suggesting that RAD52 does not play a major role in loading RAD51 upon E2F7 depletion in BRCA2-deficient cells (130). Altogether, these results suggest that E2F7 depletion may promote olaparib resistance in BRCA2-deficient cells by increasing RAD51 levels.

Recently, Chk1 was shown to phosphorylate E2F7 thereby restricting its activity in response to DNA damage (131). This raises the possibility that in BRCA2-deficient cells, Chk1 activity, by inhibiting E2F7, promotes PARPi resistance. Indeed, I found that treatment of BRCA2- knockout HeLa cells with a Chk1 inhibitor significantly sensitized them to olaparib (Figure 3.6 B). This effect was dependent at least in part on E2F7, as its knockdown alleviated this sensitization. Finally, I wanted to investigate if this novel regulatory pathway is involved in acquired resistance to PARP inhibitors. To this end, I treated BRCA2-knockout HeLa cells with a sublethal dose of olaparib (0.25 M) for 14 days, and measured mRNA expression of E2F7 and RAD51. Compared to controls, cells grown in the presence of olaparib showed a significant reduction in E2F7 levels,

with a concomitant increase in RAD51 (Figure 3.6 C). Moreover, these cells were less sensitive to olaparib than control cells (Figure 3.6D). These results suggest that prolonged olaparib treatment may result in E2F7 downregulation, as a compensatory mechanism to increase RAD51 levels and promote olaparib resistance.

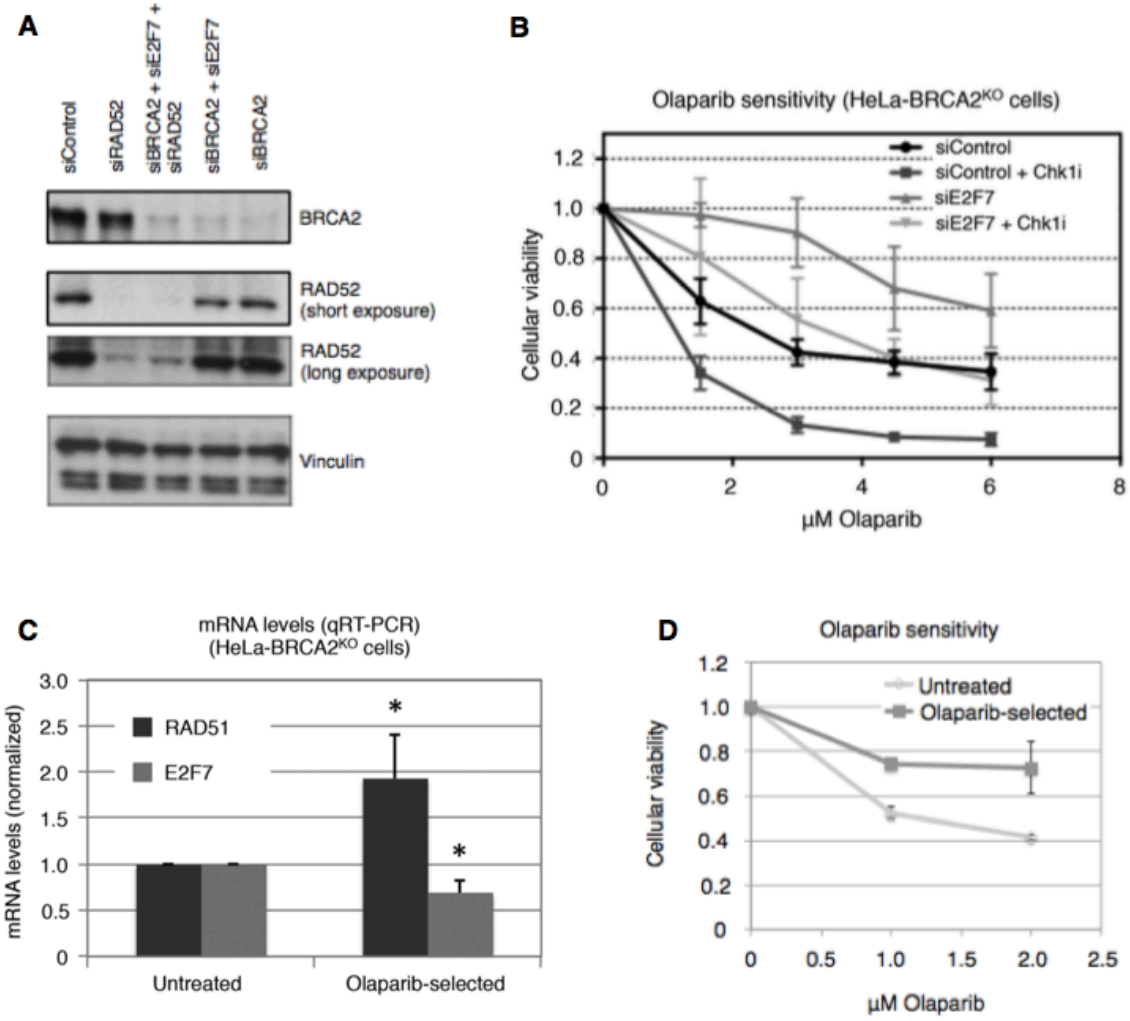

Figure 3.6. Modulation of E2F7 as a means of PARPi resistance. **(A)** Western blot showing efficient co-depletion of BRCA2, E2F7 and RAD52 in HeLa cells. (**B**) Chk1 inhibition further sensitizes BRCA2^{KO} HeLa cells to olaparib treatment, which is suppressed by E2F7 depletion. The average of three biological replicates, with standard deviations as error bars, is shown. Chk1 inhibitor used is Rabusertib (300 nM). **(C)** BRCA2-knockout HeLa cells were grown in the presence of 0.25 µM olaparib for 14 days, then subjected to qRT-PCR to detect E2F7 and RAD51 mRNA expression. The average of four biological replicates, with standard deviations as error bars, is shown. Asterisks indicate statistical significance compared to control (untreated) samples. **(D)** BRCA2-knockout HeLa cells selected with olaparib become olaparib-resistant. The average of three experiments, with standard deviations as error bars, is shown.

3.2.3. Depletion of E2F7 restores RAD51-mediated homologous recombination in BRCA2-deficient cells

Next, I sought to investigate the mechanism of the observed E2F7 depletion-mediated suppression of olaparib sensitivity in BRCA2-deficient cells. Two activities of BRCA2 have been associated with chemoresistance: repair of double stranded DNA breaks through HR (by loading of RAD51 to resected DNA ends), and protection of stalled replication forks against nucleolytic degradation by MRE11 (through loading of RAD51 to reversed replication forks) (50, 88, 93). Thus, I decided to test if the increased RAD51 levels and chromatin loading observed in E2F7-depleted cells may partially alleviate the impact of BRCA2 loss and restore HR proficiency and/or fork protection. To measure HR, I employed the DR-GFP assay that quantifies double strand break-induced recombination between direct repeats in U2OS cells (132). As expected, BRCA2 knockdown significantly reduced HR, while depletion of E2F7 alone did not affect it (Figures 3.7 A and B). However, co-depletion of E2F7 rescued the HR defect caused by BRCA2 knockdown. In contrast, E2F7 depletion could not rescue the HR defect conferred by loss of RAD51, indicating that the E2F7-mediated rescue observed in BRCA2-deficient cells requires RAD51 expression. Moreover, E2F7 co-depletion did not increase classic or alternative NHEJ rates in BRCA2-knockdown cells (Figures 3.7 C and D), indicating that its effect is specific for HR and does not occur through other double strand break repair pathways. Altogether, these results indicate that E2F7 depletion increases RAD51 levels, which promotes HR in BRCA2-deficient cells.

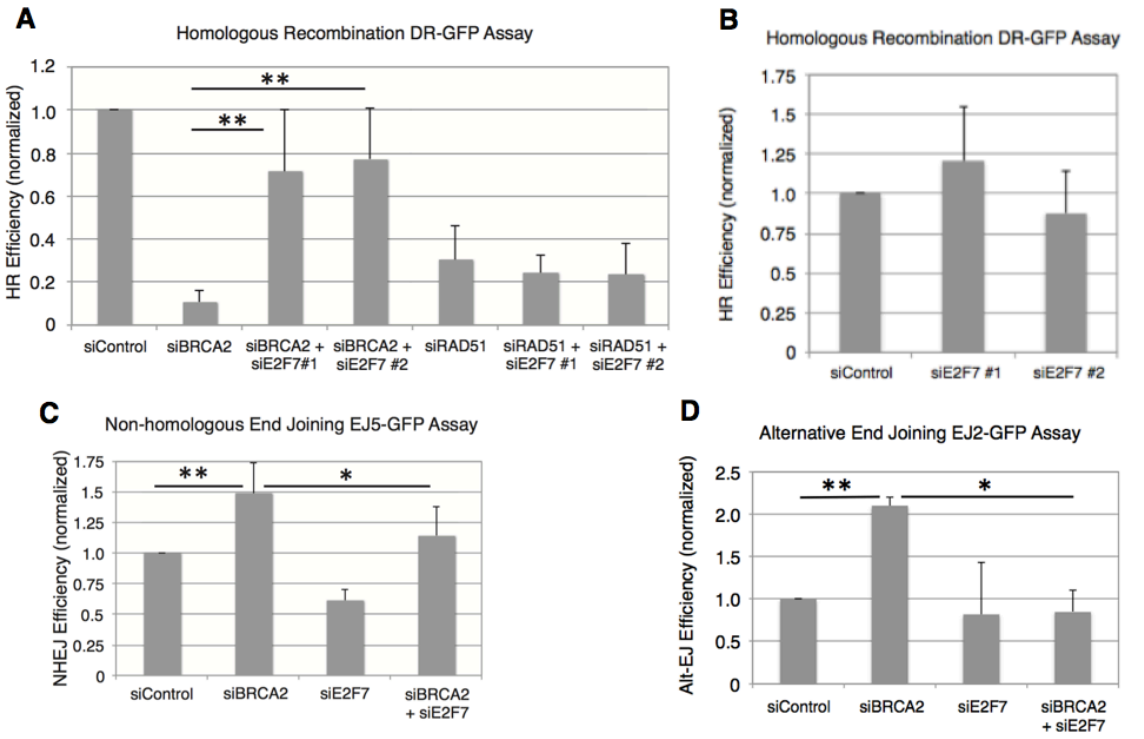

Figure 3.7. E2F7 depletion restores RAD51-mediated HR in BRCA2-deficient cells. **(A)** DR-GFP assay in U2OS cells showing that E2F7 depletion restores HR levels in BRCA2-knockdown cells, but not in RAD51-knockdown cells. The average of three to five biological replicates, with standard deviations as error bars, is shown. Asterisks indicate statistical significance. **(B)** DR-GFP assay showing no impact of E2F7 depletion alone on homologous recombination. The average of four biological replicates, with standard deviations as error bars, is shown. **(C)** EJ5-GFP assay showing no impact of E2F7 co-depletion on the NHEJ levels in BRCA2-depleted cells. The average of four to six biological replicates, with standard deviations as error bars, is shown. Asterisks indicate statistical significance. **(D)** EJ2-GFP assay showing the impact of E2F7 co-depletion on microhomology mediated (alternative) end joining levels in BRCA2-depleted cells. While BRCA2 knockdown increases Alt-EJ, E2F7 co-depletion restores it to control levels. While the reason for this effect is unclear, it may reflect the opposite (and likely compensatory) impact these gene knockdowns have on HR (which is reduced by BRCA2 knockdown, but restored by E2F7 co-depletion). The average of three experiments, with standard deviations as error bars, is shown. Asterisks indicate statistical significance.

3.2.4. E2F7 regulates replication fork stability in BRCA2-deficient cells

Next, I tested the impact of E2F7 on replication fork protection. Recently, degradation of stalled replication forks was proposed as a novel activity underlying chemosensitivity of BRCA2-deficient cells. In normal cells, BRCA2 protects against fork degradation by loading RAD51 on forks arrested at sites of DNA damage. In BRCA2-deficient cells, RAD51 cannot be loaded, thus rendering stalled forks susceptible to degradation by MRE11 nuclease (88, 89, 96). In order to test the impact of E2F7 on fork stability in BRCA2-deficient cells, I employed the DNA fiber assay, which allows detection and quantification of nascent DNA strands at molecular level. I measured the length of replication tracts in BRCA2-knockout HeLa cells upon treatment with hydroxyurea (HU), an established model of fork degradation in BRCA-deficient cells (93, 96, 133). In line with previous reports (88, 89, 96), loss of BRCA2 resulted in HU-induced degradation of nascent DNA (Figure 3.8 A-D). Importantly, E2F7 depletion could rescue the HU-induced fork degradation phenotype of BRCA2- knockout cells (Figure 3.8 A-D). This rescue requires RAD51 loading to stalled forks, as it was abolished by treatment with RAD51 inhibitor B02, previously shown to block RAD51 loading to stalled forks (96). Moreover, addition of MRE11 inhibitor mirin restored tract length to that of wild-type cells (Figure 3.8 D), confirming that forks are degraded by the canonical MRE11-mediated pathway. These findings indicate that increased RAD51 levels upon E2F7 depletion can protect stalled replication forks against MRE11-mediated degradation in BRCA2-deficient cells.

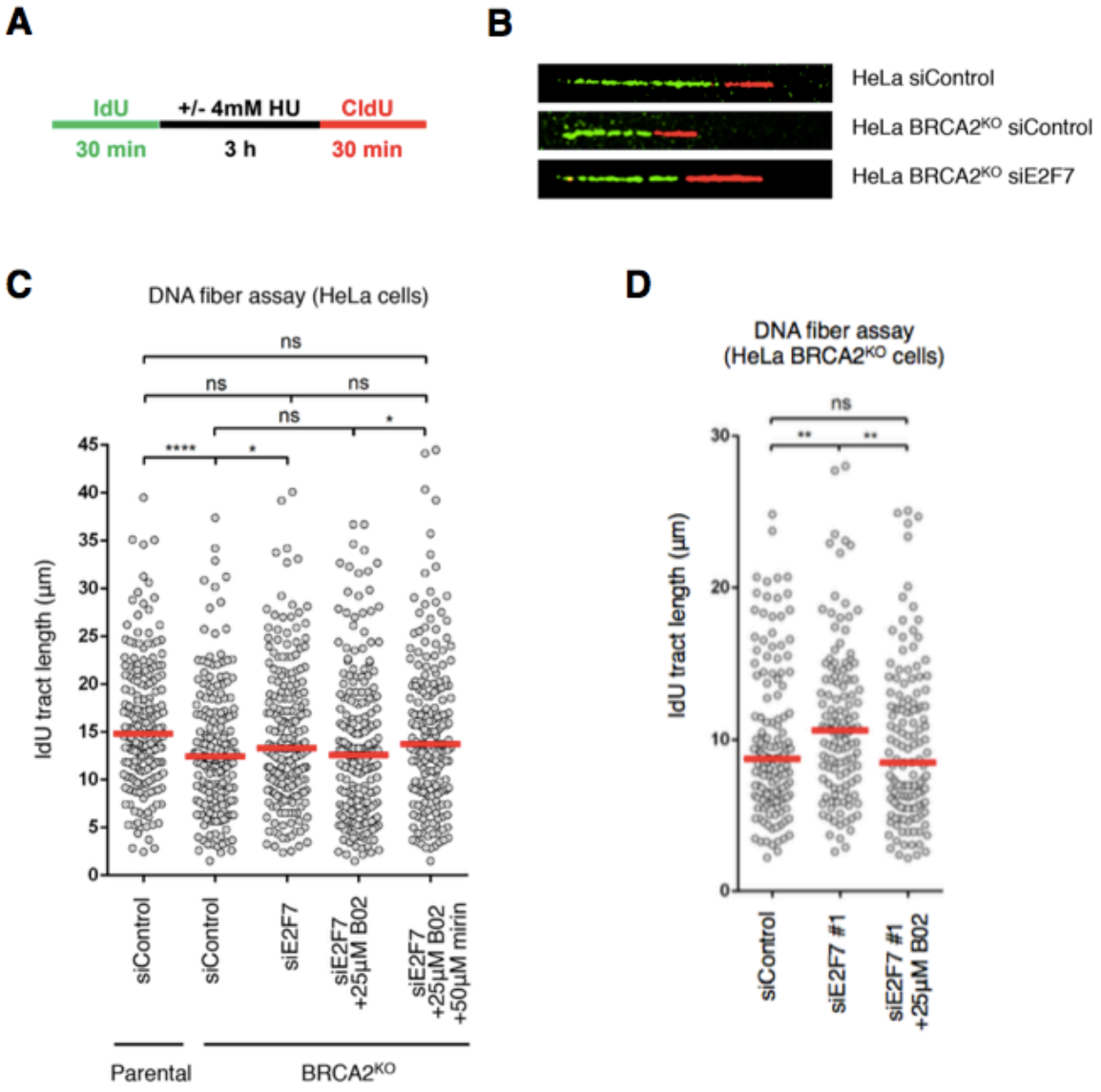

Figure 3.8. E2F7 controls replication fork stability in control and BRCA2- knockout HeLa cells. (A) Schematic representation of the experimental setup for the DNA fiber combing experiment. **(B)** Examples of replication tracts for the indicated genotypes. **(C)** Quantification of the IdU tract length. Loss of BRCA2 reduces the length of the IdU tract upon HU treatment, indicating that the nascent strand is degraded. This degradation can be suppressed by E2F7 depletion. Treatment with RAD51 inhibitor BO2 abolishes this rescue, indicating that it involves RAD51 loading to reversed forks. Incubation with the MRE11 inhibitor mirin can restore tract length, indicating that the fork degradation occurs through the classic MRE11 pathway. At least 200 tracts were analyzed for each sample. The median and statistical significance are indicated. **(D)** E2F7 knockdown using a different siRNA oligonucleotide than that shown in (B) also suppresses fork degradation in BRCA2-knockout HeLa cells, in a manner dependent on RAD51. At least 120 tracts were analyzed for each sample. The median of IdU tracts lengths and statistical significance are indicated.

3.3 Discussion

Identifying clinical biomarkers of PARPi resistance is paramount for more targeted usage of these promising drugs in cancer treatment. The work described in this chapter work identifies E2F7 as a new factor regulating PARPi and cisplatin resistance of BRCA2-deficient cells (Figure 3.9). I show that E2F7 depletion results in increased levels of RAD51, a previously described target for transcriptional repression by E2F7. This, in turn, promotes both HR and fork stability in BRCA2-deficient cells. Thus, my work suggests that E2F7 levels may represent a putative biomarker predicting PARPi responses of human tumors. Future clinical studies are important to validate this prediction. Moreover, upstream regulators of E2F7 may also serve as biomarkers and provide opportunities for therapeutic intervention. Recently, Chk1 was shown to phosphorylate E2F7 thereby restricting its activity in response to DNA damage (131). I show here that Chk1 inhibition further sensitizes BRCA2-deficient cells to olaparib, in a manner at least partially dependent on E2F7. This suggests that Chk1 activity may promote PARPi resistance by inhibiting E2F7. Pharmacological inhibition of this pathway may potentially be employed to restore PARPi sensitivity in tumors with acquired resistance. These studies also indicate the possibility that E2F7 may be involved in acquired resistance, as prolonged olaparib treatment resulted in a compensatory reduction in E2F7 levels accompanied by increased RAD51 levels and reduced sensitivity to olaparib. Whether such a downregulation occurs in patient tumors upon olaparib treatment is not yet known, but if so, it may represent one of the mechanisms explaining why despite increases in PFS, many patients eventually relapse in the clinical trials described in Chapter 1.

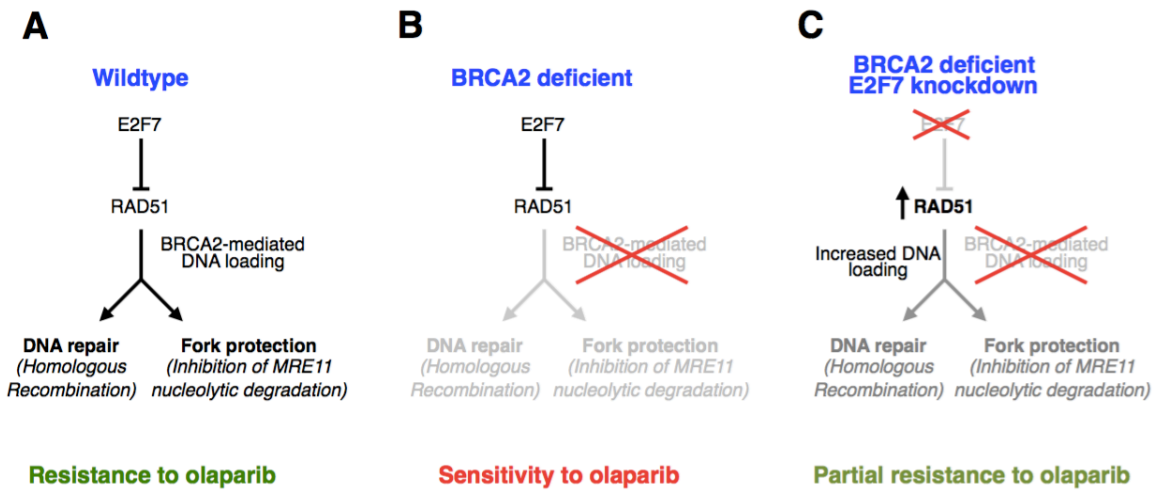

Figure 3.9. Model showing the impact of E2F7 on olaparib sensitivity of BRCA2-deficient cells. In wildtype cells, BRCA2-dependent loading of RAD51 to DNA breaks and stalled replication forks ensures correct HR and fork protection, which promote resistance to olaparib **(A)**. In BRCA2-deficient cells, RAD51 loading is reduced and both HR and fork protection are impaired, which results in olaparib sensitivity **(B)**. E2F7 represses expression of RAD51. Loss of E2F7 results in increased RAD51 levels, which allows more binding of RAD51 to damaged DNA. This promotes both HR and fork protection, restoring resistance to olaparib **(C)**.

Previous studies have suggested an association between PARPi resistance and protection against nucleolytic degradation of stalled replication forks in BRCA2-deficient cells. For example, depletion of ZRANB3, HLTF or SMARCAL1 abolishes formation of the reversed fork structures targeted by the MRE11 nuclease and results in chemoresistance of BRCA2-deficient cells (96). Inhibition of MRE11 (88, 89), or loss of PTIP (which recruits MRE11 to reversed forks) (93), or of RADX (which inhibits RAD51 accumulation to stalled replication forks) (95) can similarly rescue PARPi sensitivity of BRCA2-deficient cells without restoring HR. Finally, inhibition of a parallel fork degradation pathway governed by the chromatin modifier EZH2 which recruits the nuclease MUS81 to stalled forks (91), or channeling the processing stalled forks toward translesion synthesis-mediated lesion bypass rather than fork reversal (128), is also associated with reduced chemosensitivity of BRCA2-deficient cells. Here, I show that

depletion of E2F7, a transcriptional repressor of RAD51, also results in protection against degradation of stalled replication forks by MRE11. These data suggest that increased RAD51 levels are enough to promote its loading to stalled replication forks even in the absence of BRCA2 activity.

Additionally, I found that E2F7 knockdown also restores HR in BRCA2-deficient cells. This effect also involves regulation of RAD51 expression, as E2F7 knock-down could not rescue the HR defect of RAD51-depleted cells, thus ruling out an involvement of other E2F7 targets involved in HR (such as BRCA1). How RAD51 is loaded to DSB ends in BRCA2-depleted cells is not clear. My data indicate that it is unlikely to involve the activity of RAD52, which has been previously implicated in RAD51 loading in BRCA2-deficient cells (130).

At this time, the relative contribution of HR rescue and fork protection activities to the E2F7-mediated chemoresistance of BRCA2-depleted cells is unclear. Nevertheless, to our knowledge this is the first time that restoration of HR (independent of a reversion mutation) is identified as a mechanism of PARPi resistance in BRCA2-deficient cells. Notably, while our manuscript reporting these novel findings was under revision, another group published results corroborating my findings that E2F7 depletion in BRCA2-depleted cells results in the restoration of HR as well as the rescue of PARPi sensitivity, highlighting the reproducibility of these results (134). Recently, E2F7 was reported to bind to double strand break sites and inhibit their repair, potentially through altering chromatin status at these sites (135). While it is not known if this activity requires RAD51, it is nevertheless possible that the rescue of BRCA2 chemosensitivity by E2F7 depletion also reflects this transcription-independent role of E2F7 in repressing DNA double strand break repair.

3.4 Materials and Methods

Cell culture and protein techniques. Human HeLa, HCC1395, 293T and U2OS cells were grown in Dulbecco's modified Eagle's medium (DMEM), while SH-SY5Y were grown in DMEM/F12 (1:1). Media was supplemented with 10% fetal calf serum. U2OS DR-GFP cells were obtained from Dr. Jeremy Stark (City of Hope National Medical Center, Duarte, CA) (132). Chromatin fractionation experiments were performed as previously described (122, 136, 137). Antibodies used for Western blot (that were not previously listed in Chapter 2) were: RAD51 (Santa Cruz Biotechnology sc-8349), Vinculin (Santa Cruz Biotechnology sc-73614), RAD52 (Santa Cruz Biotechnology sc-365341).

For gene knockdown, cells were transfected with Stealth siRNA (Life Tech) using Lipofectamine RNAiMAX reagent. For co-depletion experiments, control (non-targeting) siRNA was added to the targeting siRNA in the single knockdown samples to equalize total siRNA levels. The siRNA targeting sequences used were:

E2F7 #1: GGACGATGCATTTACAGATTCTCTA;

E2F7 #2: GACTATGGGTAACAGGGCATCTATA;

E2F7 #3: AAACAAAGGTACGACGCCTCTATGA (used for E2F7 knockdown unless otherwise mentioned);

RAD51: CCATACTGTGGAGGCTGTTGCCTAT;

RAD52: GGCCAATGAGATGTTTGGTTACAAT.

Knockdown was confirmed for all proteins targeted, using western blot unless otherwise indicated. Efficacy of knockdown was confirmed in each cell line used in this dissertation, however representative western blot images for a single cell line are shown for each siRNA.

Immunofluorescence. Immunofluorescence experiments were performed as previously described (122) with small modifications. Briefly, cells were fixed with 4% paraformaldehyde for 10 min, followed by three washes with phosphate-buffered saline (PBS). Cells were then permeabilized with 0.2% Triton X-100 for 10 min. After two washes with PBS, slides were blocked with 3% bovine serum albumin (BSA) in PBS for 10 min, followed by incubation with the primary antibody diluted in 3% BSA in PBS, for 2 h at room temperature. After three washes with PBS, the secondary antibody (Alexa Fluor 488 from Invitrogen) was added for 1 h. Slides were mounted with DAPI-containing Vectashield mounting medium (Vector Labs). Antibodies used for immunofluorescence were: H2AX (Bethyl A300-081A) and 53BP1 (Bethyl A300-272A).

Functional assays. Cisplatin was obtained from Biovision. Rabusertib (Chk1 inhibitor) was obtained from Selleck Chemicals. Cellular viability and apoptosis assays were performed as described in Chapter 2. The neutral comet assay was performed using the CometAssay kit (Trevigen 4250-050).

HR and non-homologous end joining (NHEJ) assays were performed as previously described (132). Briefly, these U2OS cell lines contain integrated reporters with a GFP cassette interrupted by a restriction enzyme (I-SCEI) cut site. Repair of the I-SCEI-induced break through the DNA repair mechanism indicated (i.e. homology-dependent repair or NHEJ) results in restoration of the GFP reporter cassette and GFP-positive cells detectable via flow cytometry.

Quantification of gene expression by real-time quantitative PCR (RT-qPCR). Total mRNA was purified using TRIzol reagent (Life Tech) according to the manufacturer's instructions. To generate cDNA, 1 µg RNA was subjected to reverse transcription using the RevertAid Reverse Transcriptase Kit (Thermo Fisher Scientific) with oligo dT

primers. Real-time quantitative polymerase chain reaction (RT-qPCR) was performed with PerfeCTa SYBR Green SuperMix (Quanta), using a CFX Connect Real- Time Cycler (BioRad). The cDNA of GAPDH gene was used for normalization. Primers used were:

E2F7 for: GGAAAGGCAACAGCAAACTCT;

E2F7 rev: TGGGAGAGCACCAAGAGTAGAAGA;

RAD51 for: TGCTTATTGTAGACAGTGCCACC;

RAD51 rev: CACCAAACTCATCAGCGAGTC;

GAPDH for: AAATCAAGTGGGGCGATGCTG;

GAPDH rev: GCAGAGATGATGACCCTTTTG.

DNA fiber assay. HeLa cells, pretreated with the indicated siRNA oligonucleotides, were incubated with 100 μM IdU for 30 min. Cells were washed with PBS and incubated with 4 mM hydroxyurea (HU) (with or without 50 μM Mirin as indicated) for 3 h. Following removal of HU media and a PBS wash, fresh media containing 100 μM CldU was added for another 30 min. Next, cells were harvested and DNA fibers were obtained using the FiberPrep kit (Genomic Vision) according to the manufacturer's instructions. DNA fibers were stretched on glass slides using the FiberComb Molecular Combing instrument (Genomic Vision). Slides were incubated with primary antibodies (Abcam 6326 for detecting CIdU; BD 347580 for detecting IdU; Millipore Sigma MAB3034 for detecting DNA), washed with PBS, and incubated with Cy3, Cy5 or BV480-coupled secondary antibodies (Abcam 6946, Abcam 6565, BD Biosciences 564879). Following mounting, slides were imaged using a Leica SP5 confocal microscope. At least 200 tracts were quantified for each sample.

Statistical analyses. With the exception of the DNA fiber data, the statistical analysis performed was the t-test (two-tailed, unequal variance). For the DNA fiber data, the Mann–Whitney test was performed. Statistical significance is indicated for each graph (ns = not significant, for $P > 0.05$; * for $P \leq 0.05$; ** for $P \leq 0.01$; *** for $P \leq 0.001$; **** for $P \leq 0.0001$).

Chapter 4: TIP60 or HUWE1 depletion leads to PARPi resistance in BRCA2-deficient cells

Adapted from: Clements, K.E. et al. (2019) bioRxiv

4.1 Rationale

In the CRISPR knockout screen in BRCA2-deficient cells, guide RNAs targeting the histone acetyltransferase TIP60 as well as HUWE1, an E3 ubiquitin ligase, were significantly enriched in cells surviving olaparib treatment (logP=-3.039 and -6.33, respectively). I was interested in investigating these findings further, as both proteins have significant roles in cellular processes related to DNA replication and repair, yet they have not been directly connected to PARPi sensitivity.

A recent study has suggested that TIP60 interacts with PARP1 in untreated HeLa cells and that untreated TIP60-depleted cells demonstrated reduced PARP1 activity as well as impaired PARP1 flux after photobleaching at IR-damaged chromatin (138). Additionally, a connection between TIP60 and 53BP1, a key mediator of DSB repair pathway choice, is well-established: in wild type cells, a reduction in levels or recruitment of TIP60 leads to increased 53BP1 binding at damaged chromatin, favoring NHEJ over homology-dependent repair (HDR) (139–141). 53BP1 promotes NHEJ by preventing the resection of the ends of DSBs, a key step in HDR pathways, which include RAD51-dependent HR as well as SSA (12). Interestingly, recent work has indicated that exhaustion of 53BP1 by an abundance of DSBs (as one might expect in BRCA2-deficient cells treated with PARPi) leads to an increase in SSA, a repair pathway that results in large deletions and genomic instability, rather than error-free RAD51-dependent HR (142). Thus, I was interested in evaluating the role of TIP60 in PARPi sensitivity and testing which functions of TIP60 accounted for this novel role.

HUWE1 is a large protein, with several domains including the HECT domain, which confers its catalytic activity, as well as the WWE domain, which has been shown to interact with poly-ADP-ribose (PAR) chains *in vitro* (143). Previous work from our lab has shown that HUWE1 helps to alleviate replication stress at stalled forks (136). Furthermore, HUWE1 activity is required for the recruitment of DNA repair factors to chromatin after damage (136, 144). Interestingly, recent studies have identified PARP1, which is regulated by post-translational modifications (77), as a potential damage-related substrate of HUWE1 (144). Other known mediators of PARPi sensitivity, such as HLTF (96, 145), were also identified among HUWE1 substrates, adding that the ubiquitin is likely K6-linked and therefore involved in regulation rather than degradation (144, 146). Finally, RNA sequencing experiments previously performed in our lab in HUWE1 wildtype or knockout cells indicated that RAD51 may be upregulated upon HUWE1 depletion (data not shown), a mechanism I established in Chapter 3 as a pathway to PARPi resistance. Given these potential connections to PARPi sensitivity, I was interested in evaluating HUWE1 as a hit from the screen.

Overall, in this chapter, I validate two proteins previously unconnected to PARPi resistance, namely TIP60 and HUWE1, which cause resistance to PARPi when depleted in BRCA2-deficient cells. Furthermore, I show that the mechanism of resistance caused by TIP60 depletion involves 53BP1-mediated regulation of end resection at double-strand DNA breaks (DSBs).

4.2 Results

4.2.1. Depletion of TIP60 or HUWE1 rescues PARPi sensitivity in BRCA2-deficient cells

I first sought to validate these hits (TIP60 and HUWE1). In order to test the effect of TIP60 or HUWE1 loss on PARPi sensitivity in BRCA2-depleted cells, I knocked down

these genes and assessed cellular viability after olaparib treatment. Strikingly, TIP60 or HUWE1 knockdown in HeLa cells depleted of BRCA2 using siRNA led to PARPi resistance similar to that seen in HR-proficient controls (Figure 4.1 A).

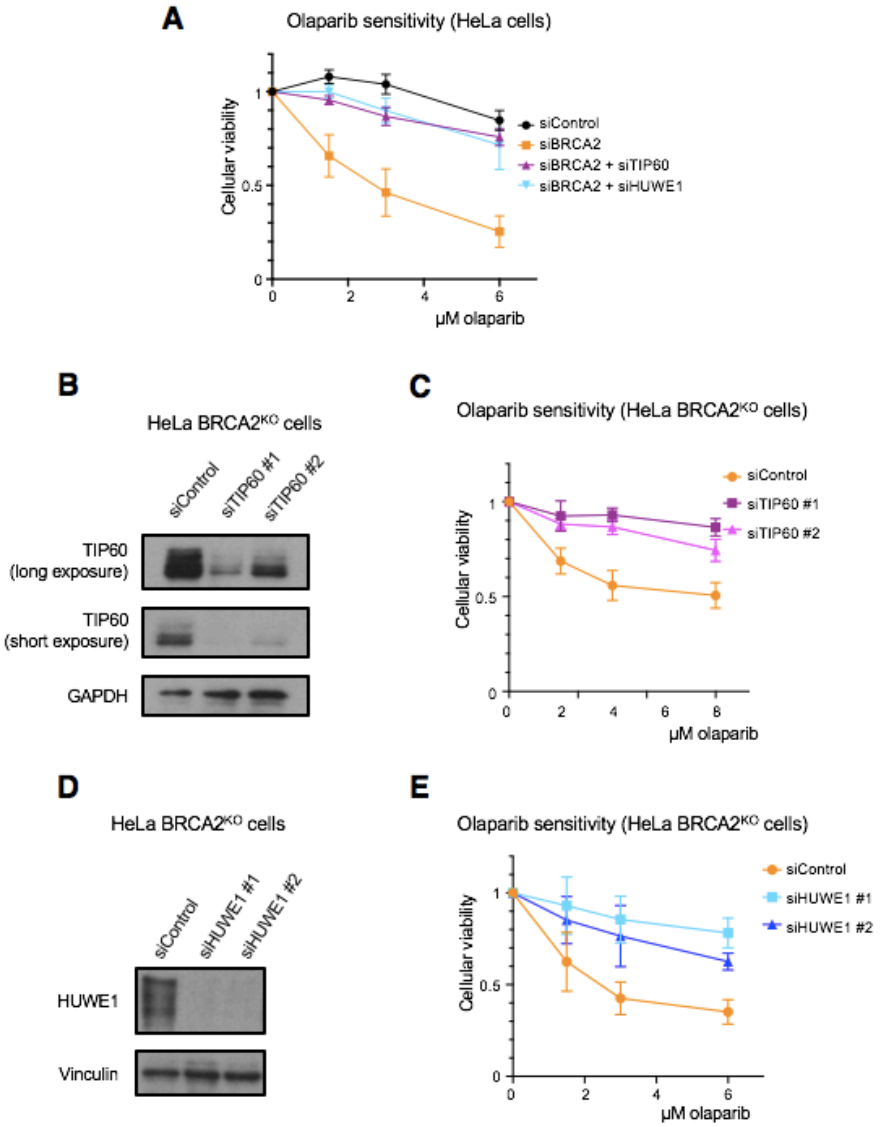

Figure 4.1. TIP60 or HUWE1 knockdown in BRCA2-depleted cells results in PARPi resistance. (A) Knockdown of TIP60 or HUWE1 rescues the olaparib sensitivity of BRCA2-knockdown HeLa cells in cellular viability assays. **(B)** Western blot showing that TIP60 is efficiently depleted with siRNA oligonucleotides employed. **(C)** Depletion of TIP60 by two siRNA oligonucleotides rescues PARPi sensitivity in HeLa BRCA2-knockout cells in cellular viability assays. **(D)** HUWE1 protein is depleted using two siRNA oligonucleotides as shown by western blot. **(E)** Depletion of HUWE1 by two siRNA oligonucleotides rescues PARPi sensitivity in HeLa BRCA2-knockout cells in cellular viability assays. All figures reflect the average of three biological replicates performed after 72 hours of treatment, with standard deviations shown as error bars.

This robust rescue of PARPi sensitivity was also observed in our HeLa BRCA2^{KO} cells upon depletion of TIP60 (Figures 4.1 B and C) or HUWE1 (Figures 4.1 D and E) using either of two siRNA targeting sequences. I next asked whether these phenotypes were cell line-specific by extending our studies into additional cell lines. While TIP60 or HUWE1 depletion alone did not affect sensitivity of wildtype controls to PARPi, co-depletion of either protein in BRCA2-depleted U2OS (Figure 4.2 A) or BRCA2-knockout DLD1 (Figure 4.2 B) cells significantly reduced PARPi sensitivity.

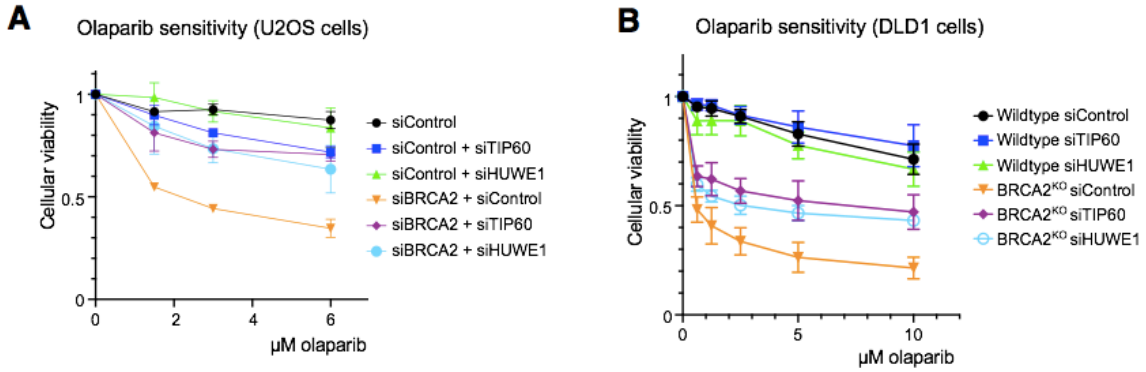

Figure 4.2. The rescue caused by TIP60 or HUWE1 depletion is not cell line-specific. **(A and B)** Knockdown of TIP60 or HUWE1 rescues the olaparib sensitivity of BRCA2-knockdown U2OS **(A)**, and BRCA2-knockout DLD1 **(B)** cells in cellular viability assays. The average of three biological replicates performed after 72 hours of treatment are shown, with standard deviations as error bars.

I next investigated the effect of TIP60 or HUWE1 depletion on olaparib-induced apoptosis using Annexin V flow cytometry. Consistent with the results of the cellular viability assays, depletion of TIP60 or HUWE1 abrogated the increase in Annexin V–positive cells caused by PARPi treatment in BRCA2-knockdown HeLa cells as well as BRCA2-knockout DLD1 cells (Figures 4.3 A and B). I observed similar phenotypes using a second siRNA oligonucleotide for each hit in HeLa BRCA2^{KO} cells (Figures 4.3 C and D).

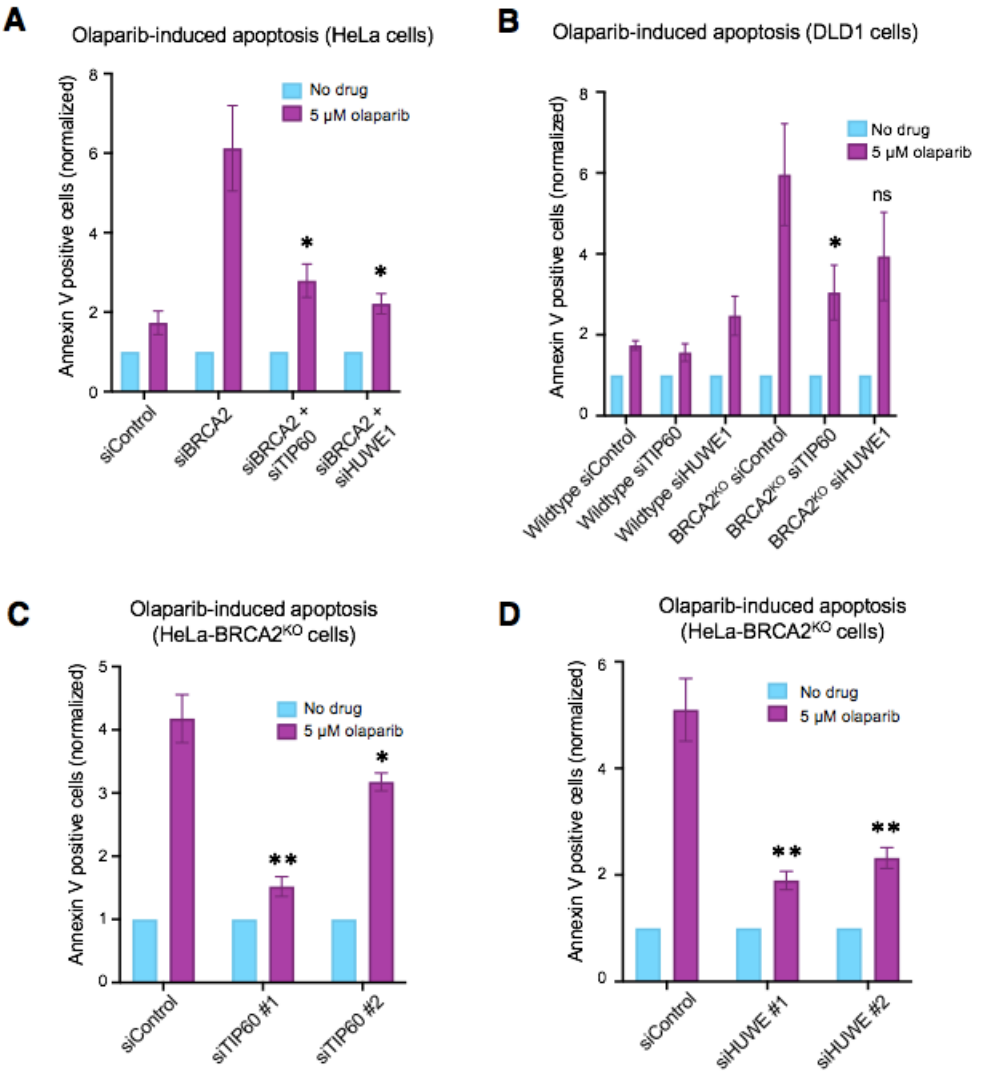

Figure 4.3. Knockdown of TIP60 or HUWE1 with either of two siRNA oligonucleotides rescues olaparib-induced apoptosis in BRCA2-depleted cells. **(A and B)** Olaparib-induced apoptosis is rescued by TIP60 or HUWE1 depletion in BRCA2-knockdown HeLa **(A)** and BRCA2-knockout DLD1 **(B)** cells. **(C and D)** Olaparib-induced apoptosis is rescued by TIP60 **(C)** or HUWE1 **(D)** depletion in BRCA2-knockout cells. Asterisks indicate statistical significance, compared to the olaparib-treated siBRCA2 **(A)** or $BRCA2^{KO}$ siControl **(B, C, D)** samples. All figures reflect the average of three biological replicates performed after 72 hours of treatment, with standard deviations shown as error bars.

In light of this increased cellular survival after PARPi treatment in BRCA2-deficient cells depleted of the two hits, I wondered if these surviving cells would demonstrate improved viability in the long-term. To test this, I performed clonogenic survival assays in HeLa $BRCA2^{KO}$ cells. Cells were pre-treated with siRNAs targeting TIP60, HUWE1, or a

control siRNA, treated with olaparib for three days, and then allowed to form colonies for two weeks in drug-free media. I found that while BRCA2^{KO} cells showed reduced colony-forming ability after olaparib treatment, TIP60- and HUWE1- depleted BRCA2^{KO} cells were able to form colonies after olaparib treatment in a manner similar to wildtype controls (Figure 4.4A). Taken together, these findings confirm the results of the CRISPR knockout screen and demonstrate that TIP60 or HUWE1 depletion leads to PARPi resistance in BRCA2-deficient cells. Several factors which confer resistance to PARPi have also been shown to rescue sensitivity to the DNA damaging agent and widely used chemotherapeutic, cisplatin (75). Thus, I reasoned that TIP60 or HUWE1 depletion may also confer resistance to cisplatin in BRCA2-deficient cells. Using a clonogenic survival assay, I found that depletion of TIP60 or HUWE1 in BRCA2-knockout HeLa cells rescues cisplatin sensitivity back to that of wildtype cells (Figure 4.4B). As cisplatin has remained a mainstay of cancer treatment for decades (147), these results indicate that TIP60 and HUWE1 status may be more broadly relevant in the clinic.

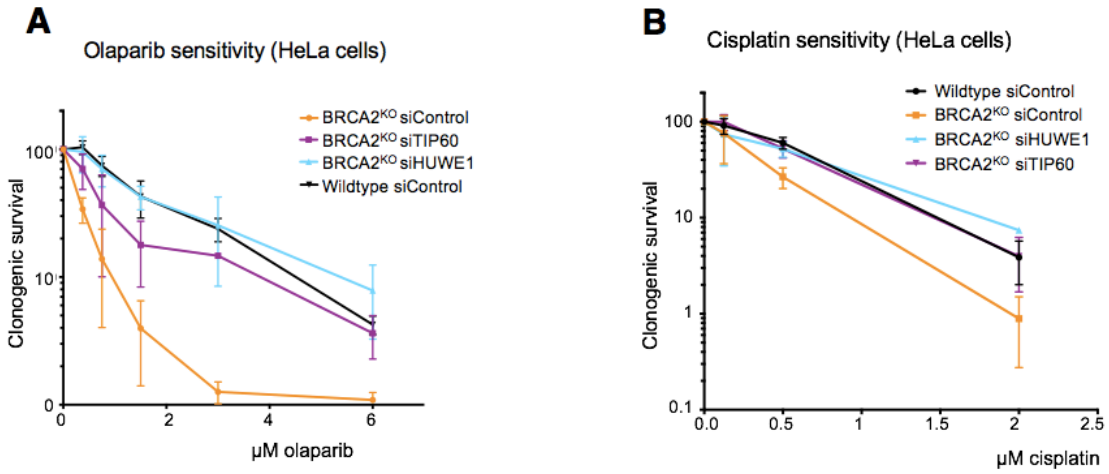

Figure 4.4. TIP60 or HUWE1 depletion rescues colony-forming ability of BRCA2-knockout cells after treatment with clinically used cancer therapies. In clonogenic survival assays, depletion of TIP60 or HUWE1 in BRCA2-knockout HeLa cells led to increased colony formation after PARPi (3 days) **(A)** or cisplatin (24 hours) **(B)** treatment. The averages of three biological replicates are shown, with standard deviations as error bars.

4.2.2. PARPi resistance caused by TIP60 depletion is dependent on the 53BP1/REV7 pathway

After observing that TIP60 depletion robustly rescued PARPi sensitivity, I sought to investigate the mechanisms through which this may occur. To this end, I tested the effect of TIP60 depletion on several previously proposed mechanisms of PARPi-induced cytotoxicity. Trapping of PARP1 on the chromatin has been suggested as an underlying cause of the toxicity of PARPi (78). Given that TIP60 has been previously connected to the flux of PARP1 on chromatin (138), I tested if TIP60 depletion may abrogate this PARP-trapping effect of the inhibitor. However, I observed no difference in trapped PARP1 after TIP60 depletion using a chromatin fractionation assay (Figure 4.5A). Furthermore, an aberrant increase in replication fork speed was recently proposed as a mechanism of action of PARPi (92). While I did observe an increase in replication fork speed upon PARPi treatment, this phenotype was not affected by TIP60 depletion (Figure 4.5B). Finally, we have previously shown that E2F7 depletion led to PARPi resistance in BRCA2-deficient cells by rescuing the defect in homologous recombination (148). In contrast, TIP60 depletion did not improve the HR efficiency of BRCA2-depleted cells (Figure 4.5C). Interestingly, however, despite no change in HR repair, I observed a reduction in olaparib-induced double-strand breaks in HeLa $BRCA2^{KO}$ cells after TIP60 depletion using a neutral comet assay (Figure 4.6A), suggesting that repair of DSBs is improved in these cells.

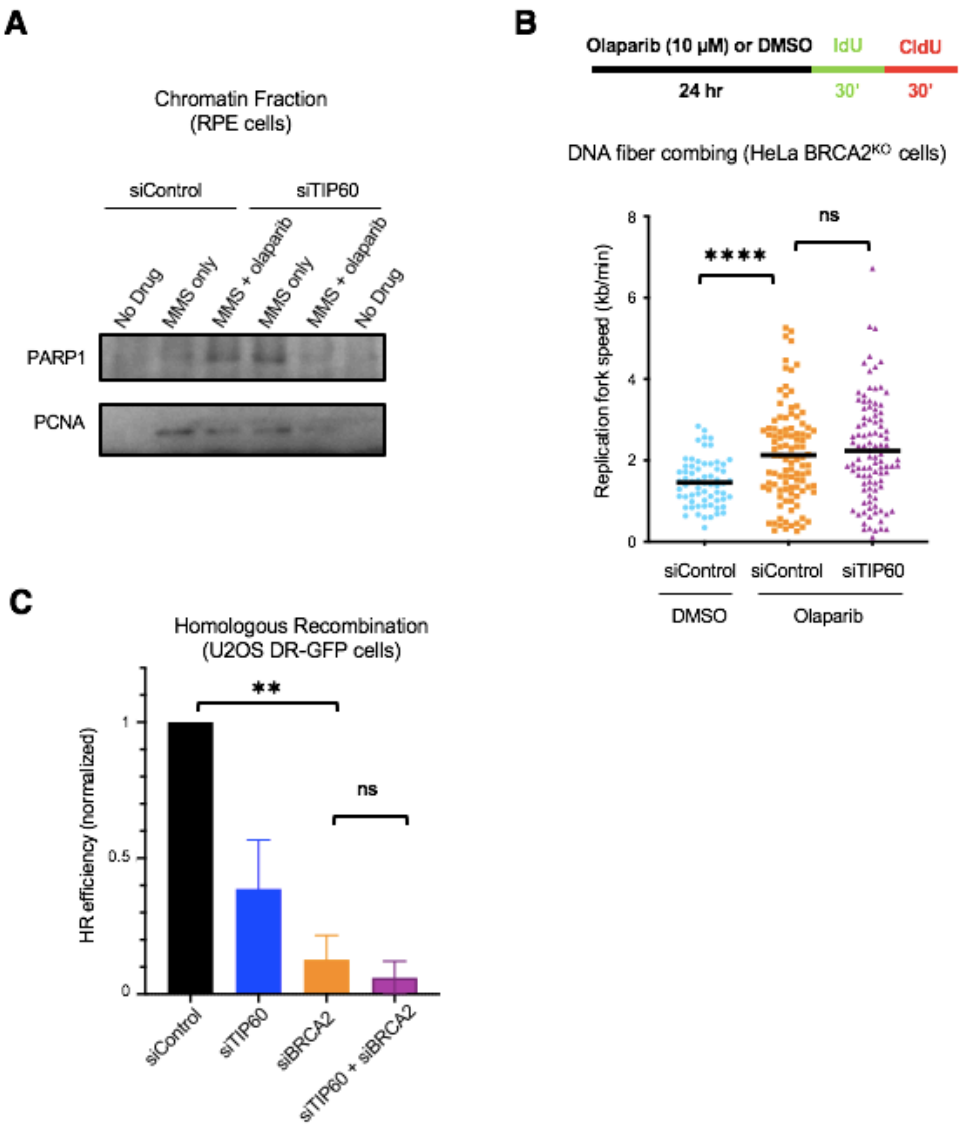

Figure 4.5. TIP60 depletion does not affect other proposed mechanisms of PARPi cytotoxicity. (A) A chromatin fractionation experiment shows that while MMS (0.01%) and olaparib (1 μM) co-treatment for 3 hours induces trapping of PARP1 on the chromatin, this effect is not rescued by TIP60 depletion. **(B)** DNA fiber assay performed in HeLa BRCA2 knockout cells demonstrates that while olaparib treatment increases replication fork speed, this phenotype is not affected by TIP60 depletion. Olaparib (10μM) was added for 24 hours prior to incubation with the thymidine analogs. Horizontal bars reflect the means of replication fork speeds calculated from measurements of CldU tracts. At least 65 fibers were quantified from one experiment. Asterisks indicate statistical significance. **(C)** TIP60 depletion does not rescue the homologous recombination defect caused by BRCA2 depletion as shown using a DR-GFP assay. The averages of three biological replicates are shown, with standard deviations as error bars. Statistical significance is indicated by asterisks.

Previous studies have indicated that TIP60 activity antagonizes the recruitment of 53BP1 to damaged DNA (139–141). 53BP1 is a key mediator of double-strand break repair pathway choice, which suppresses DNA end resection at DSBs and promotes non-homologous end joining (NHEJ) (12, 65). I reasoned that increased 53BP1 binding due to TIP60 depletion may be involved in the improved cellular viability and reduced double-strand breaks observed after olaparib treatment in BRCA2-deficient cells. To test if 53BP1 is required for PARPi resistance in BRCA2-deficient cells depleted of TIP60, I performed additional cellular viability assays. TIP60 was depleted alone or in combination with 53BP1 in HeLa BRCA2^{KO} cells and sensitivity to PARPi was assessed. I found that while TIP60 depletion alone causes resistance, co-depletion of 53BP1 with TIP60 severely diminishes this rescue (Figure 4.6B). Importantly, the magnitude of TIP60 knockdown was unaffected by 53BP1 co-depletion (Figure 4.6C). Recently, the Shieldin complex has been identified as a downstream effector of 53BP1 at the double-strand break (68, 71). Therefore, I next tested if REV7, a component of the Shieldin complex, was also required for the rescue of PARPi sensitivity caused by TIP60 loss. Indeed, co-depletion of REV7 abolished the PARPi resistance produced by the depletion of TIP60 (Figure 4.6 D and E). Taken together, these results demonstrate that the 53BP1/REV7 pathway is required for PARPi resistance caused by TIP60 depletion in BRCA2-deficient cells.

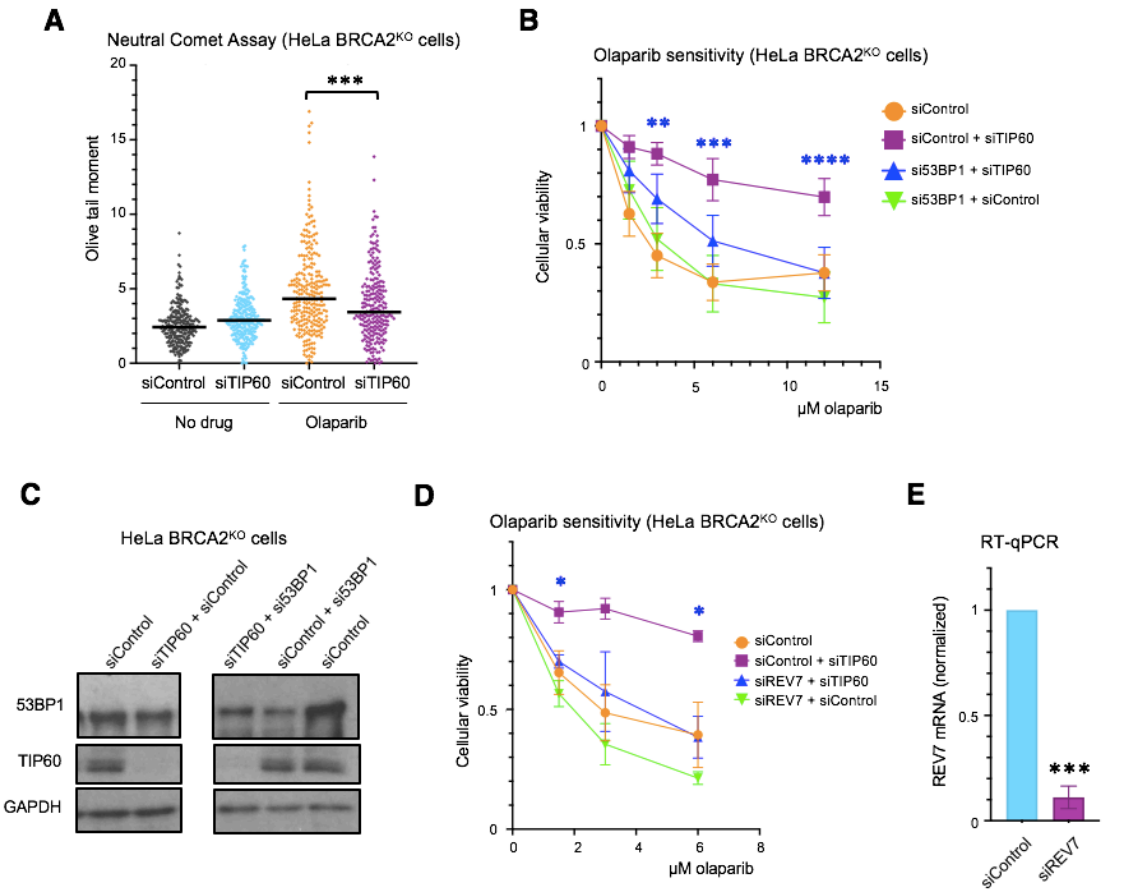

Figure 4.6. TIP60 depletion reduces olaparib-induced double-strand breaks and relies on the 53BP1/REV7 pathway to rescue olaparib-induced cytotoxicity. **(A)** Neutral Comet assay showing that olaparib treatment (10 μM for 24 hours) induces double-strand breaks in HeLa BRCA2-knockout cells, and that this effect is abrogated by TIP60 depletion. Approximately 120 comets from each of two biological replicates were pooled for each sample. Medians are shown as horizontal bars. Asterisks indicate statistical significance. **(B)** PARPi resistance caused by TIP60 depletion is dependent on 53BP1. The averages of 9 experiments are shown, with standard deviations as error bars. Asterisks indicate statistical significance between the "siControl + siTIP60" and "si53BP1 + siTIP60" conditions. **(C)** Western blot showing that 53BP1 is depleted by the siRNA oligonucleotides employed, and that TIP60 depletion is equivalent when depleted alone or in combination with 53BP1. **(D)** REV7 is required for the PARPi resistance after TIP60 knockdown. The averages of 3 biological replicates are shown, with standard deviations as error bars. Asterisks indicate statistical significance between the "siControl + siTIP60" and "siREV7 + siTIP60" conditions. **(E)** Quantitative PCR assay demonstrating the efficacy of the siRNA oligonucleotide targeting REV7. Data shown is the average of three biological replicates, normalized to the siControl condition, with standard deviations shown as error bars. Statistical significance is indicated by asterisks.

4.2.3. TIP60 depletion increases 53BP1 binding at double-strand breaks and reduces end resection

I next sought to directly assess the impact of TIP60 depletion on the binding of 53BP1 near the double-strand break site in BRCA2-deficient cells. I used a chromatin immunoprecipitation (ChIP) assay with a 53BP1 antibody to evaluate binding near the site of an inducible double-strand break within an integrated reporter in the previously described U2OS-DSB reporter cell line (141). qPCR analysis of the immunoprecipitated DNA revealed increased 53BP1 binding near the double-strand break site after TIP60 knockdown in BRCA2-depleted cells (Figure 4.7A).

As the 53BP1/Shieldin pathway functions to prevent excessive end resection at DNA ends, I sought to investigate the effect of TIP60 depletion on end resection (68). To test this, I quantified the percentage of cells that were positive for RPA, a protein which binds to single-stranded DNA produced by end resection, using flow cytometry as previously described (149, 150). I observed an accumulation of S-phase cells in control cells treated with olaparib, which was not observed in siTIP60-treated cells (Figure 4.7B). To prevent these differences from confounding our analysis, I only assessed RPA-positivity in G2 and M -phase cells. In this population of cells, olaparib treatment caused an increase in the percentage of RPA-positive cells, which was reduced upon TIP60 depletion (Figure 4.7C). Overall, these findings indicate that TIP60 depletion increases 53BP1 binding to olaparib-induced DSBs in BRCA2-deficient cells, suppressing end resection.

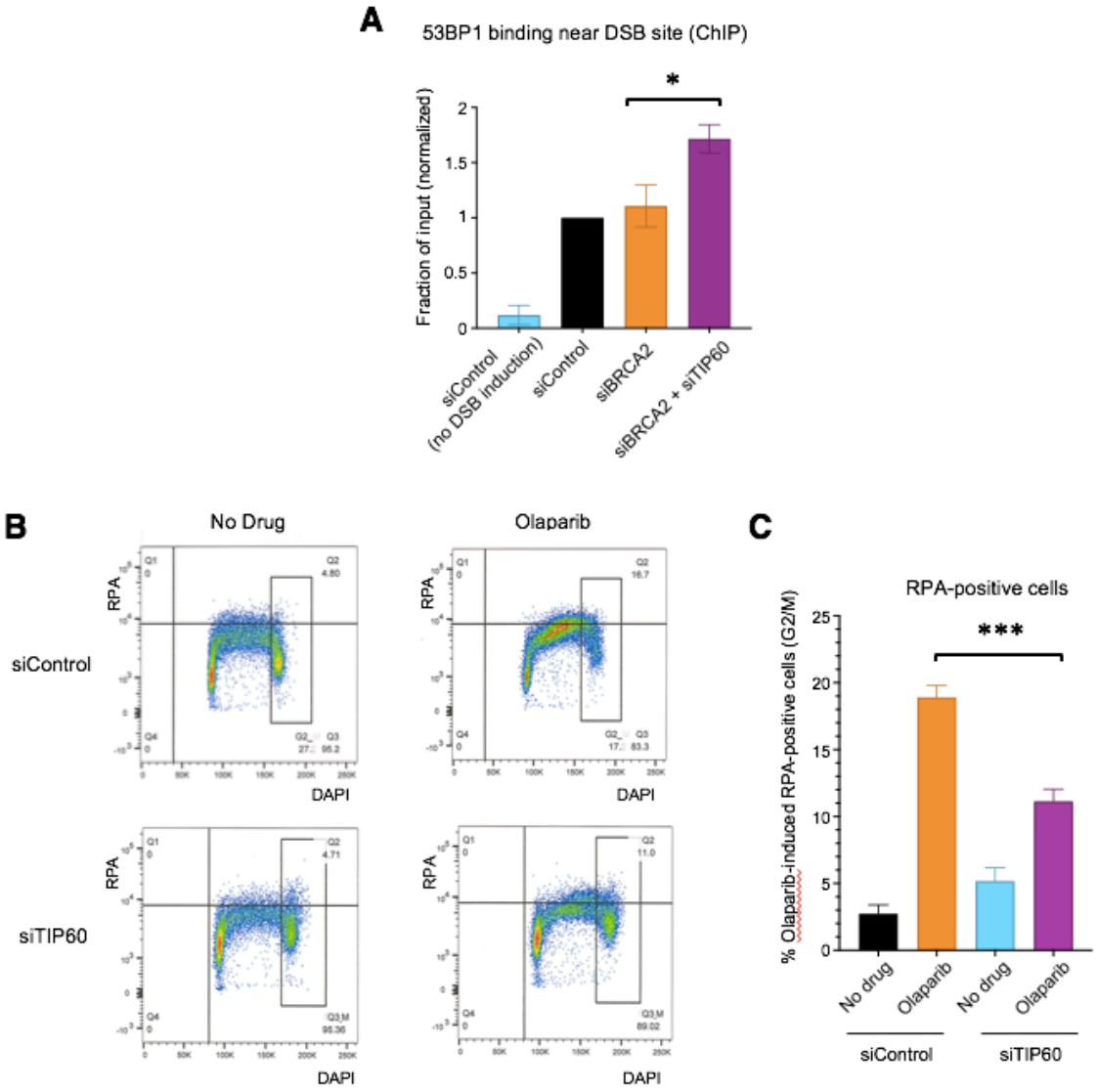

Figure 4.7. Functional consequences of TIP60 depletion (A) Depletion of TIP60 leads to increased recruitment of 53BP1 near the site of the double-strand break in BRCA2-depleted U2OS-DSB reporter cells. DSBs were generated at a specific genomic locus through induction of expression of LacI-FokI nuclease. Then, chromatin immunoprecipitation was performed with an antibody against 53BP1 and qPCR was performed using primers for the DSB site. The averages of 3 biological replicates are shown, with standard error of the mean as error bars. Asterisks indicate statistical significance from a paired TTEST. **(B and C)** Cells were treated with 10 μM olaparib for 12 hours before being harvested for flow cytometry experiments using an RPA antibody. **(B)** Flow cytometry dot plot of DAPI versus RPA staining intensity illustrates the gating (inset box) used. Cells in Quadrant 2 (Q2) were considered RPA-positive, and cells in Quadrant 3 (Q3) RPA-negative; this cutoff was determined based on the "No treatment" condition and was kept constant across all samples. Approximately 20,000 events per sample from a single experiment are shown, and similar results were obtained across 3 experiments. **(C)** TIP60 loss leads to a reduction in olaparib-induced end resection as measured by quantification of RPA-positive cells. Averages of 3 biological replicates are shown, with standard deviations as error bars. Asterisks indicate statistical significance.

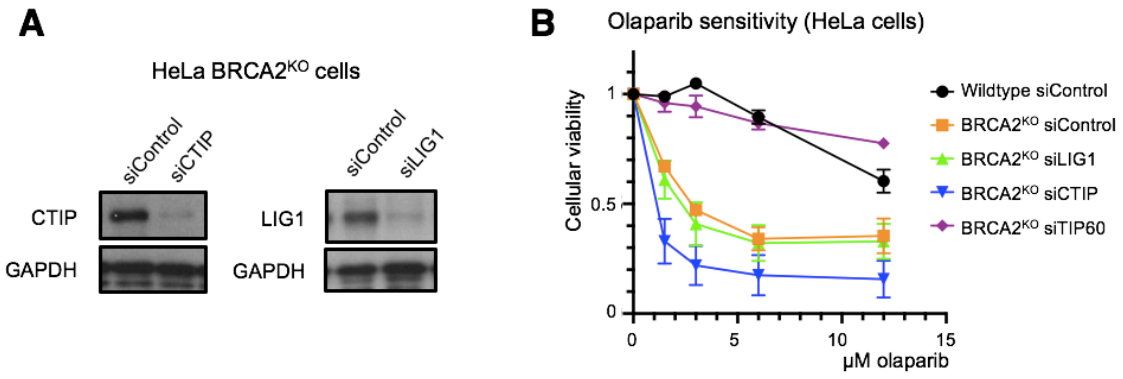

Figure 4.8. Functional impact of TIP60, LIG1, or CTIP depletion in BRCA2-knockout cells. (A) The efficacy of the siRNA oligonucleotides targeting CTIP and LIG1 are shown using western blot. **(B)** Cellular viability assays demonstrate that depletion of CTIP or LIG1 is not sufficient to cause PARPi resistance in BRCA2-knockout HeLa cells. The averages of three biological replicates are shown, with standard deviations as error bars.

Altogether, I observed that TIP60 depletion causes PARPi resistance in a manner dependent on the 53BP1/REV7 pathway, and subsequently causes a reduction in olaparib-induced end resection. Notably, inhibiting end resection directly via depletion of CTIP was not sufficient to cause PARPi resistance in BRCA2-deficient cells (Figure 4.8). Previously, exhaustion of 53BP1 by an abundance of DSBs (as one might expect in BRCA2-deficient cells treated with PARPi) was shown to lead to an increase in single strand annealing (SSA), a repair pathway downstream of end resection that results in large deletions and genomic instability (142). Therefore, we reasoned that the observed increase in 53BP1 binding may rescue PARPi sensitivity by preventing SSA. However, inhibiting SSA via depletion of LIG1 also failed to cause PARPi resistance in this context (Figure 4.8). One potential explanation for these findings is that increased 53BP1 recruitment not only reduces end resection, but also promotes DSB repair through NHEJ (12). To address this, our collaborators Anchal Sharma and Subhajyoti De investigated NHEJ DNA repair signature at somatic structural variation breakpoints in publicly available genomic datasets. Bioinformatic analysis of the Australian Ovarian Cancer Study cohort (OV-AU) dataset suggests a higher incidence of NHEJ in ovarian tumors

with low TIP60 expression, in both BRCA2-high and BRCA2-low backgrounds (data not shown) (98). Overall, this leads to a model in which TIP60 depletion increases 53BP1 binding near the double-strand break, leading to a reduction in end resection and subsequent PARPi resistance, potentially through an increase in NHEJ (Figure 4.9).

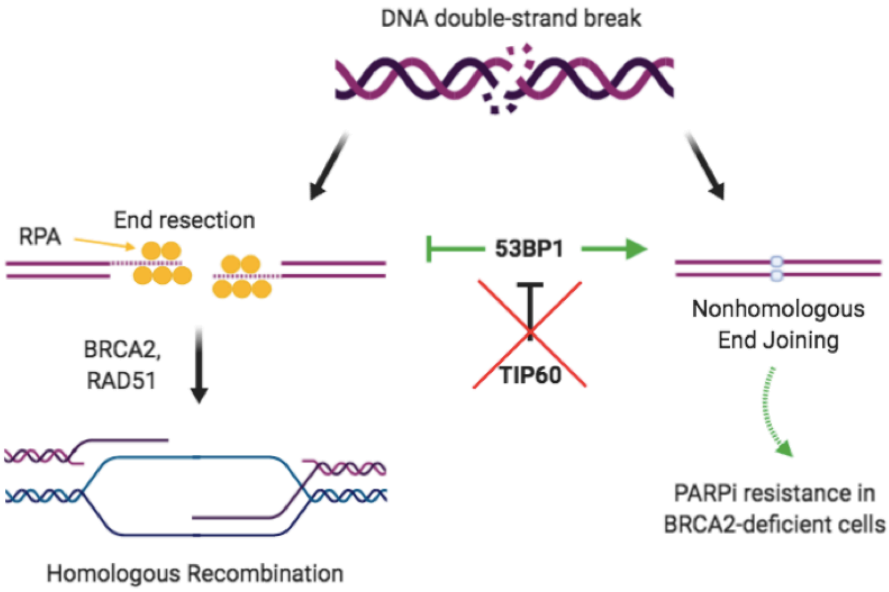

Figure 4.9. Proposed model for resistance caused by TIP60 depletion. In BRCA2-proficient cells, homologous recombination is the most accurate mechanism of double-strand break repair. However, this pathway is not functional in BRCA2-deficient cells. TIP60 depletion increases 53BP1 binding at the double-strand break in BRCA2-deficient cells, preventing the break from proceeding down the "dead-end" process of HR and instead directs it towards repair by NHEJ.

4.3 Discussion

In this chapter, I further validate the results of our CRISPR knockout screen investigating genetic factors governing resistance to PARPi in BRCA2-deficient cells. Specifically, here I test two top hits, TIP60 and HUWE1, using several cellular survival and apoptosis assays, in multiple cell lines. Furthermore, I identify the mechanisms through which TIP60 depletion leads to resistance, showing that this rescue of PARPi-

induced cytotoxicity is dependent on both 53BP1 and REV7. Functionally, TIP60 depletion increases the binding of 53BP1 near the double-strand break, reduces olaparib-induced end resection, and ameliorates the olaparib-induced increase in double-strand breaks. This is a novel mechanism of PARPi resistance in BRCA2-deficient cells, and highlights critical differences between BRCA2- and BRCA1-deficiency. In fact, whereas I show that in BRCA2-deficient cells an increase in 53BP1 binding to damaged DNA plays a role in PARPi resistance, others have shown 53BP1 loss to be a mechanism of PARPi resistance in BRCA1-deficent cells (65, 66). This divergent impact of 53BP1 on PARPi resistance in BRCA2- and BRCA1- deficient cells likely reflects the different roles of BRCA1/2 in the double-strand break repair process of homologous recombination, and is consistent with previous reports that 53BP1 depletion rescued defects in proliferation and checkpoint responses in BRCA1-deficient, but not BRCA2-deficient cells (151). BRCA1 functions early in homologous recombination, promoting end resection at the double-strand break; this is in direct opposition to the anti-resection role of 53BP1 (12). Therefore, 53BP1 depletion would be expected to alleviate the defects caused by BRCA1 deficiency and improve the ability of the cell to manage olaparib-induced damage, resulting in resistance. On the other hand, BRCA2 functions much later in the process of homologous recombination. Hence, 53BP1 depletion would not correct this defect; instead, increased 53BP1 binding would reduce end resection and prevent the break from beginning down the homologous recombination pathway, which is a “dead-end” in BRCA2-deficient cells. Altogether, my work identifies a novel mechanism of PARPi resistance in BRCA2-deficient cells and emphasizes the fact that despite both causing defects in homologous recombination, BRCA1- and BRCA2- deficiency represent distinct defects that should not always be grouped together in the laboratory or the clinic.

I show here that 53BP1 is required for the rescue of PARPi sensitivity caused by TIP60 depletion, and also that TIP60-deficient patient tumors show an increase in the non-homologous end joining pathway of double-strand break repair, consistent with the expected effects of an increase in 53BP1 binding at the double-strand break (12, 65). However, 53BP1 has been implicated in additional PARPi-relevant contexts, such as at the replication fork (152–154). The finding that REV7 is also required for the resistance caused by TIP60 depletion supports a mechanism involving activity at the double-strand break (67); however, other potential roles for REV7 at the replication fork have not yet been thoroughly characterized (155). Additionally, REV7 constitutes an important subunit of DNA polymerase zeta, which is involved in translesion synthesis (TLS) (156). This role for REV7 could theoretically contribute to the phenotypes observed here, as increasing TLS through depletion of CHD4 has been suggested to cause resistance to olaparib treatment in one study (128). However, it is important to note that the importance of TLS in response to PARPi has remained controversial as POLZ and POLH mutant cells are not sensitive to all PARPi (78). Furthermore, data indicate that the function of REV7 depletion in mediating PARPi resistance in BRCA1-deficient cells is independent of its role as a member of polymerase zeta, as depletion of REV3 or REV1, other key subunits of polymerase zeta, failed to recapitulate the PARPi resistance caused by REV7 depletion (67). Finally, it has been reported that depletion of REV7 and other polymerase zeta subunits may reduce HR repair; however, as TIP60 depletion did not restore HR repair in our already HR-deficient BRCA2 KO cells (Figure 4.5C), this is an unlikely mechanism through which REV7 depletion would prevent the rescue caused by TIP60 depletion (157). Still, other function(s) of 53BP1/REV7 may potentially be involved in the rescue of PARPi-induced cytotoxicity downstream of TIP60 depletion in BRCA2-deficient cells.

Unlike PARPi, which are relatively new agents in the clinic, cisplatin has remained a mainstay of ovarian cancer treatment for decades (147). As such, survival data and matched genotype and expression data exist in publicly available datasets. Thus, based on my cell culture experiments showing that TIP60 depletion led to cisplatin resistance in clonogenic assays, I wondered if TIP60 expression impacts survival of BRCA2-mutant ovarian cancer patients. Our collaborators Anchal Sharma and Subhajyoti De queried the OV-TCGA database and asked if ovarian cancer patients with low or high TIP60 expression showed any differences in survival, in BRCA2-mutant or BRCA2-wildtype backgrounds. They found that low TIP60 expression in tumors trended towards poorer survival in patients harboring BRCA2 mutations, but not in the BRCA2-wildtype cohort (data not shown) (98). This observation could be due to several factors in the patients with TIP60-low BRCA2-mutant tumors, including features such as increased metastasis, higher tumor burden, or even effects of low TIP60 expression on biological systems outside of the tumor that affect survival (if low TIP60 expression is due to germline, rather than somatic, changes). However, as it is highly likely that most patients in this dataset have been treated with cisplatin, these findings are also consistent with possible increased therapy resistance in the TIP60-low BRCA2 mutant group. Taken together with the results of the cell-based experiments, these data support the conclusion that TIP60 depletion not only confers resistance to PARPi, but also to cisplatin in BRCA2-deficient cells and potentially also in tumors.

4.4 Materials and Methods

Cell culture. Human HeLa, U2OS, and RPE cells were grown in Dulbecco's modified Eagle's medium (DMEM). DLD1 cells were grown in Roswell Park Memorial Institute (RPMI) 1640 medium. DMEM and RPMI were supplemented with 10% fetal bovine serum. DLD1 BRCA2^{KO} cells (Horizon HD105-007) were obtained from Dr. Robert Brosh

(National Institute on Aging, NIH). U2OS-DSB reporter cells were obtained from Dr. Roger Greenberg (University of Pennsylvania) (141).

Gene knockdowns were performed using Lipofectamine RNAiMAX reagent for transfection of Stealth siRNA (Life Tech, unless otherwise noted). Oligonucleotide sequences used were:

TIP60 #1: GATGGACGTAAGAACAAGAGTTATT

TIP60 #2: CACCCATTCATCCAGACGTTTGTTG

HUWE1 #1: TTTAAGGGTGGGCTGATGTCTCATG

HUWE1 #2: CACACCAGCAATGGCTGCCAGAATT

53BP1: TCCCAGAGTTGATGTTTCTTGTGAA

REV7: GTGGAAGAGCGCGCTCATAAA (Qiagen)

CTIP: GGGTCTGAAGTGAACAAGATCATTA

LIG1: CCAAGAACAACTATCATCCCGTGGA

For all genes, siRNA #1 was used for knockdown unless otherwise indicated. Knockdown was confirmed by western blot for all proteins targeted, except REV7, which was assessed using real-time quantitative PCR (RT-qPCR) as described in Chapter 3. Primers used were:

REV7 for: TGCTGTCCATCAGCTCAGAC;

REV7 rev: TCTTCTCCATGTTGCGAGTG.

Protein techniques. For the PARP trapping assay, cells were co-treated with MMS (0.01%) and olaparib (1μM) for 3 hours to induce trapping of PARP1 as previously described (78). Cellular fractionation was performed with the Subcellular Protein Fractionation Kit for Cultured Cells (Thermo Scientific, 78840) per manufacturer's instructions; protein was quantified using the Qubit Protein Assay Kit (Invitrogen). Antibodies used (that were not utilized in previous chapters) were: TIP60 (Santa Cruz

Biotechnology, sc-166323), HUWE1 (Bethyl, A300-486A), Vinculin (Santa Cruz Biotechnology, sc-25336), 53BP1 (Bethyl, A300-272A), CTIP (Santa Cruz Biotechnology, sc-271339), LIG1 (Bethyl, A301-136A), PARP1 (Cell Signaling, 8542), and PCNA (Cell Signaling, 2586).

Drug Sensitivity Assays. Clonogenic survival assays were performed by seeding cells in 6-well plates; after 72 hours (olaparib) or 24 hours (cisplatin) of treatment at the indicated concentrations, media was changed and colonies were allowed to form for 2 weeks. Cells were fixed with a solution of 10% methanol + 10% acetic acid and stained using crystal violet (2% solution, Aqua Solutions).

Functional assays. The chromatin immunoprecipitation (ChIP) experiments to investigate 53BP1 binding near a double-strand break site were performed as previously described with minor modifications (141). The U2OS-DSB reporter cell line, with an integrated reporter transgene and inducible expression of mCherry-LacI-FokI nuclease, were pretreated with the indicated siRNA for 48 hours, then treated with 4-hydroxytamoxifen (4-OHT, 1 μM) and shield-1 ligand (1 μM) to induce nuclease expression and subsequent double-strand break formation. Five hours after induction, cells were harvested and processed using the SimpleChIP Enzymatic Chromatin Immunoprecipitation Kit (Cell Signaling, 9003) according to the manufacturer's instructions. The antibody used for immunoprecipitation was Anti- 53BP1 (Bethyl, A300-272A). Immunoprecipitated DNA was subjected to real-time qPCR with PerfeCTa SYBR Green SuperMix (Quanta), using a CFX Connect Real-Time Cycler (BioRad). Primers used for the DSB-reporter locus were:
for: GGAAGATGTCCCTTGTATCACCAT;
rev: TGGTTGTCAACAGAGTAGAAAGTGAA.

Detection of RPA-positive cells was performed as previously described, using a BD FACSCanto 10 flow cytometer (149, 150). Data were analyzed using FlowJo software (BD). The neutral comet assay as described in Chapter 3 and olive tail moment was analyzed using CometScore.

Statistical analyses. For the neutral comet assays, the Mann-Whitney statistical test was performed. For the olaparib sensitivity assays, data were analyzed using a two-way ANOVA in GraphPad Prism with Tukey's multiple comparison post-hoc test. For all other assays, the statistical analysis performed was the t-test (two-tailed, unequal variance unless indicated). Statistical significance is indicated for each graph (ns = not significant, for $P > 0.05$; * for $P \leq 0.05$; ** for $P \leq 0.01$; *** for $P \leq 0.001$; **** for $P \leq 0.0001$).

Chapter 5: Discussion

5.1. Mechanisms of PARPi resistance in BRCA2-deficient cells identified through CRISPR screens

5.1.1. BRCA2-independent restoration of homologous recombination

In Chapter 3, I demonstrate that depletion of E2F7, a top hit from the CRISPR knockout screen, causes resistance to PARPi treatment in BRCA2-deficient cells. I show this using several methods in multiple cell lines, including cellular viability assays and measurements of olaparib-induced apoptosis. My experiments indicate that E2F7 depletion reduces double-strand break accumulation, rescues the homologous recombination defect caused by BRCA2-depletion, and confers protection of stalled replication forks. Furthermore, I show that the effects of E2F7 depletion on homologous recombination and replication fork protection are dependent on RAD51, which is upregulated at the mRNA, total protein, and chromatin-bound protein levels upon E2F7 depletion. Although restoration of HR independent of BRCA1/2 reversion mutations has been shown extensively in BRCA1-deficient cells (65–76), to our knowledge my work establishes this as a novel mechanism associated with PARPi resistance in BRCA2-deficient cells. Interestingly, at the time of publication of this work, another group independently corroborated many of my findings (134). In particular, Mitxelena et *al*. also demonstrated that depletion of E2F7 led to an increase in RAD51 at the mRNA and total protein level, and rescue of the HR defect and PARPi sensitivity caused by BRCA2 deficiency (134). Additionally, their finding that E2F7 depletion leads to an increase in RAD51 foci formation nicely supports my chromatin fractionation experiments demonstrating an increase in chromatin-bound RAD51 upon E2F7 depletion.

It is conceptually interesting that both my experiments and those of Mitxelena et al. demonstrate that increased RAD51 is able to restore HR in BRCA2-depleted cells, as

it raises the question, 'How is RAD51 loaded in the absence of BRCA2?'. As both groups used siRNA depletion of BRCA2 for the HR (DR-GFP) assay, this may be explained by incomplete knockdown of BRCA2, with residual protein remaining to load RAD51 and restore HR. However, I also observed increased RAD51 loading onto chromatin after E2F7 depletion in my BRCA2 knockout cells (Figure 3.5D), which lack full-length BRCA2 (Figure 2.1A). Our data also indicate that RAD52, a protein reported to load RAD51 in the absence of BRCA2 (130), was likely not involved (Figure 3.3D). Surprising results obtained from the CRISPR activation screen may give an indication. Even though the BRCA2 knockout cells lack full-length BRCA2 protein, lack the ability to form RAD51 foci (data not shown), and demonstrate extreme olaparib sensitivity consistent with lack of BRCA2 function, BRCA2 emerged as a top hit in the CRISPR activation screen investigating PARPi resistance in the BRCA2-knockout cells (Supplemental Table S1 of Ref (98)). This indicates that in the BRCA2-knockout cell line, transcriptional activation of the *BRCA2* gene unexpectedly yielded PARPi resistance. While I cannot rule out the possibility that very low levels of full-length BRCA2, below the detection limits of western blot, are still present in this cell line due to the aneuploidy of HeLa cells, there is another, more potentially meaningful possibility. Despite losing detectable full-length BRCA2, the BRCA2 knockout clone that I generated using CRISPR/Cas9 demonstrated the appearance of two lower molecular weight bands detected with the BRCA2 antibody (Figure 2.1A). Thus, it is possible that these cells contain truncated, hypomorphic forms of BRCA2. As the majority (80%) of pathogenic BRCA1/2 variants in the clinic are caused by nonsense mutations leading to truncated proteins, further investigating these lower molecular weight species could reveal meaningful information (16).

One major limitation of the field is that for the most part, only correlation, rather than causation, can be established between the functional phenotypes seen and the

impact on cytotoxicity. For example, in addition to HR restoration, E2F7 depletion also rescued replication fork protection after HU treatment, and the relative contributions of these two mechanisms to the observed effect on PARPi sensitivity in this case is unclear. This is due in no small part to the fact that there is much overlap with regard to proteins involved in various DNA repair processes implicated in PARPi resistance, such as replication fork protection and homologous recombination; thus, attempts to show causation by manipulating one process often affects the other. To this end, additional studies utilizing BRCA2-deficient cells corrected with S3291A mutant BRCA2 may be useful, as this mutation compromises fork protection, but not homologous recombination (88). In addition, interestingly, PARPi were recently developed which uncouple the inhibition of PARylation from PARP trapping by targeting the inhibited PARP for degradation; this may help to further parse out the contributions of these two activities of PARPi to cytotoxicity in various contexts (158). In the future, identification of additional proteins specific to each process, or of protein domains required for one process but not the other, may help to uncouple investigations into the underlying mechanisms of PARPi sensitivity and resistance.

Still, even without directly showing causation, the finding that PARPi resistance was associated with restored homologous recombination independent of a reversion mutation in BRCA2 is novel and important, as it highlights the potential advantages of using functional testing, rather than purely BRCA1/2 mutation status, to predict patients who may benefit from PARPi therapy. Currently, the closest thing to testing of homologous recombination function in the clinic is the use of Myriad Genetics' "MyChoice HRD Plus" test, which seeks to identify patients whose tumors are predicted to be deficient in homologous recombination based on genomic scars consistent with this phenotype, including loss of heterozygosity, telomeric allelic imbalance, and large-scale state transitions (159). This approach to stratifying patients has several

advantages, including identifying patients who may have homologous recombination deficiency without mutations in BRCA 1 or 2, and also avoiding the ambiguity caused by BRCA1 and 2 VUS. Consistent with this, several clinical trials described in Chapter 1 demonstrate that patients with HRD identified using similar methods benefited from PARPi therapy, despite not having confirmed deleterious mutations in BRCA1 or 2. My work indicates that such an approach may also be advantageous in that it would identify a different group of patients: those who may have deleterious BRCA2 mutations but would in fact not benefit from PARPi treatment due to restoration of homologous recombination through other mechanisms, such as E2F7 deficiency.

5.1.2. Modulation of end resection at the double-strand break

In Chapter 4, I reveal that depletion of TIP60 or HUWE1 causes PARPi resistance in BRCA2-deficient cells. This observation holds true in several cell lines, in both short-term cellular viability assays as well as long-term survival assays measuring colony-forming ability. I took a broad approach to investigating the potential mechanisms underlying the resistance caused by TIP60 depletion. I tested many of the proposed mechanisms of cytotoxicity and resistance of PARPi described in Chapter 1, and asked what effect TIP60 depletion had on these phenotypes (Figure 4.5). Consistent with many other reports, I observed that co-treatment of MMS and olaparib resulted in increased PARP1 on chromatin (78, 115), however, TIP60 depletion did not ameliorate this effect. Furthermore, I was able to reproduce one of the newest observations in the realm of PARPi: that PARPi treatment, in fact, causes an increase in replication fork speed (92). However, once again, TIP60 depletion did not impact this phenotype. Finally, TIP60 depletion did not rescue the HR defect caused by BRCA2-deficiency. While these experiments proved to be all negative results with regards to the mechanism of action of TIP60 depletion, these results are valuable for the field. In particular, these

studies are one of the first that have attempted to reproduce the reported increase in replication fork speed caused by PARPi treatment (92). While this experiment recapitulated the observed increase in speed, other data outlined here challenges this phenotype as a mechanism of cytotoxicity (see section 5.2).

I observed that TIP60 depletion rescued olaparib-induced double-strand breaks (DSBs) using the neutral comet assay (Figure 4.6). Based on this observation, coupled with the failure of TIP60 depletion to restore HR, I hypothesized that the observed resistance may depend on another mechanism of DSB repair. Importantly, I discovered that the PARPi resistance caused by TIP60 depletion is dependent on 53BP1 and REV7, proteins that are involved in preventing resection of DSBs, and promoting nonhomologous end joining (NHEJ) repair. Further supporting this mechanism, I found that TIP60 depletion increased the binding of 53BP1 near the site of a DSB in BRCA2-deficient cells, consistent with previous reports in BRCA2-wildtype cells (141). Finally, I tested the effect of loss of TIP60 on olaparib-induced end resection using a flow cytometry-based assay for the quantification of olaparib-induced RPA-positive cells (Figure 4.7). I found that 12 hours of PARPi treatment caused an accumulation of cells in S-phase, consistent with findings by other groups (81, 92). Interestingly, it seemed that TIP60 depletion ameliorated this S-phase accumulation, perhaps reflecting resistance to damage caused by PARPi (81). Thus, to eliminate any additional variables that might confound my analysis, I only assessed olaparib-induced RPA positive cells in the G2 phase of the cell cycle (Figure 4.7 C). I found that TIP60 depletion also rescued olaparib-induced end resection as measured by RPA-positive cells. Altogether, these results yield a model in which loss of TIP60 leads to an increase in 53BP1 binding near the DSB, reducing end resection and causing PARPi resistance, perhaps due to avoiding commitment to HR, which is a “dead end” in BRCA2-deficient cells (Figure 4.9).

Additionally, this model predicts that TIP60 depletion would increase NHEJ efficiency; ideally, I would have directly assessed this phenotype, however, this was prevented by technical limitations. In our laboratory, we have previously utilized reporters for various DSB repair pathways which rely on the enzymatic induction of a DSB at a specific cut site within the integrated reporter (132). However, we were unable to obtain reliable results using this method to examine the effect of TIP60 depletion. This may be due to the fact that the proposed mechanism of action of TIP60 in modulating DSB repair pathway choice is through modifying histones within the chromatin near the DSB (141). Recent work has characterized the chromatin landscape surrounding breaks throughout the genome, and found that different sites within the genome are prone to different types of repair (ie NHEJ or HR) and are associated with broad-scale chromatin remodeling (160). Thus, a reporter integrated arbitrarily within a single site of the genome may not be appropriate to investigate the effects of a histone acetyltransferase on repair pathway choice. The Traffic Light Reporter (TLR) system is also available within our lab, in which green or red fluorescence indicates the repair of a single I-SCEI induced DSB by HR or NHEJ, respectively—however the same limitations would apply (161). In the future, utilization of the DIvA (DSB inducible via AsiSI) cell line may be a good option, as it allows for the inductions of DSBs at hundreds of sites within the human genome via 4-hydroxytamoxifen-inducible AsiSI activity (160, 162–164). These sites are already well-characterized, including annotation of which sites are typically repaired by HR or NHEJ (160). Moving forward, it would be interesting to see if TIP60 depletion in BRCA2-depleted DIvA cells would be able to shift HR-prone sites toward NHEJ repair. In lieu of a dependable reporter system currently available in our lab, I asked our collaborators Anchal Sharma and Subhajyoti De to investigate this question using a bioinformatic approach. Their analysis of the Australian Ovarian Cancer Study cohort (OV-AU) suggests that ovarian tumors with low TIP60 expression

demonstrate a higher incidence of NHEJ DNA repair signature at structural variation breakpoints, in line with our model (98).

Overall, I propose a model in which TIP60 depletion leads to an increase in the binding of 53BP1 near the double-strand break, a reduction in olaparib-induced end resection, and rescue of the olaparib-induced increase in double-strand breaks. Ultimately, TIP60 depletion leads to PARPi resistance in a manner dependent on the anti-resection activities of 53BP1 and REV7 at the DSB. Not only is this a novel mechanism of PARPi resistance in BRCA2-deficient cells, but notably this model proposes that the relationship between 53BP1 and PARPi resistance is the opposite in BRCA2-deficient cells as compared to BRCA1-deficient cells. In BRCA1-deficient cells, depletion of 53BP1 or the downstream effectors of 53BP1 such as components of the Shieldin complex cause PARPi resistance by restoring HR (65–76). This is because BRCA1 acts early in the DSB response, antagonizing 53BP1 function to promote HR; in the absence of BRCA1, the balance shifts in favor of 53BP1 and NHEJ, which is corrected upon 53BP1 depletion. However, BRCA2-deficiency induces defects later in the HR process; therefore, 53BP1 depletion would not correct the defect, but rather send breaks down an ineffective pathway of repair. Overall, these findings describe a novel mechanism of PARPi resistance in BRCA2-deficient cells, and highlight critical differences between BRCA1- and BRCA2-deficient cells.

5.2. Impact of the performed CRISPR screens

In this work, I present the results of complementary genome-wide CRISPR knockout and activation screens designed to provide insight into cellular mechanisms governing sensitivity and resistance to PARPi. Although several others have reported the results of CRISPR knockout screens investigating mechanisms of PARPi resistance in BRCA1-deficient cells (70, 72, 75), our execution of this screen in BRCA2-deficient

cells represents a novel contribution to the field. Additionally, to my knowledge, this is the first instance in which genome-wide CRISPR activation screen technology has been applied to PARPi resistance. As described in Chapter 2, the results of these screens revealed several expected hits which instilled confidence in the screen results. One such hit was *ABCB1* (MDR-1), a multidrug resistance drug efflux pump which I validated by generating an overexpression cell line and testing sensitivity to PARPi. More interestingly, these screens also generated lists of novel hits which may mediate PARPi response. In Chapters 3 and 4, I present data validating three of these novel hits from the CRISPR knockout screen which investigated mediators of PARPi resistance in BRCA2-knocout cells, namely E2F7, HUWE1, and TIP60. Subsequent investigations into the processes underlying these observations revealed the novel mechanisms of PARPi resistance in BRCA2-deficient cells described above.

Furthermore, I performed pathway analysis on the results from these screens using Biological Processes Gene Ontology (GO:BP terms) analysis through NIH DAVID. The goal of this pathway analysis was to search for pathways that the three screens may have had in common, in order to draw broader conclusions regarding the pathways governing PARPi response. This pathway analysis was difficult to interpret, as confusing pathways emerged such as “regulation of the inflammatory response” and “blood vessel development” (Figure 2.5C). These unexpected results may be due to poor annotation of the GO:BP term set. For example, TIP60 (KAT5) had been previously implicated in regulating double-strand break repair pathway choice, and our work suggests that it is this role which underpins its presence among screen hits; however, this protein was annotated in the GO:BP term category, “viral process”. Moving forward, comparing different analysis platforms such as Ingenuity Pathway Analysis (Qiagen) may be helpful.

These unexpected results also likely reflect the role for underexplored pathways (and proteins) in mediating this phenotype. For example, top pathways from all three screens centered on transcription and RNA processes, such as “RNA processing,” “positive regulation of transcription”. Previously, one study reported that loss of ribonuclease H2 resulted in PARPi sensitivity due to impaired ribonucleotide excision repair and persistence of embedded genomic ribonucleotides (82). In addition to this role, Ribonuclease H2 also has important functions in resolving RNA-DNA hybrids known as R-loops (165, 166). Interestingly, another recent study found that overexpression of the microRNA miR-493-5p in BRCA2-mutated cells was associated with a significant increase in R-loops, and PARPi resistance (167). The presence of many RNA and transcription-related pathways within the results of my three screens, and the seemingly contradictory results of these studies indicate that the relationships between transcription, RNA processing, and PARPi resistance will be worthwhile areas of investigation moving forward. Another process which emerged in the top pathways of all three screens was translation (such as “translation” and “translation initiation” pathways). It will be interesting to further research whether the process of translation itself, or rather production of specific proteins in particular, affect PARPi response. As our lab has interest and expertise in DNA replication and repair, I chose hits within these categories (E2F7, HUWE1, and TIP60) for further investigation; however, it is my hope that with publication of these screen results, labs from diverse areas will be able to pursue other hits from the screens.

The screens also provided potential insight into previously proposed mechanisms of PARPi sensitivity and resistance other than those detailed here for E2F7 and TIP60. One example relates to one of the newest proposed models of PARPi-induced cytotoxicity: that PARPi treatment leads to an aberrant increase in replication fork speed, resulting in DNA damage and cytotoxicity (92). Maya-Mendoza et al. propose that

PARP1 is involved in two arms of a "fork speed regulatory network." In one arm, PARylation by PARP1 acts as a sensor of replication stress at ongoing forks, reducing speed accordingly (92, 97). In the other arm of the proposed regulatory network, speed is also restrained by p21, which is transcriptionally downregulated by PARP1 (92, 97). According to this model, after PARPi treatment, both arms of this network would be unable to restrain replication fork speed: PARPi treatment diminishes PARylation, without reducing PARP1 levels; thus, the PARylation-independent transcriptional repression of p21 via PARP1 is still intact. Consistent with the proposed model, they found that PARP1 knockdown prevented the increase in fork speed and the DNA damage response (DDR) caused by PARPi by increasing p21 levels. To verify the role of p21 in this mechanism, they tested the effects of PARP1 knockdown in HeLa cells, which have low p21 expression; PARP1 knockdown did not upregulate p21 or prevent PARPi-induced increase in fork speed (92). If an aberrant increase in replication fork speed is responsible for the cytotoxicity of PARPi, one might expect that factors which ameliorate this phenotype would rescue cytotoxicity, while those that do not do not correct it may not. Thus, this model predicts that since PARP1 knockdown in HeLa cells was unable to prevent the PARPi-induced increase in replication fork speed, PARP1 knockdown in HeLa cells would likely not rescue PARPi-induced cytotoxicity; Maya-Mendoza et al. do not test this hypothesis. However, in our CRISPR knockout screen which investigated PARPi resistance in HeLa BRCA2-knockout cells, I found that PARP1 was one of the top hits (Figure 2.3). This would suggest that in fact, PARP1 depletion can rescue PARPi-induced cytotoxicity in a HeLa background. Importantly though, I have not yet validated this screen result with additional experiments (although it is consistent with previous reports (86)), and it is unclear what impact BRCA2-deficiency would have on this mechanism. As I have been able to perform this DNA fiber-based replication speed assay successfully (Figure 4.5B), future work could focus

on investigating this conceptual discrepancy in order to test the contributions of aberrant replication fork speed to the cytotoxicity of PARPi.

My screen results also relate to another proposed mechanism of PARPi resistance: activation of Wnt signaling (104). Bitler et al. identified increased Wnt signaling as being associated with olaparib resistance in an unbiased transcriptome analysis of matched PARPi -resistant and -sensitive ovarian cancer cell lines (104). They then further show that activation of Wnt signaling through overexpression of WNT3A conferred resistance in previously PARPi-sensitive lines. In light of these findings, I wondered if mediators of Wnt signaling were identified as hits within the results of my CRISPR activation screen which identified genes that, when transcriptionally activated (overexpressed), led to PARPi resistance in BRCA2-deficient HeLa cells. Interestingly, I found that guides targeting WNT1 for activation were significantly enriched in the cells surviving olaparib treatment (Supplemental Table S1 of Ref (98)). Additionally, guides targeting several other genes connected to Wnt signaling (KIF2C, KIF18B, BCL9L, and PRICKLE4) were associated with PARPi resistance (Supplemental Table S1 of Ref (98)). Although requiring validation through additional viability experiments, these screen results support an increase in Wnt signaling as a mechanism of PARPi resistance. The results presented by Bitler et al. indicate that several transcription factors, including TCF, LEF, and AP-1, are likely involved in the relationship between Wnt signaling and PARPi resistance; however, the specific mechanisms underlying these observations are not yet clear (104). The results of my CRISPR activation screen indicate that additional research into Wnt signaling as a mechanism of PARPi resistance is warranted, as the presence of so many related proteins within the screen results suggest that this may be a robust mechanism of resistance. Overall, the complementary screens reported here provide insight into both previously reported and novel mechanisms of PARPi sensitivity and resistance.

5.3 Perspective: Potential for translation of CRIPSR screen results to the clinic

While I performed the CRISPR screens in part to provide a better understanding of the fundamental processes underlying PARPi response to advance human knowledge, a major reason for undertaking these investigations was the hopes of discovering something that may actually benefit patients in the future. While certainly findings from CRISPR screens must be validated through many subsequent studies and in many models before being implemented in the clinic, there are several ways that one could envision results from screens in general, or my validated hits in particular, affecting patient care.

5.3.1 Limitations of performed CRISPR screens

Before the results of these CRISPR screens may be applied to patient care, further study is warranted given the limitations of this work. One such limitation is that this work was performed in human cell lines. While cell lines were the best model system for these experiments given the ease of genetic manipulation and high-throughput capability of the system, other systems such as patient-derived xenografts and patient-derived organoids allow for better modelling of the biologically complex environment observed in patients (168). Other caveats involve the specific characteristics of the cell line used for the screens, HeLa cells. These cells were derived from cervical tissue and contain human papillomavirus (HPV) proteins, which interfere with the p53 pathway. This cell line was chosen for several reasons, including that cell lines with active p53 pathways may pose challenges for precision CRISPR-Cas9 gene editing, the foundation of our screens (169). Still, it is clear from the clinical trials described in Chapter 1 of this dissertation that PARPi may have different efficacies in different tissue types; for this reason and to rule out any cell-line specific effects of HeLa cells, we tested the validity of the hits described here (E2F7, HUWE1, and TIP60) in many different cell lines, which originate from different tissues and are not HPV-infected. Additionally, these screens

were performed using the HeLa BRCA2-knockout cells that I generated, which may contain hypomorphic BRCA2 as described above, despite the lack of full-length BRCA2 protein, the inability to form RAD51 foci, and extreme olaparib sensitivity consistent with lack of BRCA2 function. To address this limitation, we confirmed our results using other BRCA2-deficient cells, as well as siRNA knockdown of BRCA2 in additional lines. Such approaches would be important to validate any other hits pursued from these screens.

Furthermore, the screens and subsequent experiments described here tested only one of the six PARPi being clinically explored. For these studies, I chose to use olaparib, the PARPi being studied most widely in the clinical setting (roughly 50% of the Phase III clinical trials utilize olaparib, as described in Chapter 1). Despite having similar mechanisms of action, there are slight differences between different PARPi both at the molecular level and in terms of clinical efficacy, indicating that distinct resistance mechanisms could theoretically be possible. As our data suggest that the two hits mechanistically investigated here, namely E2F7 and TIP60, cause resistance to PARPi through mitigating the downstream effects of PARP1 inhibition rather than directly affecting the action of olaparib on PARP1, I would expect depletion of these hits to have similar effects on sensitivity to other PARPi. However, this is an important consideration to investigate during further pre-clinical validation, and is especially important for hits whose mechanism of resistance remains unknown. Another caveat is that changes in cellular survival at short-term endpoints may not translate to long-term patient response. For the experiments described in this dissertation, cells were treated continuously with olaparib for 3-4 days, at which point cells were assessed for viability (the CRISPR screen and cell titer glo and annexin assays) or allowed to form colonies for 2 weeks (Clonogenic assays). For patients, time during and after treatment is measured in months and years, rather than the days and weeks used here. For this reason, additional

validation, including the bioinformatic association studies using patient genotype and survival data described below in section 5.3.2, are essential.

Finally, it is likely that clinical resistance to PARPi in patients may be both due to features present within patients' cells before treatment (intrinsic resistance) as well as those which arise in cells during the course of the treatment (acquired resistance) (170). However, due to the design of the screen in which proteins were knocked out or activated prior to drug treatment, the results of the screen only indicate the ability of the knockout or activation to cause intrinsic resistance; it is theoretically possible, though, that these mechanisms could also be acquired in certain cases. While recent work suggests that long-term PARPi treatment may cause little to no increased mutagenesis (171), acquired resistance may develop through phenomena such as epigenetic or post-translational modifications. Interestingly, I investigated modulation of E2F7 as a potential mechanism of acquired resistance, showing that growth of BRCA2-knockout HeLa cells in low-dose olaparib for 2 weeks led to a significant reduction in E2F7 transcription, a concomitant increase in RAD51 transcription, and PARPi resistance. While I have not directly investigated roles for HUWE1 or TIP60 in acquired resistance, both of these proteins may be regulated at the transcriptional and post-translational levels, suggesting that acquired resistance may be possible through these routes as well (172–176).

5.3.2. Potential applications of CRISPR screen results in the clinic

One way in which these results could be used in the clinic is as biomarkers to stratify patients into groups according to those who would be expected to respond to treatment and those who would likely not benefit. Due to inter-tumor heterogeneity, it is likely that most specific biomarkers would only be found to cause resistance in a small percentage of patients tested (1). However, research is being done on ways to make biomarker screening more efficient. For example, the National Cancer Institute's Clinical

Proteomic Tumor Analysis Consortium (CPTAC) is working to apply high-throughput proteogenomic methods to questions of therapy resistance in clinical trials (177). A major obstacle in the PARPi field however, is the fact that since these agents are relatively new in the clinic, the survival and matched genotype/expression data needed to assess the potential clinical relevance of a screen hit as a biomarker is not currently available. Homologous recombination-deficient cells demonstrate sensitivity to cisplatin in vitro, and many clinical studies have used platinum sensitivity as a surrogate marker to try to predict PARPi response (26). Furthermore, recent work has suggested that similar cellular pathways mediate sensitivity to PARPi and cisplatin (129). Therefore, since cisplatin has been used for decades and much survival and genotype/expression data is publicly available, researchers have evaluated genetic perturbations that lead to PARPi and cisplatin resistance in the lab as potential predictors of clinical response to cisplatin (75). In our case, we tested this approach to evaluate the effects of TIP60, as I showed in clonogenic survival assays that TIP60 depletion also causes resistance to cisplatin (Figure 4.4B). Our collaborators, Anchal Sharma and Subhajyoti De, investigated the effect of TIP60 expression on survival of patients with BRCA2-mutant or -wildtype tumors using data from the Cancer Genome Atlas Ovarian Cancer (OV-TCGA) dataset. Although there is a trend in which low TIP60 expression in tumors trends toward poorer survival in patients with BRCA2 mutations, possibly consistent with increased therapy resistance in this cohort, the association is not statistically significant (Figure 6B of Ref (98)). This reflects another challenge: although there are publicly available datasets based on patient response to cisplatin, only a small number of those patients are confirmed to have mutations in BRCA1 or BRCA2, limiting the power of the analyses. Thus, while hits identified from CRISPR PARPi sensitivity/resistance screens, such as TIP60 identified here, hold great promise as potential biomarkers, significant hurdles complicate the evaluation of their potential utility in actual patients.

Beyond purely serving to predict patient response to PARPi, hits identified through CRISPR screens could theoretically also be targeted to actively sensitize (or re-sensitize) cancer cells to PARPi. In this case, CRISPR transcriptional activation (overexpression) screens such as the one I report in Chapter 2 are particularly useful, as overexpression of genes is easier to target in the clinic, through the use of drugs such as inhibitors. For example, mouse experiments indicate that this may be possible for the hit which I validated from the activation screen, the drug efflux pump MDR-1 *(ABCB1).* In a BRCA1-deficient mouse mammary tumor model, up-regulation of ABCB1 was identified as a mechanism of acquired resistance after PARPi treatment, and sensitivity was restored upon treatment with the MDR-1 inhibitor, tariquidar (a specific third-generation P- glycoprotein inhibitor) (99). Furthermore, verapamil or elacridar treatment was reported to re-sensitize a human ovarian cancer cell line demonstrating PARPi resistance due to ABCB1 overexpression (85, 101). While not as straightforward as directly inhibiting overexpressed genes, genes whose loss confers resistance to PARPi, such as E2F7, may also be pharmacologically manipulated to re-sensitize cells, through targeting proteins which regulate it. For example, based on previous reports that CHk1 restricts the activity of E2F7, we tested the effect of CHk1 inhibition on PARPi sensitivity (131). We found that Chk1 inhibition further sensitized BRCA2-deficient cells to PARPi treatment (Figure 3.6B). Altogether, this indicates that hits from CRISPR knockout or activation screens, such as ABCB1 or E2F7 reported from my screens, may be used not only to predict PARPi response, but may also be exploited as targets to re-sensitize resistant cancer cells to treatment.

5.4. Conclusions

Through a series of complementary CRISPR knockout and activation screens, I provide an unbiased catalog of genes that mediate PARPi response. In wildtype cells, I

utilized a CRISPR knockout library to reveal genes which, when knocked out, sensitize cells to PARPi treatment. Furthermore, I identify genes which cause resistance to PARPi when depleted or overexpressed in BRCA2-deficient cells, using CRISPR-knockout and transcriptional activation libraries, respectively. These studies fill a gap in the field, as to my knowledge, a knockout screen has not been reported to assess PARPi resistance in BRCA2-deficient cells, despite several screens in the context of BRCA1-deficiency. This is also the first time a CRISPR activation library has been utilized to this end. These screens identified several hits connected to previously described mechanisms of PARPi response, and in so doing, provided a new perspective which supported certain models and challenged others, as described above. Importantly, these screens revealed many novel mediators of PARPi response—three of which, namely, E2F7, HUWE1 and TIP60—I further validate here.

Subsequent investigations into the processes underlying the PARPi resistance caused by E2F7 or TIP60 depletion revealed two novel mechanisms of resistance in BRCA2-depleted cells. Specifically, I found that E2F7 depletion causes resistance to PARPi through an increase in RAD51 at the mRNA, total protein, and chromatin-bound protein levels. This increase in RAD51 led to both a restoration of homologous recombination as well as protection of stalled replication forks. Notably, restoration of homologous recombination independent of a reversion mutation is a novel mechanism of resistance in BRCA2-deficient cells. On the other hand, loss of TIP60 leads to PARPi resistance in a manner dependent on 53BP1 and REV7, key mediators of double-strand break repair pathway choice. In particular, TIP60 depletion leads to an increase in 53BP1 binding at the site of the break, a reduction in olaparib-induced end resection, and rescue of PARPi-induced double-strand breaks. Importantly, these findings reveal a that the impact of 53BP1 in PARPi resistance in BRCA2-deficient cells opposite to its role in this process in BRCA1-deficient cells; this underscores key differences between

BRCA1 and BRCA2 deficiency that are often under-recognized, especially in clinical studies. Overall, my work provides much-needed insight into the players and processes mediating response to PARPi, a targeted cancer therapy with rapidly expanding uses in the clinic.

BIBLIOGRAPHY

1. Schütte,M., Ogilvie,L.A., Rieke,D.T., Lange,B.M.H., Yaspo,M.-L. and Lehrach,H. (2017) Cancer Precision Medicine: Why More Is More and DNA Is Not Enough. *Public Health Genomics*, **20**, 70–80.

2. O'Neil,N.J., Bailey,M.L. and Hieter,P. (2017) Synthetic lethality and cancer. *Nat. Rev. Genet.*, **18**, 613–623.

3. Lord,C.J. and Ashworth,A. (2017) PARP inhibitors: Synthetic lethality in the clinic. *Science (80-.).*, **355**, 1152–1158.

4. Narod,S.A. and Foulkes,W.D. (2004) BRCA1 and BRCA2: 1994 and beyond. *Nat. Rev. Cancer*, **4**, 665–676.

5. Takaoka,M. and Miki,Y. (2018) BRCA1 gene: function and deficiency. *Int. J. Clin. Oncol.*, **23**, 36–44.

6. Wang,B., Matsuoka,S., Ballif,B.A., Zhang,D., Smogorzewska,A., Gygi,S.P. and Elledge,S.J. (2007) Abraxas and RAP80 form a BRCA1 protein complex required for the DNA damage response. *Science (80-.).*, **316**, 1194–1198.

7. Daley,J.M. and Sung,P. (2014) 53BP1, BRCA1, and the Choice between Recombination and End Joining at DNA Double-Strand Breaks. *Mol. Cell. Biol.*, **34**, 1380–1388.

8. Gupta,R., Sharma,S., Sommers,J.A., Kenny,M.K., Cantor,S.B. and Brosh,R.M. (2007) FANCJ (BACH1) helicase forms DNA damage inducible foci with replication protein a and interacts physically and functionally with the single-stranded DNA-binding protein. *Blood*, **110**, 2390–2398.

9. Zhang,F., Fan,Q., Ren,K., Auerbach,A.D. and Andreassen,P.R. (2010) FANCJ/BRIP1 recruitment and regulation of FANCD2 in DNA damage responses. *Chromosoma*, **119**, 637–649.

10. Fradet-Turcotte,A., Sitz,J., Grapton,D. and Orthwein,A. (2016) BRCA2 functions:

From DNA repair to replication fork stabilization. *Endocr. Relat. Cancer*, **23**, T1–T17.

11. Shailani,A., Kaur,R.P. and Munshi,A. (2018) A comprehensive analysis of BRCA2 gene: focus on mechanistic aspects of its functions, spectrum of deleterious mutations, and therapeutic strategies targeting BRCA2-deficient tumors. *Med. Oncol.*, **35**, 1–10.
12. Ceccaldi,R., Rondinelli,B. and D'Andrea,A.D. (2016) Repair Pathway Choices and Consequences at the Double-Strand Break. *Trends Cell Biol.*, **26**, 52–64.
13. Collins,N., McManus,R., Wooster,R., Mangion,J., Seal,S., Lakhani,S.R., Ormiston,W., Daly,P.A., Ford,D., Easton,D.F., *et al.* (1995) Consistent loss of the wild type allele in breast cancers from a family linked to the BRCA2 gene on chromosome 13q12-13. *Oncogene*, **10**, 1673–1675.
14. Gudmundsson,J., Johannesdottir,G., Bergthorsson,J.T., Arason,A., Ingvarsson,S., Egilsson,V. and Barkardottir,R.B. (1995) Different tumor types from BRCA2 carriers show wild-type chromosome deletions on 13q12-q13. *Cancer Res.*, **55**, 4830–2.
15. Merajver,S.D., Frank,T.S., Xu,J., Pham,T.M., Calzone,K.A., Bennett-Baker,P., Chamberlain,J., Boyd,J., Garber,J.E., Collins,F.S., *et al.* (1995) Germline BRCA1 Mutations and Loss of the Wild-Type Allele in Tumors from Families with Early Onset Breast and Ovarian Cancer. *Clin. Cancer Res.*, **1**, 539–544.
16. Venkitaraman,A.R. (2019) How do mutations affecting the breast cancer genes BRCA1 and BRCA2 cause cancer susceptibility? *DNA Repair (Amst).*, **81**, 102668.
17. Rebbeck,T.R., Mitra,N., Wan,F., Sinilnikova,O.M., Healey,S., McGuffog,L., Chenevix-Trench,G., Easton,D.F., Antoniou,A.C., Nathanson,K.L., *et al.* (2015) Association of type and location of BRCA1 and BRCA2 mutations with risk of breast and ovarian cancer. *JAMA - J. Am. Med. Assoc.*, **313**, 1347–1361.
18. Hawsawi,Y.M., Al-Numair,N.S., Sobahy,T.M., Al-Ajmi,A.M., Al-Harbi,R.M.,

Baghdadi,M.A., Oyouni,A.A. and Alamer,O.M. (2019) The role of BRCA1/2 in hereditary and familial breast and ovarian cancers. *Mol. Genet. Genomic Med.*, **7**.

19. Armstrong,N., Ryder,S., Forbes,C., Ross,J. and Quek,R.G.W. (2019) A systematic review of the international prevalence of BRCA mutation in breast cancer. *Clin. Epidemiol.*, **11**, 543–561.
20. Mahdavi,M., Nassiri,M., Kooshyar,M.M., Vakili-Azghandi,M., Avan,A., Sandry,R., Pillai,S., Lam,A.K. yin and Gopalan,V. (2019) Hereditary breast cancer; Genetic penetrance and current status with BRCA. *J. Cell. Physiol.*, **234**, 5741–5750.
21. Kuchenbaecker,K.B., Hopper,J.L., Barnes,D.R., Phillips,K.A., Mooij,T.M., Roos-Blom,M.J., Jervis,S., Van Leeuwen,F.E., Milne,R.L., Andrieu,N., *et al.* (2017) Risks of breast, ovarian, and contralateral breast cancer for BRCA1 and BRCA2 mutation carriers. *JAMA - J. Am. Med. Assoc.*, **317**, 2402–2416.
22. Schultz,N., Lopez,E., Saleh-Gohari,N. and Helleday,T. (2003) Poly(ADP-ribose) polymerase (PARP-1) has a controlling role in homologous recombination. *Nucleic Acids Res.*, **31**, 4959–4964.
23. Bryant,H.E., Schultz,N., Thomas,H.D., Parker,K.M., Flower,D., Lopez,E., Kyle,S., Meuth,M., Curtin,N.J. and Helleday,T. (2005) Specific killing of BRCA2-deficient tumours with inhibitors of poly(ADP-ribose) polymerase. *Nature*, **434**, 913–917.
24. Farmer,H., McCabe,N., Lord,C.J., Tutt,A.N.J., Johnson,D.A., Richardson,T.B., Santarosa,M., Dillon,K.J., Hickson,I., Knights,C., *et al.* (2005) Targeting the DNA repair defect in BRCA mutant cells as a therapeutic strategy. *Nature*, **434**, 917–921.
25. Menear,K.A., Adcock,C., Boulter,R., Cockcroft,X.L., Copsey,L., Cranston,A., Dillon,K.J., Drzewiecki,J., Garman,S., Gomez,S., *et al.* (2008) 4-[3-(4-Cyclopropanecarbonylpiperazine-1-carbonyl)-4-fluorobenzyl] -2H-phthalazin-1-one: A novel bioavailable inhibitor of poly(ADP-ribose) polymerase-1. *J. Med. Chem.*, **51**, 6581–6591.

26. Hoppe,M.M., Sundar,R., Tan,D.S.P. and Jeyasekharan,A.D. (2018) Biomarkers for homologous recombination deficiency in cancer. *J. Natl. Cancer Inst.*, **110**, 704–713.

27. Del Campo,J.M., Matulonis,U.A., Malander,S., Provencher,D., Mahner,S., Follana,P., Waters,J., Berek,J.S., Woie,K., Oza,A.M., *et al.* (2019) Niraparib Maintenance Therapy in Patients With Recurrent Ovarian Cancer After a Partial Response to the Last Platinum-Based Chemotherapy in the ENGOT-OV16/NOVA Trial. *J. Clin. Oncol.*, **37**, 2968–2973.

28. Mirza,M.R., Monk,B.J., Herrstedt,J., Oza,A.M., Mahner,S., Redondo,A., Fabbro,M., Ledermann,J.A., Lorusso,D., Vergote,I., *et al.* (2016) Niraparib maintenance therapy in platinum-sensitive, recurrent ovarian cancer. *N. Engl. J. Med.*, **375**, 2154–2164.

29. Pujade-Lauraine,E., Ledermann,J.A., Selle,F., Gebski,V., Penson,R.T., Oza,A.M., Korach,J., Huzarski,T., Poveda,A., Pignata,S., *et al.* (2017) Olaparib tablets as maintenance therapy in patients with platinum-sensitive, relapsed ovarian cancer and a BRCA1/2 mutation (SOLO2/ENGOT-Ov21): a double-blind, randomised, placebo-controlled, phase 3 trial. *Lancet Oncol.*, **18**, 1274–1284.

30. Coleman,R.L., Oza,A.M., Lorusso,D., Aghajanian,C., Oaknin,A., Dean,A., Colombo,N., Weberpals,J.I., Clamp,A., Scambia,G., *et al.* (2017) Rucaparib maintenance treatment for recurrent ovarian carcinoma after response to platinum therapy (ARIEL3): a randomised, double-blind, placebo-controlled, phase 3 trial. *Lancet*, **390**, 1949–1961.

31. Oza,A.M., Matulonis,U.A., Malander,S., Hudgens,S., Sehouli,J., del Campo,J.M., Berton-Rigaud,D., Banerjee,S., Scambia,G., Berek,J.S., *et al.* (2018) Quality of life in patients with recurrent ovarian cancer treated with niraparib versus placebo (ENGOT-OV16/NOVA): results from a double-blind, phase 3, randomised controlled

trial. *Lancet Oncol.*, **19**, 1117–1125.

32. Friedlander,M., Gebski,V., Gibbs,E., Davies,L., Bloomfield,R., Hilpert,F., Wenzel,L.B., Eek,D., Rodrigues,M., Clamp,A., *et al.* (2018) Health-related quality of life and patient-centred outcomes with olaparib maintenance after chemotherapy in patients with platinum-sensitive, relapsed ovarian cancer and a BRCA1/2 mutation (SOLO2/ENGOT Ov-21): a placebo-controlled, phase 3 randomised tria. *Lancet Oncol.*, **19**, 1126–1134.
33. Tesaro Inc (2019) ZEJULA (Niraparib): US prescribing information.
34. Clovis Oncology Inc. (2018) Rubraca (rucaparib): US prescribing information.
35. AstraZeneca Pharmaceuticals (2019) LYNPARZA (olaparib): US prescribing information.
36. Moore,K., Colombo,N., Scambia,G., Kim,B.G., Oaknin,A., Friedlander,M., Lisyanskaya,A., Floquet,A., Leary,A., Sonke,G.S., *et al.* (2018) Maintenance olaparib in patients with newly diagnosed advanced ovarian cancer. *N. Engl. J. Med.*, **379**, 2495–2505.
37. González-Martín,A., Pothuri,B., Vergote,I., DePont Christensen,R., Graybill,W., Mirza,M.R., McCormick,C., Lorusso,D., Hoskins,P., Freyer,G., *et al.* (2019) Niraparib in Patients with Newly Diagnosed Advanced Ovarian Cancer. *N. Engl. J. Med.*, 10.1056/nejmoa1910962.
38. Coleman,R.L., Fleming,G.F., Brady,M.F., Swisher,E.M., Steffensen,K.D., Friedlander,M., Okamoto,A., Moore,K.N., Efrat Ben-Baruch,N., Werner,T.L., *et al.* (2019) Veliparib with First-Line Chemotherapy and as Maintenance Therapy in Ovarian Cancer. *N. Engl. J. Med.*, 10.1056/nejmoa1909707.
39. Ray-Coquard,I., Pautier,P., Pignata,S., Pérol,D., González-Martín,A., Berger,R., Fujiwara,K., Vergote,I., Colombo,N., Mäenpää,J., *et al.* (2019) Olaparib plus Bevacizumab as First-Line Maintenance in Ovarian Cancer.

10.1056/NEJMoa1911361.

40. Robson,M., Im,S.A., Senkus,E., Xu,B., Domchek,S.M., Masuda,N., Delaloge,S., Li,W., Tung,N., Armstrong,A., *et al.* (2017) Olaparib for metastatic breast cancer in patients with a germline BRCA mutation. *N. Engl. J. Med.*, **377**, 523–533.
41. Robson,M.E., Tung,N., Conte,P., Im,S.A., Senkus,E., Xu,B., Masuda,N., Delaloge,S., Li,W., Armstrong,A., *et al.* (2019) OlympiAD final overall survival and tolerability results: Olaparib versus chemotherapy treatment of physician's choice in patients with a germline BRCA mutation and HER2-negative metastatic breast cancer. *Ann. Oncol.*, **30**, 558–566.
42. Robson,M., Ruddy,K.J., IM,S.A., Senkus,E., Xu,B., Domchek,S.M., Masuda,N., Li,W., Tung,N., Armstrong,A., *et al.* (2019) Patient-reported outcomes in patients with a germline BRCA mutation and HER2-negative metastatic breast cancer receiving olaparib versus chemotherapy in the OlympiAD trial. *Eur. J. Cancer*, **120**, 20–30.
43. Litton,J.K., Rugo,H.S., Ettl,J., Hurvitz,S.A., Gonçalves,A., Lee,K.H., Fehrenbacher,L., Yerushalmi,R., Mina,L.A., Martin,M., *et al.* (2018) Talazoparib in patients with advanced breast cancer and a germline BRCA mutation. *N. Engl. J. Med.*, **379**, 753–763.
44. Ettl,J., Quek,R.G.W., Lee,K.H., Rugo,H.S., Hurvitz,S., Gonçalves,A., Fehrenbacher,L., Yerushalmi,R., Mina,L.A., Martin,M., *et al.* (2018) Quality of life with talazoparib versus physician's choice of chemotherapy in patients with advanced breast cancer and germline BRCA1/2 mutation: Patient-reported outcomes from the EMBRACA phase III trial. *Ann. Oncol.*, **29**, 1939–1947.
45. Pfizer Labs (2019) TALZENNA (talazoparib): US prescribing information.
46. Loibl,S., O'Shaughnessy,J., Untch,M., Sikov,W.M., Rugo,H.S., McKee,M.D., Huober,J., Golshan,M., von Minckwitz,G., Maag,D., *et al.* (2018) Addition of the

PARP inhibitor veliparib plus carboplatin or carboplatin alone to standard neoadjuvant chemotherapy in triple-negative breast cancer (BrighTNess): a randomised, phase 3 trial. *Lancet Oncol.*, **19**, 497–509.

47. Bang,Y.J., Xu,R.H., Chin,K., Lee,K.W., Park,S.H., Rha,S.Y., Shen,L., Qin,S., Xu,N., Im,S.A., *et al.* (2017) Olaparib in combination with paclitaxel in patients with advanced gastric cancer who have progressed following first-line therapy (GOLD): a double-blind, randomised, placebo-controlled, phase 3 trial. *Lancet Oncol.*, **18**, 1637–1651.
48. Golan,T., Hammel,P., Reni,M., Van Cutsem,E., Macarulla,T., Hall,M.J., Park,J.O., Hochhauser,D., Arnold,D., Oh,D.Y., *et al.* (2019) Maintenance olaparib for germline BRCA-mutated metastatic pancreatic cancer. *N. Engl. J. Med.*, **381**, 317–327.
49. Hammel,P., Kindler,H.L., Reni,M., Van Cutsem,E., Macarulla,T., Hall,M.J., Park,J.O., Hochhauser,D., Arnold,D., Oh,D.-Y., *et al.* (2019) Health-related quality of life in patients with a germline BRCA mutation and metastatic pancreatic cancer receiving maintenance olaparib. *Ann. Oncol.*, 10.1093/annonc/mdz406.
50. Bitler,B.G., Watson,Z.L., Wheeler,L.J. and Behbakht,K. (2017) PARP inhibitors: Clinical utility and possibilities of overcoming resistance. *Gynecol. Oncol.*, **147**, 695–704.
51. Lord,C.J. and Ashworth,A. (2013) Mechanisms of resistance to therapies targeting BRCA-mutant cancers. *Nat. Med.*, **19**, 1381–1388.
52. Ledermann,J.A., Drew,Y. and Kristeleit,R.S. (2016) Homologous recombination deficiency and ovarian cancer. *Eur. J. Cancer*, **60**, 49–58.
53. Rimar,K.J., Tran,P.T., Matulewicz,R.S., Hussain,M. and Meeks,J.J. (2017) The emerging role of homologous recombination repair and PARP inhibitors in genitourinary malignancies. *Cancer*, **123**, 1912–1924.
54. Helleday,T. (2011) The underlying mechanism for the PARP and BRCA synthetic

lethality: Clearing up the misunderstandings. *Mol. Oncol.*, **5**, 387–393.

55. Fisher,A.E.O., Hochegger,H., Takeda,S. and Caldecott,K.W. (2007) Poly(ADP-Ribose) Polymerase 1 Accelerates Single-Strand Break Repair in Concert with Poly(ADP-Ribose) Glycohydrolase. *Mol. Cell. Biol.*, **27**, 5597–5605.
56. Satoh,M.S. and Lindahl,T. (1992) Role of poly(ADP-ribose) formation in DNA repair. *Nature*, **356**, 356–358.
57. Podhorecka,M., Skladanowski,A. and Bozko,P. (2010) H2AX phosphorylation: Its role in DNA damage response and cancer therapy. *J. Nucleic Acids*, **2010**.
58. Rothkamm,K., Barnard,S., Moquet,J., Ellender,M., Rana,Z. and Burdak-Rothkamm,S. (2015) DNA damage foci: Meaning and significance. *Environ. Mol. Mutagen.*, **56**, 491–504.
59. Patel,A.G., Sarkaria,J.N. and Kaufmann,S.H. (2011) Nonhomologous end joining drives poly(ADP-ribose) polymerase (PARP) inhibitor lethality in homologous recombination-deficient cells. *Proc. Natl. Acad. Sci. U. S. A.*, **108**, 3406–11.
60. Gottipati,P., Vischioni,B., Schultz,N., Solomons,J., Bryant,H.E., Djureinovic,T., Issaeva,N., Sleeth,K., Sharma,R.A. and Helleday,T. (2010) Poly(ADP-ribose) polymerase is hyperactivated in homologous recombination-defective cells. *Cancer Res.*, **70**, 5389–5398.
61. Ström,C.E., Johansson,F., Uhlén,M., Szigyarto,C.A.K., Erixon,K. and Helleday,T. (2011) Poly (ADP-ribose) polymerase (PARP) is not involved in base excision repair but PARP inhibition traps a single-strand intermediate. *Nucleic Acids Res.*, **39**, 3166–3175.
62. Kubalanza,K. and Konecny,G.E. (2020) Mechanisms of PARP inhibitor resistance in ovarian cancer. *Curr. Opin. Obstet. Gynecol.*, **32**, 36–41.
63. D'Andrea,A.D. (2018) Mechanisms of PARP inhibitor sensitivity and resistance. *DNA Repair (Amst).*, **71**, 172–176.

64. Kass,E.M., Moynahan,M.E. and Jasin,M. (2010) Loss of 53BP1 Is a Gain for BRCA1 Mutant Cells. *Cancer Cell*, **17**, 423–425.

65. Bunting,S.F., Callén,E., Wong,N., Chen,H.-T., Polato,F., Gunn,A., Bothmer,A., Feldhahn,N., Fernandez-Capetillo,O., Cao,L., *et al.* (2010) 53BP1 inhibits homologous recombination in Brca1-deficient cells by blocking resection of DNA breaks. *Cell*, **141**, 243–54.

66. Jaspers,J.E., Kersbergen,A., Boon,U., Sol,W., van Deemter,L., Zander,S.A., Drost,R., Wientjens,E., Ji,J., Aly,A., *et al.* (2013) Loss of 53BP1 Causes PARP Inhibitor Resistance in *Brca1* -Mutated Mouse Mammary Tumors. *Cancer Discov.*, **3**, 68–81.

67. Xu,G., Chapman,J.R., Brandsma,I., Yuan,J., Mistrik,M., Bouwman,P., Bartkova,J., Gogola,E., Warmerdam,D., Barazas,M., *et al.* (2015) REV7 counteracts DNA double-strand break resection and affects PARP inhibition. *Nature*, **521**, 541–544.

68. Gupta,R., Somyajit,K., Narita,T., Maskey,E., Stanlie,A., Kremer,M., Typas,D., Lammers,M., Mailand,N., Nussenzweig,A., *et al.* (2018) DNA Repair Network Analysis Reveals Shieldin as a Key Regulator of NHEJ and PARP Inhibitor Sensitivity. *Cell*, **173**, 972–988.e23.

69. Findlay,S., Heath,J., Luo,V.M., Malina,A., Morin,T., Coulombe,Y., Djerir,B., Li,Z., Samiei,A., Simo-Cheyou,E., *et al.* (2018) SHLD 2/ FAM 35A co-operates with REV 7 to coordinate DNA double-strand break repair pathway choice . *EMBO J.*, **37**, 1–20.

70. Dev,H., Chiang,T.W.W., Lescale,C., de Krijger,I., Martin,A.G., Pilger,D., Coates,J., Sczaniecka-Clift,M., Wei,W., Ostermaier,M., *et al.* (2018) Shieldin complex promotes DNA end-joining and counters homologous recombination in BRCA1-null cells. *Nat. Cell Biol.*, **20**, 954–965.

71. Noordermeer,S.M., Adam,S., Setiaputra,D., Barazas,M., Pettitt,S.J., Ling,A.K., Olivieri,M., Álvarez-Quilón,A., Moatti,N., Zimmermann,M., *et al.* (2018) The shieldin complex mediates 53BP1-dependent DNA repair. *Nature*, **560**, 117–121.

72. Barazas,M., Annunziato,S., Pettitt,S.J., de Krijger,I., Ghezraoui,H., Roobol,S.J., Lutz,C., Frankum,J., Song,F.F., Brough,R., *et al.* (2018) The CST Complex Mediates End Protection at Double-Strand Breaks and Promotes PARP Inhibitor Sensitivity in BRCA1-Deficient Cells. *Cell Rep.*, **23**, 2107–2118.

73. Becker,J.R., Cuella-Martin,R., Barazas,M., Liu,R., Oliveira,C., Oliver,A.W., Bilham,K., Holt,A.B., Blackford,A.N., Heierhorst,J., *et al.* (2018) The ASCIZ-DYNLL1 axis promotes 53BP1-dependent non-homologous end joining and PARP inhibitor sensitivity. *Nat. Commun.*, **9**, 1–12.

74. West,K.L., Kelliher,J.L., Xu,Z., An,L., Reed,M.R., Eoff,R.L., Wang,J., Huen,M.S.Y. and Leung,J.W.C. (2019) LC8/DYNLL1 is a 53BP1 effector and regulates checkpoint activation. *Nucleic Acids Res.*, **47**, 6236–6249.

75. He,Y.J., Meghani,K., Caron,M.-C., Yang,C., Ronato,D.A., Bian,J., Sharma,A., Moore,J., Niraj,J., Detappe,A., *et al.* (2018) DYNLL1 binds to MRE11 to limit DNA end resection in BRCA1-deficient cells. *Nature*, **563**, 522–526.

76. Zalmas,L.-P., Lu,W.-T. and Kanu,N. (2019) An emerging regulatory network of NHEJ via DYNLL1-mediated 53BP1 redistribution. *Ann. Transl. Med.*, **7**, S93–S93.

77. Ko,H.L. and Ren,E.C. (2012) Functional Aspects of PARP1 in DNA Repair and Transcription. *Biomolecules*, **2**, 524–48.

78. Murai,J., Huang,S.N., Das,B.B., Renaud,A., Zhang,Y., Doroshow,J.H., Ji,J., Takeda,S. and Pommier,Y. (2012) Trapping of PARP1 and PARP2 by Clinical PARP Inhibitors. *Cancer Res.*, **72**, 5588–99.

79. Murai,J., Zhang,Y., Morris,J., Ji,J., Takeda,S., Doroshow,J.H. and Pommier,Y. (2014) Rationale for poly(ADP-ribose) polymerase (PARP) inhibitors in combination

therapy with camptothecins or temozolomide based on PARP trapping versus catalytic inhibition. *J. Pharmacol. Exp. Ther.*, **349**, 408–416.

80. Murai,J., Huang,S.Y.N., Renaud,A., Zhang,Y., Ji,J., Takeda,S., Morris,J., Teicher,B., Doroshow,J.H. and Pommier,Y. (2014) Stereospecific PARP trapping by BMN 673 and comparison with olaparib and rucaparib. *Mol. Cancer Ther.*, **13**, 433–443.
81. Michelena,J., Lezaja,A., Teloni,F., Schmid,T., Imhof,R. and Altmeyer,M. (2018) Analysis of PARP inhibitor toxicity by multidimensional fluorescence microscopy reveals mechanisms of sensitivity and resistance. *Nat. Commun.*, **9**, 2678.
82. Zimmermann,M., Murina,O., Reijns,M.A.M., Agathanggelou,A., Challis,R., Tarnauskaitė,Ž., Muir,M., Fluteau,A., Aregger,M., McEwan,A., *et al.* (2018) CRISPR screens identify genomic ribonucleotides as a source of PARP-trapping lesions. *Nature*, **559**, 285–289.
83. Liu,X., Han,E.K., Anderson,M., Shi,Y., Semizarov,D., Wang,G., McGonigal,T., Roberts,L., Lasko,L., Palma,J., *et al.* (2009) Acquired resistance to combination treatment with temozolomide and ABT-888 is mediated by both base excision repair and homologous recombination DNA repair pathways. *Mol. Cancer Res.*, **7**, 1686–1692.
84. Pettitt,S.J., Rehman,F.L., Bajrami,I., Brough,R., Wallberg,F., Kozarewa,I., Fenwick,K., Assiotis,I., Chen,L., Campbell,J., *et al.* (2013) A Genetic Screen Using the PiggyBac Transposon in Haploid Cells Identifies Parp1 as a Mediator of Olaparib Toxicity. *PLoS One*, **8**.
85. Noordermeer,S.M. and van Attikum,H. (2019) PARP Inhibitor Resistance: A Tug-of-War in BRCA-Mutated Cells. *Trends Cell Biol.*, **29**, 820–834.
86. Pettitt,S.J., Krastev,D.B., Brandsma,I., Dréan,A., Song,F., Aleksandrov,R., Harrell,M.I., Menon,M., Brough,R., Campbell,J., *et al.* (2018) Genome-wide and high-density CRISPR-Cas9 screens identify point mutations in PARP1 causing

PARP inhibitor resistance. *Nat. Commun.*, **9**, 1849.

87. Gogola,E., Duarte,A.A., de Ruiter,J.R., Wiegant,W.W., Schmid,J.A., de Bruijn,R., James,D.I., Guerrero Llobet,S., Vis,D.J., Annunziato,S., *et al.* (2018) Selective Loss of PARG Restores PARylation and Counteracts PARP Inhibitor-Mediated Synthetic Lethality. *Cancer Cell*, **33**, 1078–1093.e12.

88. Schlacher,K., Christ,N., Siaud,N., Egashira,A., Wu,H. and Jasin,M. (2011) Double-strand break repair-independent role for BRCA2 in blocking stalled replication fork degradation by MRE11. *Cell*, **145**, 529–542.

89. Schlacher,K., Wu,H. and Jasin,M. (2012) A Distinct Replication Fork Protection Pathway Connects Fanconi Anemia Tumor Suppressors to RAD51-BRCA1/2. *Cancer Cell*, **22**, 106–116.

90. Lemaçon,D., Jackson,J., Quinet,A., Brickner,J.R., Li,S., Yazinski,S., You,Z., Ira,G., Zou,L., Mosammaparast,N., *et al.* (2017) MRE11 and EXO1 nucleases degrade reversed forks and elicit MUS81-dependent fork rescue in BRCA2-deficient cells. *Nat. Commun.*, **8**.

91. Rondinelli,B., Gogola,E., Yücel,H., Duarte,A.A., van de Ven,M., van der Sluijs,R., Konstantinopoulos,P.A., Jonkers,J., Ceccaldi,R., Rottenberg,S., *et al.* (2017) EZH2 promotes degradation of stalled replication forks by recruiting MUS81 through histone H3 trimethylation. *Nat. Cell Biol.*, **19**, 1371–1378stabili.

92. Maya-Mendoza,A., Moudry,P., Merchut-Maya,J.M., Lee,M., Strauss,R. and Bartek,J. (2018) High speed of fork progression induces DNA replication stress and genomic instability. *Nature*, 10.1038/s41586-018-0261-5.

93. Ray Chaudhuri,A., Callen,E., Ding,X., Gogola,E., Duarte,A.A., Lee,J.-E., Wong,N., Lafarga,V., Calvo,J.A., Panzarino,N.J., *et al.* (2016) Replication fork stability confers chemoresistance in BRCA-deficient cells. *Nature*, **535**, 382–387.

94. Schlacher,K. (2017) PARPi focus the spotlight on replication fork protection in

cancer. *Nat. Cell Biol.*, **19**, 1309–1310.

95. Dungrawala,H., Bhat,K.P., Le Meur,R., Chazin,W.J., Ding,X., Sharan,S.K., Wessel,S.R., Sathe,A.A., Zhao,R. and Cortez,D. (2017) RADX Promotes Genome Stability and Modulates Chemosensitivity by Regulating RAD51 at Replication Forks. *Mol. Cell*, **67**, 374–386.e5.

96. Taglialatela,A., Alvarez,S., Leuzzi,G., Sannino,V., Ranjha,L., Huang,J.W., Madubata,C., Anand,R., Levy,B., Rabadan,R., *et al.* (2017) Restoration of Replication Fork Stability in BRCA1- and BRCA2-Deficient Cells by Inactivation of SNF2-Family Fork Remodelers. *Mol. Cell*, **68**, 414–430.e8.

97. Quinet,A. and Vindigni,A. (2018) Superfast DNA replication causes damage in cancer cells. *Nature*, **559**, 186–187.

98. Clements,K.E., Hale,A., Tolman,N.J., Nicolae,C.M., Sharma,A., Thakar,T., Liang,X., Kawasawa,Y.I., Wang,H.-G., De,S., *et al.* (2019) Identification of regulators of poly-ADP-ribose polymerase (PARP) inhibitor response through complementary CRISPR knockout and activation screens. *bioRxiv*, 10.1101/871970.

99. Rottenberg,S., Jaspers,J.E., Kersbergen,A., Van Der Burg,E., Nygren,A.O.H., Zander,S.A.L., Derksen,P.W.B., De Bruin,M., Zevenhoven,J., Lau,A., *et al.* (2008) High sensitivity of BRCA1-deficient mammary tumors to the PARP inhibitor AZD2281 alone and in combination with platinum drugs. *Proc. Natl. Acad. Sci. U. S. A.*, **105**, 17079–17084.

100. Jaspers,J.E., Sol,W., Kersbergen,A., Schlicker,A., Guyader,C., Xu,G., Wessels,L., Borst,P., Jonkers,J. and Rottenberg,S. (2015) BRCA2-deficient sarcomatoid mammary tumors exhibit multidrug resistance. *Cancer Res.*, **75**, 732–741.

101. Vaidyanathan,A., Sawers,L., Gannon,A.-L., Chakravarty,P., Scott,A.L., Bray,S.E., Ferguson,M.J. and Smith,G. (2016) ABCB1 (MDR1) induction defines a common resistance mechanism in paclitaxel- and olaparib-resistant ovarian cancer cells. *Br.*

J. Cancer, **115**, 431–41.

102. Christie,E.L., Pattnaik,S., Beach,J., Copeland,A., Rashoo,N., Fereday,S., Hendley,J., Alsop,K., Brady,S.L., Lamb,G., *et al.* (2019) Multiple ABCB1 transcriptional fusions in drug resistant high-grade serous ovarian and breast cancer. *Nat. Commun.*, **10**.
103. Schoonen,P.M., Talens,F., Stok,C., Gogola,E., Heijink,A.M., Bouwman,P., Foijer,F., Tarsounas,M., Blatter,S., Jonkers,J., *et al.* (2017) Progression through mitosis promotes PARP inhibitor-induced cytotoxicity in homologous recombination-deficient cancer cells. *Nat. Commun.*, **8**, 15981.
104. Yamamoto,T.M., McMellen,A., Watson,Z.L., Aguilera,J., Ferguson,R., Nurmemmedov,E., Thakar,T., Moldovan,G.L., Kim,H., Cittelly,D.M., *et al.* (2019) Activation of Wnt signaling promotes olaparib resistant ovarian cancer. *Mol. Carcinog.*, **58**, 1770–1782.
105. Morgens,D.W., Deans,R.M., Li,A. and Bassik,M.C. (2016) Systematic comparison of CRISPR/Cas9 and RNAi screens for essential genes. *Nat. Biotechnol.*, **34**, 634–636.
106. Evers,B., Jastrzebski,K., Heijmans,J.P.M., Grernrum,W., Beijersbergen,R.L. and Bernards,R. (2016) CRISPR knockout screening outperforms shRNA and CRISPRi in identifying essential genes. *Nat. Biotechnol.*, **34**, 631–633.
107. Housden,B.E. and Perrimon,N. (2016) Comparing CRISPR and RNAi-based screening technologies. *Nat. Biotechnol.*, **34**, 621–623.
108. Dhanjal,J.K., Radhakrishnan,N. and Sundar,D. (2017) Identifying synthetic lethal targets using CRISPR/Cas9 system. *Methods*, **131**, 66–73.
109. Thompson,J.M., Nguyen,Q.H., Singh,M. and Razorenova,O. V. (2015) Approaches to identifying synthetic lethal interactions in cancer. *Yale J. Biol. Med.*, **88**, 145–155.
110. Agrotis,A. and Ketteler,R. (2015) A new age in functional genomics using

CRISPR/Cas9 in arrayed library screening. *Front. Genet.*, **6**.

111. Fang,P., De Souza,C., Minn,K. and Chien,J. (2019) Genome-scale CRISPR knockout screen identifies TIGAR as a modifier of PARP inhibitor sensitivity. *Commun. Biol.*, **2**.
112. Doench,J.G., Fusi,N., Sullender,M., Hegde,M., Vaimberg,E.W., Donovan,K.F., Smith,I., Tothova,Z., Wilen,C., Orchard,R., *et al.* (2016) Optimized sgRNA design to maximize activity and minimize off-target effects of CRISPR-Cas9. *Nat. Biotechnol.*, **34**, 184–191.
113. Swisher,E.M., Lin,K.K., Oza,A.M., Scott,C.L., Giordano,H., Sun,J., Konecny,G.E., Coleman,R.L., Tinker,A. V, O'Malley,D.M., *et al.* (2017) Rucaparib in relapsed, platinum-sensitive high-grade ovarian carcinoma (ARIEL2 Part 1): an international, multicentre, open-label, phase 2 trial. *Lancet Oncol.*, **18**, 75–87.
114. Pettitt,S.J., Rehman,F.L., Bajrami,I., Brough,R., Wallberg,F., Kozarewa,I., Fenwick,K., Assiotis,I., Chen,L., Campbell,J., *et al.* (2013) A Genetic Screen Using the PiggyBac Transposon in Haploid Cells Identifies Parp1 as a Mediator of Olaparib Toxicity. *PLoS One*, **8**, e61520.
115. Pettitt,S.J., Krastev,D.B., Brandsma,I., Dréan,A., Song,F., Aleksandrov,R., Harrell,M.I., Menon,M., Brough,R., Campbell,J., *et al.* (2018) Genome-wide and high-density CRISPR- Cas9 screens identify point mutations in PARP1 causing PARP inhibitor resistance. 10.1038/s41467-018-03917-2.
116. Sanson,K.R., Hanna,R.E., Hegde,M., Donovan,K.F., Strand,C., Sullender,M.E., Vaimberg,E.W., Goodale,A., Root,D.E., Piccioni,F., *et al.* (2018) Optimized libraries for CRISPR-Cas9 genetic screens with multiple modalities. *Nat. Commun.*, **9**, 5416.
117. Fang,P., De Souza,C., Minn,K. and Chien,J. (2019) Genome-scale CRISPR knockout screen identifies TIGAR as a modifier of PARP inhibitor sensitivity. *Commun. Biol.*, **2**, 335.

118. Hustedt,N., Álvarez-Quilón,A., McEwan,A., Yuan,J.Y., Cho,T., Koob,L., Hart,T. and Durocher,D. (2019) A consensus set of genetic vulnerabilities to ATR inhibition. *Open Biol.*, **9**, 190156.

119. Wang,T., Lander,E.S. and Sabatini,D.M. (2016) Viral Packaging and Cell Culture for CRISPR-Based Screens. *Cold Spring Harb. Protoc.*, **2016**, pdb.prot090811.

120. Joung,J., Konermann,S., Gootenberg,J.S., Abudayyeh,O.O., Platt,R.J., Brigham,M.D., Sanjana,N.E. and Zhang,F. (2017) Genome-scale CRISPR-Cas9 knockout and transcriptional activation screening. *Nat. Protoc.*, **12**, 828–863.

121. König,R., Chiang,C., Tu,B.P., Yan,S.F., DeJesus,P.D., Romero,A., Bergauer,T., Orth,A., Krueger,U., Zhou,Y., *et al.* (2007) A probability-based approach for the analysis of large-scale RNAi screens. *Nat. Methods*, **4**, 847–849.

122. Nicolae,C.M., Aho,E.R., Vlahos,A.H.S., Choe,K.N., De,S., Karras,G.I. and Moldovan,G.-L. (2014) The ADP-ribosyltransferase PARP10/ARTD10 Interacts with Proliferating Cell Nuclear Antigen (PCNA) and Is Required for DNA Damage Tolerance. *J. Biol. Chem.*, **289**, 13627–13637.

123. De Bruin,A., Maiti,B., Jakoi,L., Timmers,C., Buerki,R. and Leone,G. (2003) Identification and Characterization of E2F7, a Novel Mammalian E2F Family Member Capable of Blocking Cellular Proliferation. *J. Biol. Chem.*, **278**, 42041–42049.

124. Di Stefano,L., Jensen,M.R. and Helin,K. (2003) E2F7, a novel E2F featuring DP-independent repression of a subset of E2F-regulated genes. *EMBO J.*, **22**, 6289–6298.

125. Panagiotis Zalmas,L., Zhao,X., Graham,A.L., Fisher,R., Reilly,C., Coutts,A.S. and La Thangue,N.B. (2008) DNA-damage response control of E2F7 and E2F8. *EMBO Rep.*, **9**, 252–259.

126. Carvajal,L.A., Hamard,P.J., Tonnessen,C. and Manfredi,J.J. (2012) E2F7, a novel

target, is up-regulated by p53 and mediates DNA damage-dependent transcriptional repression. *Genes Dev.*, **26**, 1533–1545.

127. Westendorp,B., Mokry,M., Groot Koerkamp,M.J.A., Holstege,F.C.P., Cuppen,E. and De Bruin,A. (2012) E2F7 represses a network of oscillating cell cycle genes to control S-phase progression. *Nucleic Acids Res.*, **40**, 3511–3523.
128. Guillemette,S., Serra,R.W., Peng,M., Hayes,J.A., Konstantinopoulos,P.A., Green,M.R. and Cantor,S.B. (2015) Resistance to therapy in BRCA2 mutant cells due to loss of the nucleosome remodeling factor CHD4. *Genes Dev.*, **29**, 489–94.
129. Hu,H.M., Zhao,X., Kaushik,S., Robillard,L., Barthelet,A., Lin,K.K., Shah,K.N., Simmons,A.D., Raponi,M., Harding,T.C., *et al.* (2018) A Quantitative Chemotherapy Genetic Interaction Map Reveals Factors Associated with PARP Inhibitor Resistance. *Cell Rep.*, **23**, 918–929.
130. Feng,Z., Scott,S.P., Bussen,W., Sharma,G.G., Guo,G., Pandita,T.K. and Powell,S.N. (2011) Rad52 inactivation is synthetically lethal with BRCA2 deficiency. *Proc. Natl. Acad. Sci.*, **108**, 686–691.
131. Yuan,R., Vos,H.R., Es,R.M., Chen,J., Burgering,B.M., Westendorp,B. and Bruin,A. (2018) Chk1 and 14-3-3 proteins inhibit atypical E2Fs to prevent a permanent cell cycle arrest. *EMBO J.*, **37**.
132. Gunn,A. and Stark,J.M. (2012) DNA Repair Protocols: I-SceI-Based Assays to Examine Distinct Repair Outcomes of Mammalian Chromosomal Double Strand Breaks. *Methods Mol. Biol.*, **920**, 379–391.
133. Mijic,S., Zellweger,R., Chappidi,N., Berti,M., Jacobs,K., Mutreja,K., Ursich,S., Ray Chaudhuri,A., Nussenzweig,A., Janscak,P., *et al.* (2017) Replication fork reversal triggers fork degradation in BRCA2-defective cells. *Nat. Commun.*, **8**.
134. Mitxelena,J., Apraiz,A., Vallejo-Rodríguez,J., García-Santisteban,I., Fullaondo,A., Alvarez-Fernández,M., Malumbres,M. and Zubiaga,A.M. (2018) An E2F7-

dependent transcriptional program modulates DNA damage repair and genomic stability. *Nucleic Acids Res.*, **46**, 4546–4559.

135. Zalmas,L.P., Coutts,A.S., Helleday,T. and Thangue,N.B.L. (2013) E2F-7 couples DNA damage-dependent transcription with the DNA repair process. *Cell Cycle*, **12**, 3037–3051.
136. Choe,K.N., Nicolae,C.M., Constantin,D., Kawasawa,Y.I., Delgado-Diaz,M.R., De,S., Freire,R., Smits,V.A.J. and Moldovan,G.-L. (2016) HUWE1 interacts with PCNA to alleviate replication stress. *EMBO Rep.*, **17**, 1–13.
137. Nicolae,C.M., Aho,E.R., Choe,K.N., Constantin,D., Hu,H.-J., Lee,D., Myung,K. and Moldovan,G.-L. (2015) A novel role for the mono-ADP-ribosyltransferase PARP14/ARTD8 in promoting homologous recombination and protecting against replication stress. *Nucleic Acids Res.*, **43**, 3143–3153.
138. Ikura,M., Furuya,K., Fukuto,A., Matsuda,R., Adachi,J., Matsuda,T., Kakizuka,A. and Ikura,T. (2016) Coordinated Regulation of TIP60 and Poly(ADP-Ribose) Polymerase 1 in Damaged-Chromatin Dynamics. *Mol. Cell. Biol.*, **36**, 1595–607.
139. Renaud,E., Barascu,A. and Rosselli,F. (2016) Impaired TIP60-mediated H4K16 acetylation accounts for the aberrant chromatin accumulation of 53BP1 and RAP80 in Fanconi anemia pathway-deficient cells. *Nucleic Acids Res.*, **44**, 648–656.
140. Jacquet,K., Fradet-Turcotte,A., Avvakumov,N., Lambert,J.-P., Roques,C., Pandita,R.K., Paquet,E., Herst,P., Gingras,A.-C., Pandita,T.K., *et al.* (2016) The TIP60 Complex Regulates Bivalent Chromatin Recognition by 53BP1 through Direct H4K20me Binding and H2AK15 Acetylation. *Mol. Cell*, **62**, 409–421.
141. Tang,J., Cho,N.W., Cui,G., Manion,E.M., Shanbhag,N.M., Botuyan,M.V., Mer,G. and Greenberg,R.A. (2013) Acetylation limits 53BP1 association with damaged chromatin to promote homologous recombination. *Nat. Struct. Mol. Biol.*, **20**, 317–325.

142. Ochs,F., Somyajit,K., Altmeyer,M., Rask,M.-B., Lukas,J. and Lukas,C. (2016) 53BP1 fosters fidelity of homology-directed DNA repair. *Nat. Struct. Mol. Biol.*, **23**, 714–721.

143. Wang,Z., Michaud,G.A., Cheng,Z., Zhang,Y., Hinds,T.R., Fan,E., Cong,F. and Xu,W. (2012) Recognition of the iso-ADP-ribose moiety in poly(ADP-ribose) by WWE domains suggests a general mechanism for poly(ADP-ribosyl)ation-dependent ubiquitination. *Genes Dev.*, **26**, 235–40.

144. Mandemaker,I.K., Van Cuijk,L., Janssens,R.C., Lans,H., Bezstarosti,K., Hoeijmakers,J.H., Demmers,J.A., Vermeulen,W. and Marteijn,J.A. (2017) DNA damage-induced histone H1 ubiquitylation is mediated by HUWE1 and stimulates the RNF8-RNF168 pathway. *Sci. Rep.*, **7**, 1–11.

145. Kolinjivadi,A.M., Sannino,V., De Antoni,A., Zadorozhny,K., Kilkenny,M., Técher,H., Baldi,G., Shen,R., Ciccia,A., Pellegrini,L., *et al.* (2017) Smarcal1-Mediated Fork Reversal Triggers Mre11-Dependent Degradation of Nascent DNA in the Absence of Brca2 and Stable Rad51 Nucleofilaments. *Mol. Cell*, **67**, 867–881.e7.

146. Heidelberger,J.B., Voigt,A., Borisova,M.E., Petrosino,G., Ruf,S., Wagner,S.A. and Beli,P. (2018) Proteomic profiling of VCP substrates links VCP to K6-linked ubiquitylation and c-Myc function. *EMBO Rep.*, **19**, e44754.

147. Markman,M. (2019) Pharmaceutical Management of Ovarian Cancer: Current Status. *Drugs*, **79**, 1231–1239.

148. Clements,K.E., Thakar,T., Nicolae,C.M., Liang,X., Wang,H.-G. and Moldovan,G.-L. (2018) Loss of E2F7 confers resistance to poly-ADP-ribose polymerase (PARP) inhibitors in BRCA2-deficient cells. *Nucleic Acids Res.*, 10.1093/nar/gky657.

149. Forment,J. V., Walker,R. V. and Jackson,S.P. (2012) A high-throughput, flow cytometry-based method to quantify DNA-end resection in mammalian cells. *Cytom. Part A*, **81A**, 922–928.

150. Forment,J. V and Jackson,S.P. (2015) A flow cytometry-based method to simplify the analysis and quantification of protein association to chromatin in mammalian cells. *Nat. Protoc.*, **10**, 1297–307.

151. Bouwman,P., Aly,A., Escandell,J.M., Pieterse,M., Bartkova,J., van der Gulden,H., Hiddingh,S., Thanasoula,M., Kulkarni,A., Yang,Q., *et al.* (2010) 53BP1 loss rescues BRCA1 deficiency and is associated with triple-negative and BRCA-mutated breast cancers. *Nat. Struct. Mol. Biol.*, **17**, 688–695.

152. Spies,J., Lukas,C., Somyajit,K., Rask,M.-B., Lukas,J. and Neelsen,K.J. (2019) 53BP1 nuclear bodies enforce replication timing at under-replicated DNA to limit heritable DNA damage. *Nat. Cell Biol.*, **21**, 487–497.

153. Xu,Y., Ning,S., Wei,Z., Xu,R., Xu,X., Xing,M., Guo,R. and Xu,D. (2017) 53BP1 and BRCA1 control pathway choice for stalled replication restart. *Elife*, **6**.

154. Her,J., Ray,C., Altshuler,J., Zheng,H. and Bunting,S.F. (2018) 53BP1 Mediates ATR-Chk1 Signaling and Protects Replication Forks under Conditions of Replication Stress. *Mol. Cell. Biol.*, **38**.

155. Rickman,K. and Smogorzewska,A. (2019) Advances in understanding DNA processing and protection at stalled replication forks. *J. Cell Biol.*, **218**, 1096–1107.

156. Martin,S.K. and Wood,R.D. (2019) DNA polymerase ζ in DNA replication and repair. *Nucleic Acids Res.*, **47**, 8348–8361.

157. Sharma,S., Hicks,J.K., Chute,C.L., Brennan,J.R., Ahn,J.Y., Glover,T.W. and Canman,C.E. (2012) REV1 and polymerase ζ facilitate homologous recombination repair. *Nucleic Acids Res.*, **40**, 682–691.

158. Wang,S., Han,L., Han,J., Li,P., Ding,Q., Zhang,Q.J., Liu,Z.P., Chen,C. and Yu,Y. (2019) Uncoupling of PARP1 trapping and inhibition using selective PARP1 degradation. *Nat. Chem. Biol.*, **15**, 1223–1231.

159. Clinical OMICs Staff Writer AZ to Use Myriad's myChoice HRD Plus Test in Phase

III Trial.

160. Clouaire,T., Rocher,V., Lashgari,A., Arnould,C., Aguirrebengoa,M., Biernacka,A., Skrzypczak,M., Aymard,F., Fongang,B., Dojer,N., *et al.* (2018) Comprehensive Mapping of Histone Modifications at DNA Double-Strand Breaks Deciphers Repair Pathway Chromatin Signatures. *Mol. Cell*, **72**, 250–262.e6.
161. Certo,M.T., Ryu,B.Y., Annis,J.E., Garibov,M., Jarjour,J., Rawlings,D.J. and Scharenberg,A.M. (2011) Tracking genome engineering outcome at individual DNA breakpoints. *Nat. Methods*, **8**, 671–6.
162. Massip,L., Caron,P., Iacovoni,J.S., Trouche,D. and Legube,G. (2010) Deciphering the chromatin landscape induced around DNA double strand breaks. *Cell Cycle*, **9**, 2963–2972.
163. Iacovoni,J.S., Caron,P., Lassadi,I., Nicolas,E., Massip,L., Trouche,D. and Legube,G. (2010) High-resolution profiling of γh2AX around DNA double strand breaks in the mammalian genome. *EMBO J.*, **29**, 1446–1457.
164. Aymard,F., Bugler,B., Schmidt,C.K., Guillou,E., Caron,P., Briois,S., Iacovoni,J.S., Daburon,V., Miller,K.M., Jackson,S.P., *et al.* (2014) Transcriptionally active chromatin recruits homologous recombination at DNA double-strand breaks. *Nat. Struct. Mol. Biol.*, **21**, 366–374.
165. Santos-Pereira,J.M. and Aguilera,A. (2015) R loops: new modulators of genome dynamics and function. *Nat. Rev. Genet.*, **16**, 583–597.
166. Aguilera,A. and García-Muse,T. (2012) R Loops: From Transcription Byproducts to Threats to Genome Stability. *Mol. Cell*, **46**, 115–124.
167. Meghani,K., Fuchs,W., Detappe,A., Drané,P., Gogola,E., Rottenberg,S., Jonkers,J., Matulonis,U., Swisher,E.M., Konstantinopoulos,P.A., *et al.* (2018) Multifaceted Impact of MicroRNA 493-5p on Genome-Stabilizing Pathways Induces Platinum and PARP Inhibitor Resistance in BRCA2-Mutated Carcinomas. *Cell Rep.*, **23**, 100–

111.

168. Waddell,N., Pajic,M., Patch,A.-M., Chang,D.K., Kassahn,K.S., Bailey,P., Johns,A.L., Miller,D., Nones,K., Quek,K., *et al.* (2015) Whole genomes redefine the mutational landscape of pancreatic cancer. *Nature*, **518**, 495–501.
169. Haapaniemi,E., Botla,S., Persson,J., Schmierer,B. and Taipale,J. (2018) CRISPR-Cas9 genome editing induces a p53-mediated DNA damage response. *Nat. Med.*, **24**, 927–930.
170. Holohan,C., Van Schaeybroeck,S., Longley,D.B. and Johnston,P.G. (2013) Cancer drug resistance: An evolving paradigm. *Nat. Rev. Cancer*, **13**, 714–726.
171. Póti,Á., Berta,K., Xiao,Y., Pipek,O., Klus,G.T., Ried,T., Csabai,I., Wilcoxen,K., Mikule,K., Szallasi,Z., *et al.* (2018) Long-term treatment with the PARP inhibitor niraparib does not increase the mutation load in cell line models and tumour xenografts. *Br. J. Cancer*, **119**, 1392–1400.
172. Gong,X., Du,D., Deng,Y., Zhou,Y., Sun,L. and Yuan,S. (2020) The structure and regulation of the E3 ubiquitin ligase HUWE1 and its biological functions in cancer. *Invest. New Drugs*, **38**, 515–524.
173. Canfield,K., Wells,W., Geradts,J., Kinlaw,W.B., Cheng,C. and Kurokawa,M. (2016) Inverse association between MDM2 and HUWE1 protein expression levels in human breast cancer and liposarcoma. *Int. J. Clin. Exp. Pathol.*, **9**, 6342–6349.
174. Atsumi,Y., Minakawa,Y., Ono,M., Dobashi,S., Shinohe,K., Shinohara,A., Takeda,S., Takagi,M., Takamatsu,N., Nakagama,H., *et al.* (2015) ATM and SIRT6/SNF2H Mediate Transient H2AX Stabilization When DSBs Form by Blocking HUWE1 to Allow Efficient γH2AX Foci Formation. *Cell Rep.*, **13**, 2728–2740.
175. Wang,P., Bao,H., Zhang,X., Liu,F. and Wang,W. (2019) Regulation of Tip60-dependent p53 acetylation in cell fate decision. *FEBS Lett.*, **593**, 13–22.
176. Brauns-Schubert,P., Schubert,F., Wissler,M., Weiss,M., Schlicher,L., Bessler,S.,

Safavi,M., Miething,C., Borner,C., Brummer,T., *et al.* (2018) CDK9-mediated phosphorylation controls the interaction of TIP60 with the transcriptional machinery. *EMBO Rep.*, **19**, 244–256.

177. CPTAC | Office of Cancer Clinical Proteomics Research.

VITA
Kristen Clements

Education:

Pennsylvania State University College of Medicine, Hershey, PA
MD/PhD candidate (Thesis Mentor: George-Lucian Moldovan, PhD)
June 2014- present

Siena College, Loudonville, NY
B.S. in Biochemistry, Minor in Spanish Language
2014, *Summa Cum Laude*

Publications:

Clements K.E., Thakar T., Nicolae C.M., Liang X., Wang H.G., and Moldovan G.L. Loss of E2F7 confers resistance to poly-ADP-ribose polymerase (PARP) inhibitors in BRCA2-deficient cells. *Nucleic Acids Res. 2018 Jul 19. doi: 10.1093/nar/gky657. PMID: 30032296*

Pending publications:

Clements K.E., Hale A., Tolman N.J., Nicolae C.M., Sharma A., Thakar T., Liang X., Kawasawa Y.I., Wang H.G., De S., and Moldovan G.L. Identification of regulators of poly-ADP-ribose polymerase (PARP) inhibitor response through complementary CRISPR knockout and activation screens. *doi: https://doi.org/10.1101/871970*. *Manuscript under review (Nature Communications).*

Clements K.E. and Moldovan G.L. PARP inhibitor response at the bedside and the bench. (*Review; To be submitted by Jan. 2020*.)

Thakar T., Leung W., Nicolae C.M., **Clements K.E.**, Shen B., Bielinsky A.K., and Moldovan G.L. PCNA ubiquitination protects stalled replication forks from DNA2-mediated degradation by regulating Okazaki fragment maturation and chromatin assembly. *BioRxiv, 2019 September 05. doi: https://doi.org/10.1101/759985. Manuscript in revision (Nature Communications).*

Schleicher E.M., **Clements K.E.**, Dhoonmoon A., Nicolae C.M., and Moldovan G.L. CRISPR/Cas9 genome-wide genetic screens uncover novel mechanisms of resistance to ATR inhibitors. (*To be submitted by Jan. 2020*)

Hornick J., **Clements K.E.**, Canfield V.A., Selkirk J., Opiteck G.J., Moldovan G.L., and Broach J.R. Natural human genetic variants affect efficacy and coupling of spingosine-1-phosphate receptors. *Manuscript in revision (J. Biol. Chem).*

Liu Q., Atkinson J.M., Gebru M.T., **Clements K.E.**, Moldovan G.L., and Wang H.G. A luciferase-based assay identifies niclosamide derivatives antagonizing Mcl-1 through post-translational down-regulation. *BioRxiv. 2019 June 08. doi: https://doi.org/10.1101/665505.*